2019

Physicochemical, permeability, antioxidant and anti-inflammatory properties of oxyresveratrol ester prodrugs

Wuttinont Thaweesest
Faculty of Pharmaceutical Sciences

PHYSICOCHEMICAL, PERMEABILITY, ANTIOXIDANT AND ANTI-INFLAMMATORY PROPERTIES OF OXYRESVERATROL ESTER PRODRUGS

Mr. Wuttinont Thaweesest

A Dissertation Submitted in Partial Fulfillment of the Requirements
for the Degree of Doctor of Philosophy in Pharmaceutical Chemistry and Natural Products
Department of Food and Pharmaceutical Chemistry
FACULTY OF PHARMACEUTICAL SCIENCES
Chulalongkorn University
Academic Year 2019

สมบัติทางเคมีกายภาพ การซึมผ่าน การต้านออกซิเดชันและการต้านการอักเสบของออกซีเรสเวอราทรอลเอสเทอร์โปรดรักส์

นายวุฒินนท์ ทวีเศรษฐ

วิทยานิพนธ์นี้เป็นส่วนหนึ่งของการศึกษาตามหลักสูตรปริญญาวิทยาศาสตรดุษฎีบัณฑิต
สาขาวิชาเภสัชเคมีและผลิตภัณฑ์ธรรมชาติ ภาควิชาอาหารและเภสัชเคมี
คณะเภสัชศาสตร์ จุฬาลงกรณ์มหาวิทยาลัย
ปีการศึกษา 2562

Thesis Title	PHYSICOCHEMICAL, PERMEABILITY, ANTIOXIDANT AND ANTI-INFLAMMATORY PROPERTIES OF OXYRESVERATROL ESTER PRODRUGS
By	Mr. Wuttinont Thaweesest
Field of Study	Pharmaceutical Chemistry and Natural Products
Thesis Advisor	ASSOCIATE PROFESSOR PORNCHAI ROJSITTHISAK, Ph.D.
Thesis Co Advisor	PROFESSOR PAITOON RASHATASAKHON, Ph.D.

Accepted by the FACULTY OF PHARMACEUTICAL SCIENCES, Chulalongkorn University in Partial Fulfillment of the Requirement for the Doctor of Philosophy

..... Dean of the FACULTY OF PHARMACEUTICAL SCIENCES

(ASSISTANT PROFESSOR RUNGPETCH SAKULBUMRUNGSIL, Ph.D.)

DISSERTATION COMMITTEE

..... Chairman

(PROFESSOR SOMBOON TANASUPAWAT, Ph.D.)

..... Thesis Advisor

(ASSOCIATE PROFESSOR PORNCHAI ROJSITTHISAK, Ph.D.)

..... Thesis Co-Advisor

(PROFESSOR PAITOON RASHATASAKHON, Ph.D.)

..... Examiner

(ASSOCIATE PROFESSOR BOONCHOO SRITULARAK, Ph.D.)

..... Examiner

(ASSOCIATE PROFESSOR BODIN TUESUWAN, Ph.D.)

..... Examiner

(ASSISTANT PROFESSOR ROSSARIN TANSAWAT, Ph.D.)

..... External Examiner

(ASSOCIATE PROFESSOR SIRIPORN TUNTIPOPIPAT, Ph.D.)

วุฒินนท์ ทวีเศรษฐ : สมบัติทางเคมีกายภาพ การซึมผ่าน การต้านออกซิเดชันและการต้านการอักเสบของออกซีเรสเวอราทรอลเอสเทอร์โปรดรักส์. (PHYSICOCHEMICAL, PERMEABILITY, ANTIOXIDANT AND ANTI-INFLAMMATORY PROPERTIES OF OXYRESVERATROL ESTER PRODRUGS) อ.ที่ปรึกษาหลัก : รศ. ภก. ดร.พรชัย โรจน์สิทธิศักดิ์, อ.ที่ปรึกษาร่วม : ศ. ดร.ไพฑูรย์ รัชตะสาคร

ออกซีเรสเวอราทรอล (OXY) เป็นที่ทราบกันดีว่ามีสมบัติต้านออกซิเดชันและต้านการอักเสบ แต่มีความสามารถในการดูดซึมทางปากต่ำในหนูและความสามารถในการซึมผ่านระดับกลางในแบบจำลองโมโนเลเยอร์ของ Caco-2 ออกซีเรสเวอราทรอลเอสเทอร์โปรดรักส์ (OXY ester prodrugs) ที่มีความยาวโซ่ของหมู่เอซิลที่ต่างกัน (ออกซีเรสเวอราทรอลเตตระอะซีเตต (OXY-TAc), ออกซีเรสเวอราทรอลเตตระโพรพิโอเนต (OXY-TPr) และออกซีเรสเวอราทรอลเตตระบิวทีเรต (OXY-TBu) ถูกสังเคราะห์เพื่อปรับปรุงการซึมผ่านของ OXY การขนส่งของ OXY ester prodrugs ทั้งสามผ่านโมโนเลย์ของ Caco-2 สูงกว่า OXY โดย OXY-TAc มีการซึมผ่านสูงที่สุด การสลายตัวของ OXY-TAc ในบัฟเฟอร์ไฮโดรคลอริก (pH 1.2) บัฟเฟอร์ฟอสเฟต (pH 6.8 และ 7.4) ของเหลวจำลองภาวะในกระเพาะอาหารและลำไส้รวมทั้งพลาสมาของมนุษย์ที่อุณหภูมิ 37 °C เป็นไปตามจลนศาสตร์อันดับหนึ่งเทียม ฤทธิ์ต้านออกซิเดชันและต้านการอักเสบตลอดจนกลไกการออกฤทธิ์ในเซลล์แมคโครฟาจ RAW264.7 ที่กระตุ้นความเครียดออกซิเดชันและการอักเสบด้วยลิโปโพลีแซ็กคาไรด์ (LPS) ของส่วนที่ดูดซึมผ่านเซลล์ลำไส้ของ OXY-TAc (BF-OXY-TAc) ได้ถูกตรวจสอบและเปรียบเทียบกับส่วนที่ดูดซึมผ่านเซลล์ลำไส้ของ OXY (BF-OXY) การทดสอบการต้านออกซิเดชันทั้งหมด (1,1-diphenyl-2-picrylhydrazyl (DPPH) ferric reducing antioxidant power (FRAP) และ oxygen radical absorbance capacity (ORAC) assays) แสดงให้เห็นว่า BF-OXY-TAc มีฤทธิ์การต้านออกซิเดชันสูงกว่า BF-OXY BF-OXY-TAc สามารถลดระดับรีแอคทีฟออกซิเจนสปีชีส์ (ROS) ไนตริกออกไซด์ (NO) และอินเตอร์ลิวคิน-6 (IL-6) ในเซลล์แมคโครฟาจ RAW264.7 ที่กระตุ้นด้วย LPS ได้ดีกว่า BF-OXY 2.5, 2.5, 1.6 เท่าตามลำดับ จากการวิเคราะห์ western blot พบว่า BF-OXY-TAc ลดการแสดงออกของเอนไซม์ไนตริกออกไซด์ (iNOS) และไซโคลออกซีจีเนส -2 (COX-2) มากกว่า BF-OXY 1.2 และ 1.4 เท่าตามลำดับ ผลการวิจัยชี้ให้เห็นว่า OXY-TAc สามารถเอาชนะข้อจำกัดของ OXY ในแง่ของการเพิ่มการซึมผ่านซึ่งนำไปสู่การต้านออกซิเดชันและการต้านการอักเสบที่ดีขึ้น OXY ต่อความเครียดออกซิเดชันและการอักเสบที่กระตุ้นด้วย LPS ในเซลล์แมคโครฟาจ RAW264.7

สาขาวิชา	เภสัชเคมีและผลิตภัณฑ์ธรรมชาติ	ลายมือชื่อนิสิต .....
ปีการศึกษา	2562	ลายมือชื่อ อ.ที่ปรึกษาหลัก .....
		ลายมือชื่อ อ.ที่ปรึกษาร่วม .....

5876455633 : MAJOR PHARMACEUTICAL CHEMISTRY AND NATURAL PRODUCTS
KEYWORD: Oxyresveratrol, Ester prodrug, Antioxidant activity, Anti-inflammatory activity
Wuttinont Thaweesest : PHYSICOCHEMICAL, PERMEABILITY, ANTIOXIDANT AND ANTI-INFLAMMATORY PROPERTIES OF OXYRESVERATROL ESTER PRODRUGS . Advisor: ASSOC. PROF. PORNCHAI ROJSITTHISAK, Ph.D. Co-advisor: PROF. PAITOON RASHATASAKHON, Ph.D.

Oxyresveratrol (OXY) is known to exert antioxidant and anti-inflammatory properties but has low oral bioavailability in rats and low permeability in the Caco-2 cell monolayer model. Three ester prodrugs with different acyl chain lengths (oxyresveratrol tetraacetate (OXY-TAc), oxyresveratrol tetrapropionate (OXY-TPr), and oxyresveratrol tetrabutyrate (OXY-TBu) were synthesized to improve the permeability of OXY. Transport of three OXY ester prodrugs across Caco-2 monolayers was higher than that of OXY, and OXY-TAc exhibited the highest permeation. The degradation of OXY-TAc in HCl buffer (pH 1.2), phosphate buffer (pH 6.8 and 7.4), simulated gastric and intestinal fluids, as well as human plasma at 37 °C was followed pseudo-first-order kinetics. Antioxidant and anti-inflammatory effects, as well as mechanisms of action in LPS-stimulated murine macrophage cells (RAW264.7) under oxidative stress and inflammation of bioavailable fraction of OXY-TAc (BF-OXY-TAc), were investigated and compared with the bioavailable fraction of OXY (BF-OXY). All three antioxidant assays (1,1-diphenyl-2-picrylhydrazyl (DPPH), ferric reducing antioxidant power (FRAP), and oxygen radical absorbance capacity (ORAC) assays) showed that BF-OXY-TAc exhibited higher antioxidant activities than that of BF-OXY. In the LPS-stimulated RAW264.7 macrophage cells, BF-OXY-TAc attenuated the LPS-induced reactive oxygen species (ROS), nitric oxide (NO), and interleukin-6 (IL-6) levels were 2.5, 2.5, and 1.6-fold higher than that of BF-OXY respectively. Western blot analysis revealed that BF-OXY-TAc decreased inducible nitric oxide synthase (iNOS) and cyclooxygenase-2 (COX-2) protein expressions were 1.2 and 1.4-fold higher than that of BF-OXY, respectively. The results suggest that OXY-TAc can overcome the limitations of OXY in terms of improving permeation, leading to better antioxidant and anti-inflammatory activities of OXY against LPS-stimulated oxidative stress and inflammation in RAW264.7 macrophage cells.

Field of Study:	Pharmaceutical Chemistry and Natural Products	Student's Signature .....
Academic Year:	2019	Advisor's Signature .....
		Co-advisor's Signature .....

ACKNOWLEDGEMENTS

First of all, I would like to pay my special regards to my supervisor, Associate Professor Pornchai Rojsitthisak, for the support of my Ph.D. study and related research for his patience, motivation, and immense knowledge. Without his persistent help, the goal of this project would not have been realized.

My sincere gratitude is also conferred to Associate Professor Paitoon Rashatasakhon, my co-advisor who always gives me valuable comments, suggestions, and helping my laboratory work, especially the part of synthesis and characterization.

My sincere gratitude has been contributing to Professor Somboon Tanasupawat for being the thesis chairperson, and Associate Professor Boonchoo Sritularak, Assistant Professor Bodin Tuesuwan and Assistant Professor Rossarin Tansawat for being the committee, and Professor Siriporn Tuntipopipat for being the external examiner member and their kind suggestions to make my thesis complete.

This study is supported by The Scholarship from the Graduate School, Chulalongkorn University to commemorate The Celebrations on the Auspicious Occasion of Her Royal Highness Princess Maha Chakri Sirindhorn's 5th Cycle (60th) Birthday. I would like to thank the Pharmaceutical Research Instrument Center, Faculty of Pharmaceutical Sciences, Chulalongkorn University, for supplying instruments. I also would like staff from Chulalongkorn University for their kind suggestions, help, and support.

I sincerely thank everyone who has assisted in the completion of this project. I thank my fellow labmates for the discussions, for many nights we were working together, and for all good moments we have had in the last five years. In particular, I would like to acknowledge Dr. Chawanphat Muangnoi, who offered me valuable suggestions for this study. During the preparation of the dissertation, he spent a lot of time improving the publication and provide me relevant advice. This research would not be possible without their invaluable support.

Last but not least, I would like to express my sincere gratitude to my family and friends for providing me with continued support, motivation, and affection during my years of study and through the process of studying and writing this dissertation. This achievement would not have been possible without them. Thank you.

Wuttinont Thaweesest

TABLE OF CONTENTS

LIST OF TABLES

Page

LIST OF FIGURES

Page

LIST OF ABBREVIATION

ATCC	American Type Culture Collection
ºC	Degree Celsius
BF	Bioavailable fraction
COX-2	Cyclooxygenase-2
DMEM	Dulbecco's modified Eagle's medium
DMSO	Dimethyl sulfoxide
DPPH	2,2-Diphenyl-1-picrylhydrazyl
ELISA	Enzyme-linked immunosorbent assay
FRAP	Ferric Reducing Antioxidant Power
GI	Gastrointestinal
h	Hour
HPLC	High-performance liquid chromatography
iNOS	Inducible nitric oxide synthase
IL-6	Interleukin-6
LPS	Lipopolysaccharide
m/z	Mass-to-charge ratio
MW	Molecular weight
MTT	Thiazolyl blue tetrazolium bromide
µg	Microgram
µL	Microliter
µmol	Micromol
µM	Micromolar
mg	Milligram
mL	Milliliter
mM	Millimolar
mmol	Millimol
min	Minute

nm	Nanometer
NO	Nitric oxide
OXY	Oxyresveratrol
OXY-TAc	Oxyresveratrol tetraacetate
OXY-TBu	Oxyresveratrol tetrabutyrate
OXY-TPr	Oxyresveratrol tetrapropionate
P_{app}	Apparent permeability coefficient
ROS	Reactive oxygen species
rpm	Revolutions per minute
s	Second
v/v	Volume-by-volume
w/v	Weight-by-volume

CHAPTER 1

INTRODUCTION

1.1 Background

Several non-communicable diseases are associated with oxidative stress and inflammation, including atherosclerosis, diabetes, and neurodegenerative diseases. The protective effect may, therefore, provide an avenue for preventive and curative approaches through antioxidation and anti-inflammation [1]. Oxyresveratrol (trans-2′,3,4′,5-tetramethoxy stilbene; OXY) is a naturally occurring polyphenolic stilbene abundant in the heartwood of the Thai traditional medicinal plant *Artocarpus lakoocha* Buch.-Ham. or " Ma-Haad" (Figure 1) [2]. OXY has various bioactivities, including anti-inflammatory [3-5], anti-oxidant and free radical scavenging [6-10], anti-viral [11, 12], tyrosinase inhibitory activities [13], anti-hyperlipidemic [14, 15], anti-diabetic [16], neuroprotective [17], and anti-cancer [18, 19].

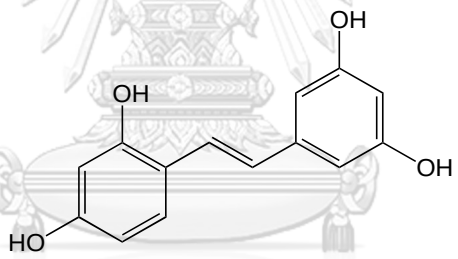

Figure 1 The chemical structures of oxyresveratrol.

However, there are some limitations to the oral delivery of OXY. The pharmacokinetic study of OXY was conducted in rats by oral dosing at 100-400 μmol/kg. OXY exhibited low oral bioavailability (approximately 10-15%), with a rapid maximum plasma concentration (T_{max}) occurring at about 15 min after dosing [20]. The oral bioavailability (% F) of the compound can be classified into two groups: low bioavailable (% F <50) and high bioavailable (% F≥50) [21, 22]. OXY was biotransformed by phase II conjugation within 12 h after oral administration at a dose of 100 mg/kg of OXY. The majority of metabolites were presented in rat urine or bile as conjugated forms, including glucuronidated, methylated, and sulfated conjugates.

Conjugation reaction of OXY in urine or bile led not only to produce an inactivation of phase II metabolites but also to increase the hydrophilicity and hence to enhance the excretion of OXY after orally administered OXY [23]. OXY had a low permeability with a permeability coefficient of approximately <1-2 x 10^{-6} cm/s in the Caco-2 monolayers model [24]. Permeability depends on the following factors: 1) octanol-water partition coefficient (logP) 2) molecular weight 3) hydrogen bond donor 4) hydrogen bond acceptor. Compounds with good permeability should have logP <5, molecular weight. <500 g / mol, hydrogen bond donor <5 and hydrogen bond acceptor <10 [25-27].

In order to improve permeability, oral bioavailability of OXY, and avoid the modification of OXY by enterocytic transferases *in vivo*, synthesis of ester prodrugs OXY has been used to overcome these problems. Ester prodrugs are designed to enhance the lipophilicity and passive membrane permeability [28]. Many studies have reported that esterification of natural compounds with a phenolic hydroxyl group is an effective way to improve permeability. Interestingly, there are many cases where ester prodrug appeared to be more effective than their parent compounds. For example, quercetin (QU) had a lower permeability coefficient (2.82 x 10^{-6} cm/s), whereas the transport rate of QU ester derivative (3,7,3′,4′-*O*-tetraethyl acetate QU) (5.23 x 10^{-6} cm/s) was greater than that of QU. These results suggested that improving the lipophilicity of QU by esterification could increase the transport of QU across Caco-2 cells [29]. Ginsenoside compound K (CK), one of the main pharmacologically active metabolites of protopanaxadiol ginsenosides, had a low permeability coefficient (8.65 x 10^{-7} cm/s), while the transport rate of CK butyl ester (2.97 x 10^{-6} cm/s) and CK octyl ester (2.84 x 10^{-6} cm/s) was greater than that of CK. These results suggested that improving the lipophilicity of CK by acylation could significantly improve transport across Caco-2 cells [30]. Esculin (6,7-dihydroxy-coumarin-6-O-glucoside) had a low permeability coefficient (0.71 x 10^{-6} cm/s), while five esculin ester derivatives with different acyl chain lengths had a greater bioavailability than

the esculin. Esculin-6'-O-octanoate, ester derivative with a medium alkyl chain, had a much better bioavailability (36.7 x 10^{-6} cm/s) than the esculin [31].

It was therefore hypothesized that the chemical capping of the hydroxyl group with an appropriate acyl length chain in OXY through ester prodrugs should improve its permeability potential by enhancing its suitable lipophilicity. However, the permeability of OXY ester prodrug across Caco-2 monolayers has not been reported. Notably, antioxidant and anti-inflammatory activities after intestinal absorption have not yet been investigated so far. In this study, OXY ester prodrugs were synthesized by carrying a different acyl substituent conjugated with hydroxyl groups on the backbone of OXY and explored the transport of OXY ester prodrugs across Caco-2 monolayers. In addition, the stability of OXY ester prodrug in buffers at various pHs, simulated gastric fluid, simulated intestinal fluid, and human plasma was investigated. The effect of the bioavailable fraction (BF) of OXY ester prodrug after permeation on antioxidant and anti-inflammatory activities was determined in LPS-stimulated murine macrophage cell line (RAW264.7 cells).

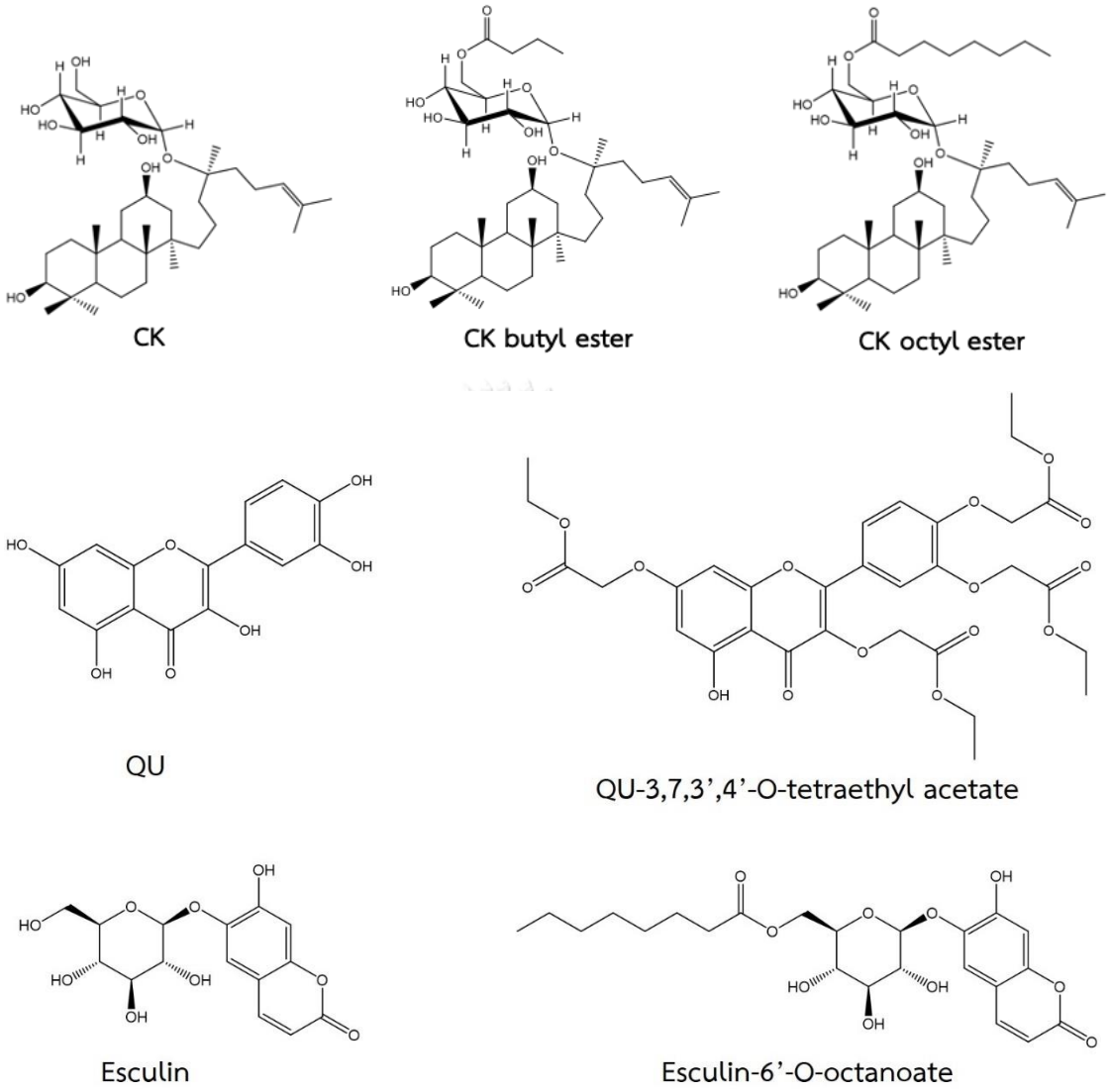

Figure 2 Chemical structure of ester prodrug of natural compounds.

1.2 Objectives

1.2.1 To synthesize and structural elucidate prodrugs of OXY

1.2.2 To determine cellular transport of OXY ester prodrugs across the Caco-2 cell monolayers

1.2.3 To study the stability of OXY ester prodrugs in buffer solutions, simulated gastric fluid, simulated intestinal fluid, and human plasma

1.2.4 To assess antioxidant and anti-inflammatory activities of bioavailable fraction of OXY ester prodrug on LPS-stimulated oxidative stress and inflammation in RAW264.7 macrophage cell line

CHAPTER 2
LITERATURE REVIEW

2.1 Oxyresveratrol

OXY is a member of the stilbene family of polyphenols and is officially known in its IUPAC name 4-[(E)-2-(3,5-dihydroxyphenyl)ethenyl]benzene-1,3-diol. It has a molecular weight of 244.24 g/mol and a molecular formula of $C_{14}H_{12}O_4$. OXY is a derivative of resveratrol; RES). Additionally, OXY is a yellow solid with a melting point of 199 - 204 ℃ and exhibits blue fluorescence under a UV lamp in a TLC reaction [32, 33]. OXY is a stilbenoid which contains four hydroxyl groups and a conjugated system of *trans* C=C bond in its structure [34]. This compound was first isolated from the heartwood of the *Artocarpus lakoocha* [35] and was later isolated from branches and roots of *Morus alba* [36], *Smilax china* [37], *Maclura pomifera* [38], *Veratrum nigrum* [39]. Among these plant species, *Morus alba* (mulberry) is the most studied source for the production of OXY [40-43]. OXY is produced from enzymatic hydrolysis of mulberroside A, a glycoside found in large amounts in mulberry. In addition, it can also be synthesized chemically using 3,5-dihydroxy-acetophenone as a starting material [44]. Recently, OXY has various bioactivities, including anti-oxidant [6-8, 10, 45] and anti-inflammatory [3-5] activities.

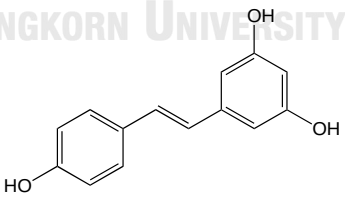

Resveratrol

Figure 3 The chemical structure of resveratrol.

2.2 Oxidative stress and inflammation

Oxidative stress refers to the excessive reactive oxygen species (ROS) production in the cells and tissues, and the antioxidant system cannot be able to reduce them. An imbalance between the ROS production and the antioxidant system

can lead to damage proteins, DNA, and lipids. ROS are produced from either an endogenous source (inflammation, mental stress, infection, aging, etc.) or an exogenous source (ultraviolet light, tobacco smoke, drugs, etc.) [46]. ROS are generally produced within the body in limited quantities. The major ROS players in biological systems are the highly reactive hydroxyl radical (HO·), superoxide anion (O_2^-), hydrogen peroxide (H_2O_2), singlet oxygen ($^1O_2$), and ozone (O_3). Besides ROS, the other physiologically essential reactive species are the reactive nitrogen species (RNS) comprising of nitric oxide (NO·) and the reactive radicals, peroxynitrite anion ($ONOO^-$, produced via interaction of $O_2^{\cdot-}$ and NO·). NO can be converted into peroxynitrous acid and, ultimately, into HO· and nitrite anion (NO_2^-) [47]. ROS and RNS are summarized in Table 1.

Table 1 Reactive oxygen species and reactive nitrogen species

ROS			
Radicals		Non-radicals	
Hydroxyl radical	HO·	Hydrogen peroxide	H_2O_2
Superoxide radical	$O_2^{\cdot-}$	Singlet oxygen	$^1O_2$
Hydroperoxyl radical	HOO·	Ozone	O_3
Peroxyl radical	ROO·		
RNS			
Radicals		Non-radicals	
Nitrogen dioxide radical	NO_2·	Peroxynitrite	$ONOO^-$
Nitric oxide radical	NO·		

ROS are essential compounds involved in the regulation of various biological processes involving the maintaining of cell homeostasis and functions such as activation of receptors, signal transduction, and gene expression. In the cells, mitochondrial oxidative metabolism produces ROS species and organic peroxides during cellular respiration [48]. The main targets of oxidative stress are proteins, DNA/RNA, and lipids. These oxidatively modified molecules may increase the chances of mutagenesis. ROS overproduction can cause damage to cellular structure

and functions. Then, excessive ROS production in cells and tissues may be harmful if not removed rapidly [49]. Indeed, ROS overproduction may cause irreversible damage to cells resulting in cell death processes (necrosis and apoptosis) [50].

ROS produced by cells, such as endothelial, inflammatory, and immune cells, has two faces; first is its participation in redox signaling, and the second is its role in oxidative stress or injury. Redox signaling occurred when low levels of ROS produced induce activation of signaling pathways to initiate biological processes, while oxidative stress defines high levels of ROS production that damages biomolecules. Oxidative stress contributes to the pathophysiology of many diseases. There is increasingly evident that both redox signaling and oxidative stress are underly conditions ranging from cardiovascular to neurodegenerative diseases [51]. Inflammation is a host defense mechanism against pathogens which involves an enhanced or exaggerated ROS production by activated inflammatory and immune cells. ROS is produced as part of the inflammatory response facilitates clearance of tissue-invasive bacteria, but when produced for prolonged periods can promote oxidative stress and chronic inflammation-associated disorders. Additionally, although inflammation induces oxidant injury, the reverse sequence of events is also true. Thus inflammation and oxidative stress are inextricably interrelated [52].

Inflammation is a response to pathogens and tissue injury. Cellular damage or pathogen-associated molecular patterns (PAMPs) expressed by microbes are recognized by innate immune cells (macrophages, leukocytes, neutrophils, and mast cells), which are thus drawn to the site of injury. These cells then release various inflammatory mediators, which include cytokines, histamine, NO, leukotrienes, and prostaglandins (PGs). Cytokines (Tumor necrosis factor-α (TNF-α) and interleukin (IL)) are released by macrophages for repairing local damage and, through binding to G protein-coupled receptors, cause expression of selectins and integrins. Histamine is released by mast cells and causes vasodilation and increases vascular permeability. NO, which is released by endothelial cells, diffuses into smooth muscle cells and causes their relaxation and thus promotes vasodilation. PGs and leukotrienes are synthesized by endothelial cells from phospholipids of damaged membranes and enhance vessel dilation and permeability. Altogether, these inflammatory mediators

promote further recruitment of immune cells into the site of injury, and there they elicit fever, redness, edema, and pain [53]. Also, during inflammation, an enormous amount of ROS is generated. Intracellularly produced ROS are key suppressors of inflammation as they initiate neutrophil apoptosis. However, prolonged inflammatory and oxidative reactions lead to chronic inflammation characterized by abnormal accumulation of inflammatory cells and release of inflammatory mediators along with ROS-mediated toxic oxidative reactions damaging lipids, proteins, and nucleic acids. Chronic inflammation is the major cause of aging and severe diseases, such as asthma, arthritis, inflammatory bowel diseases, bronchitis, pancreatitis, liver fibrosis, cardiovascular diseases, neurodegenerative disorders, and cancer [54]. Mechanistically, chronic inflammation activates Toll-like receptors (TLRs) expressed on macrophages to induce the overproduction of inflammatory mediators. These mediators activate the transcription factors, such as NFkB, nuclear factor of activated T-cells (NFAT), nuclear factor erythroid 2-related factor 2 (Nrf2), and activator protein 1 (AP-1), which are all either directly or indirectly regulated via MAPKs (extracellular signal-regulated kinases (ERK), c-JUN N-terminal kinases (JNK) and p38 mitogen-activated protein kinases [55]. Besides, several enzymes are activated, such as inhibitor of nuclear factor-KB (IKB) kinase (IKK), iNOS, COX-2, and 5-lipoxygenase (5-LOX) [56, 57]. In general, most of the nutraceuticals are antioxidant and/or anti-inflammatory agents with good tolerability. Plant polyphenols, including stilbenes, are prominent examples [58]. The relation between oxidative stress and inflammation is illustrated in Figure 4. The factors that cause inflammation and its amplification, leading to oxidative stress and the reverse sequence of events (oxidative stress-induced inflammation), and the intersection of these are also reviewed. Finally, the antioxidant regulatory mechanisms that modulate the balance between host defense, inflammation, and oxidative stress are discussed.

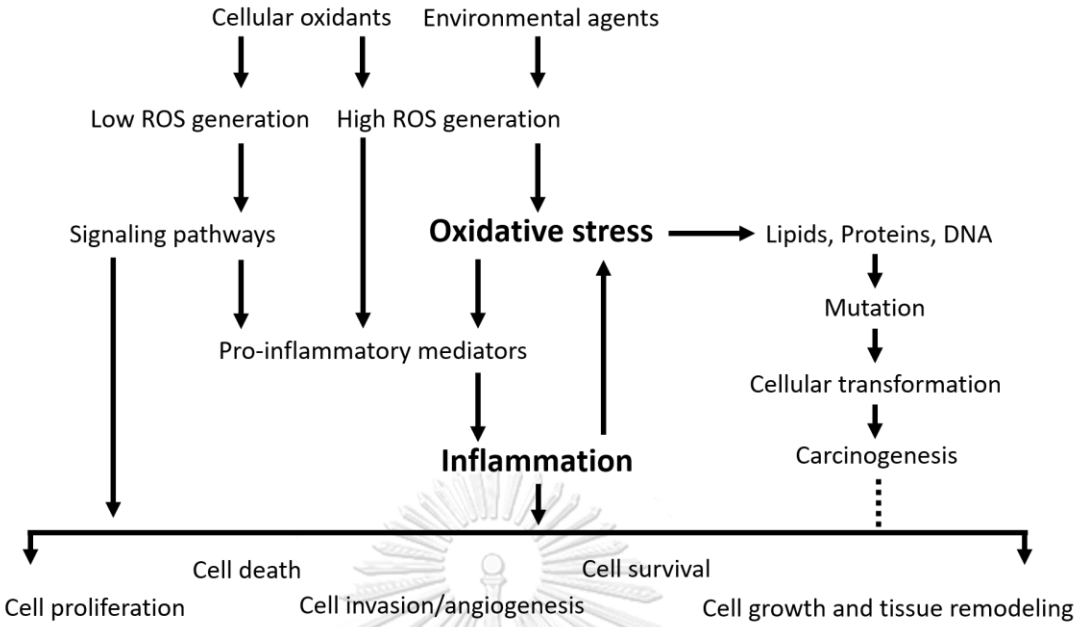

Figure 4 The interrelationship between ROS, oxidative stress, inflammation, and cellular physiology and pathology (modified from [52]).

2.3 Antioxidant and anti-inflammatory activities of OXY

During oxidative stress and inflammation, cell response follows two pathways mediated by mitogen-activated protein kinases (MAP kinases), shown in Figure 5. The first pathway is the NF-kB pathway. It has an essential role in the regulation of transcription of pro-inflammatory mediators like cytokines and chemokines. In the presence of oxidative stress and inflammation, the inactive form of NF-kB (NF-kB-IkB complexes) present in the cytoplasm is converted to the active form (NF-kB) by activated-MAP kinases. And then activated NF-kB translocate to the nucleus resulting in the expression of pro-inflammatory mediators such as interleukin-6 (IL-6), TNF-α, iNOS, and COX-2. iNOS and COX-2 are important enzymes that play a key role in the inflammatory process. These enzymes are responsible for NO and PGs production [59]. iNOS is a critical enzyme that produces large amounts of NO from L-arginine. NO can react with $O_2^{\cdot-}$ to form $ONOO^-$, which can cause damage to cell membranes and lead to cell death [50]. Meanwhile, COX-2 produces a large amount of PGE_2 from arachidonic acid, causing inflammatory reactions (Figure 6) [60]. On the other hand, the second pathway is the Nrf2 pathway. It has a central role in the transcriptional

regulation of antioxidants like antioxidant enzymes, non-enzymatic antioxidants, and detoxifying enzymes. During oxidative stress and inflammation, an inactive form of Nrf2 (Nrf2-keap1 complexes) in the cytoplasm is converted to an active form (Nrf2) by activated-MAP kinases. Freeform of Nrf2 is then translocated to the nucleus resulting in the expression of antioxidant enzymes (superoxide dismutase, glutathione peroxidase, and catalase), non-enzymatic antioxidant (glutathione), and detoxifying enzymes (HO-1, NAD(P)H dehydrogenase quinone 1 (NQO1) and glutathione S-transferase) [61, 62].

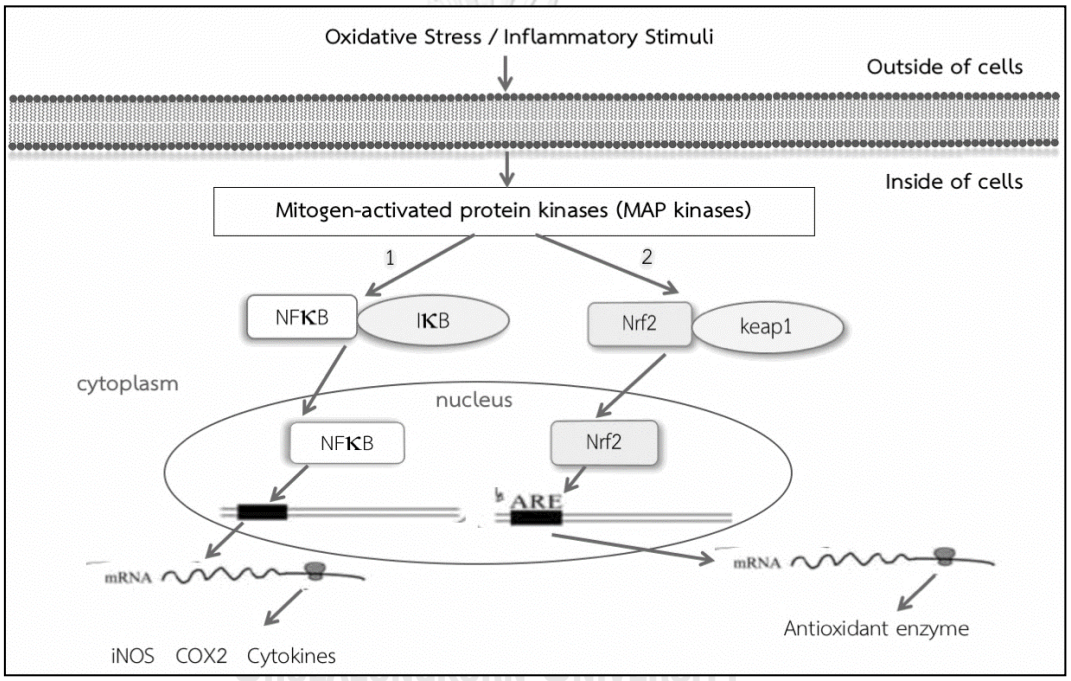

Figure 5 The mechanism of cell response to oxidative stress and inflammation (modified from [62]).

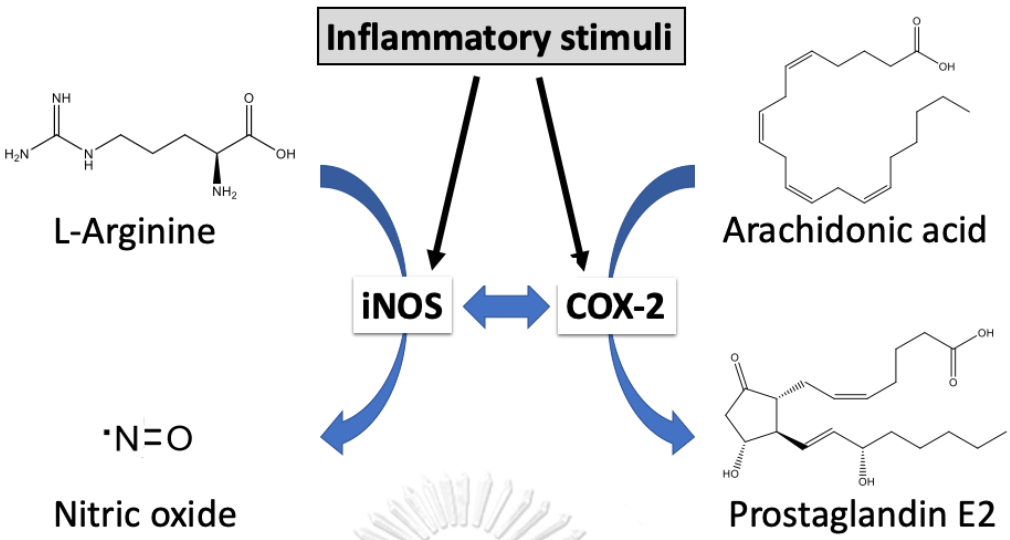

Figure 6 The role of iNOS and COX-2 (modified from [63]).

2.3.1 Antioxidant activity of OXY

OXY has demonstrated strong antioxidant activity [6, 64]. It has been shown to be an effective scavenger against free radicals such as 2,2'-Azinobis-(3-ethylbenzthiazoline-6-sulphonate (ABTS) and 2,2-diphenyl-1-picrylhydrazyl (DPPH) radicals [65]. OXY also was found to be near twice as strong as RES in the thiobarbituric acid reactive substances (TBARS) method [7]. Another study found that OXY was a more effective scavenger for DPPH radical used as a general free radical model and was a potential protectant against ROS and reactive nitrogen species (RNS) compared with RES [10]. OXY has a higher DPPH radical scavenging capacity than RES and mulberroside A [66].

OXY is a bioactive compound that has demonstrated strong antioxidant activity [6]. The high concentration of ROS is known to cause oxidative stress and potentially harm the cells. Therefore, many studies have been proceeded to decrease the concentration of ROS. Currently, there has been a rising interest in phytochemicals showing antioxidant activity. Antioxidant activity studies on flavonoids, polyphenols, and stilbenes have been reported [67, 68]. The DPPH assay results showed that the IC_{50} values of OXY and RES were 28.9 μM and 38.5 μM, respectively. The primary glial cell cultures pretreated with OXY (100 μM, 30 min) showed the lowest rise in the dichlorofluorescein (DCF) fluorescence signal equal to

250%. In contrast, RES had a less pronounced effect under the same conditions, whereby the fluorescence increased up to 370% [10]. Moreover, the cells pretreated with OXY were found out to increase nuclear translocation and transactivation of Nrf2 and transactivated expression of HO-1 [69]. HO-1 is an antioxidant enzyme with potent anti-inflammatory and antioxidant effects [70]. OXY showed superoxide radical scavenging effect (IC_{50} = 3.81 ± 0.5 μM) [45]. Another study found that isolated OXY exhibited IC_{50} values for antioxidant activity of 0.43 ± 0.03 mg/mL (TBARS assay) and 0.1 ± 0.01 mg/mL (DPPH assay) which were stronger than RES [7]. Human epidermal keratinocytes (HEK cells) were pretreated with OXY at concentrations of 5 and 10 μM, and OXY exhibited suppressions on UVA- or H_2O_2-induced cellular ROS production [8].

2.3.2 Anti-inflammatory activity of OXY

The inhibition of inflammatory reactions related to various diseases is helpful in the treatment and prevention of many kinds of diseases. Medicinal plants containing a large amount of OXY, especially mulberry extract, showed an excellent anti-inflammatory effect. Studies on the anti-inflammatory response using methanol extract of mulberry leaf demonstrated the inhibition in the production of NO in the LPS-induced RAW264.7 macrophage inflammation model. Furthermore, the production of inflammatory mediators such as iNOS, COX-2, and TNF-α, was shown to be inhibited in these studies. These results indicate that mulberry leaf extract containing OXY as the active ingredient exhibited an excellent anti-inflammatory effect [71]. It has also been reported that OXY isolated from *A. heterophyllus* extract of *Rhododendron japonica* reduced NO production in a concentration-dependent manner in RAW264.7 macrophage cells induced by LPS [5].

OXY can inhibit the productions of nitrite, PGE_2, and the expressions of nitric oxide synthase (iNOS) and cyclooxygenase (COX-2) through the nuclear factor-kB (NF-kB) activation pathway on LPS-induced RAW264.7 macrophage cells [3, 72]. Apart from the NF-kB signaling pathway, the anti-inflammatory effect of OXY in LPS-stimulated RAW264.7 macrophage cells has been reported as also occurring through the inhibition of the mitogen-activated protein kinase (MAPK) pathway [73].

In vivo and *in vitro* anti-inflammatory activities of OXY isolated from mulberry extract showed that nitrite accumulation was inhibited by LPS-induced RAW264.7 macrophage cells but not specifically inhibited by iNOS enzyme activity. However, Chung *et al*. [74] reported that OXY could inhibit iNOS expression in a dose-dependent manner and was observed to affect the expression rather than iNOS enzyme activity.

OXY was also found out to inhibit the nuclear translocation of NF-kB by LPS and markedly inhibited COX-2 activity. Another anti-inflammatory mechanism of OXY that has been reported is the inhibition of the MEK/ERK signaling cascade and, subsequently, the induction of anti-inflammatory responses by reducing CXC chemokine receptor type 4 (CXCR4) mediated T cell migration [42]. Experimental results on the immune response using mulberry leaf methanol extract showed that the level of immunoglobulin in the serum was increased by treatment with the extract, and the mortality rate induced by *Pasteurella multocida* infection was decreased. In addition, the effect of the carbon clearance test on the phagocytic index of the macrophage was significantly increased. The phagocytic index was considerably increased, and the protection against neutrophilia was induced by cyclophosphamide, and it has been reported to increase not only humoral immunity but also cell-mediated immunity [75].

OXY inhibited the productions of NO, PGE_2, IL-6, and granulocyte-macrophage colony-stimulating factor (GM-CSF) in LPS-induced RAW264.7 macrophage cells. It suppressed mRNA and protein expressions of iNOS, COX-2, IL-6, and GM-CSF in LPS-induced RAW264.7 macrophage cells. It also suppressed the phosphorylation of Akt and JNK and p38 MAPKs and the translocation of NF-kB p65 subunit into the nucleus. These results indicate that OXY inhibits LPS-induced inflammatory responses though the blocking of MAPK and NF-kB signaling pathway in macrophages, and suggest that OXY possesses anti-inflammatory effects [76].

The ethanol extract of *Ramulus mori* containing OXY (ERMO) decreased levels of NO and PGE_2 significantly and markedly diminished iNOS and COX-2 at both mRNA and protein levels in a dose-dependent manner. Pro-inflammatory cytokines (TNF-α and IL-6) and a chemokine (MCP-1) also decreased, both as mRNA and

protein, which indicates that ERMO has an anti-inflammatory effect in RAW 264.7 macrophage cells [4]. Recently *R. mori* ethanol extract showed anti-inflammatory action in RAW264.7 macrophage cells via blocking the leukotriene B4 receptor-2 (BLT2)-linked cascade that is involved in inflammatory bowel disease (IBD) by the generation of ROS [77]. The BLT2-linked cascade might be a possible target of the anti-inflammatory action of *R. mori* ethanol extract. These results suggest that OXY is a highly potent anti-inflammatory agent that can control inflammation through various pathways.

2.4 RAW264.7 macrophage cells

Macrophages play key roles in the host immune defense system during infection and disease development. It serves as the body's first line of defense in the body against invading pathogens and promotes cell protection and repair processes [78]. Macrophages also produce inflammatory mediators, including pro-inflammatory cytokines (TNF-α and IL-6), chemokines (IL-8 and MCP-1), and inflammatory enzymes (iNOS and COX-2) [79]. LPS is a main outer component of the Gram-negative bacterial cell wall. In addition, LPS-activated macrophage produces a variety of ROS, IL-6, NO, and PGE_2, which can promote the development of inflammation [80, 81]. Inflammation is a protective reaction of the immune system. However, uncontrolled and prolonged inflammation importantly contributes to the initiation and progression of many diseases, such as arthritis, asthma, arthrophlogosis, and so on [82]. Therefore, regulation of inflammation and maintaining proper levels of other immune responses help prevent those diseases.

RAW264.7 macrophage cells are monocyte/macrophage-like cells originating from Abelson leukemia virus-transformed cell line derived from BALB/c mice. The cells are defined as an appropriate model of macrophages. They can conduct pinocytosis and phagocytosis. Upon LPS activation, RAW264.7 macrophage cells increase NO production and enhance phagocytosis. In addition, these cells are capable of killing target cells with antibody-dependent cytotoxicity [16]. RAW264.7 macrophage cells are well accepted as a suitable macrophage model [83]. LPS is commonly used for the induction of inflammatory models because of its ability to

regulate the expression of inflammatory enzymes and the release of inflammatory mediators by activating multiple signaling pathways [84].

2.5 Pharmacokinetic of OXY

Huang et al. [85] reported a method to verify the pharmacokinetic of OXY in rat plasma using HPLC. Oxyresveratrol is the most important constituents of the traditional Chinese medicine *Smilax china*. The cumulative excretion of oxyresveratrol was 0.84% and 0.29% in urine and bile samples, respectively. The results of LC-MS/MS analysis of urine and bile samples after oral administration to rats of OXY purified from *Cheongyigea japonica* extract showed that seven metabolites were isolated, but the main metabolites were monoglucuronidated and monosulfated oxyresveratrol (Figure 7) [86]. Glucuronidation was the most common metabolic pathway of oxyresveratrol in the urine and bile of rats. On the other hand, only sulfated metabolites were isolated in bile. This conjugation seems to increase the hydrophilicity of oxyresveratrol and improve its release. Mulberroside A was biotransformed by intestinal bacteria into oxyresveratrol. Oxyresveratrol was observed to have significantly increased permeability to Caco-2 cells compared to mulberroside A [87].

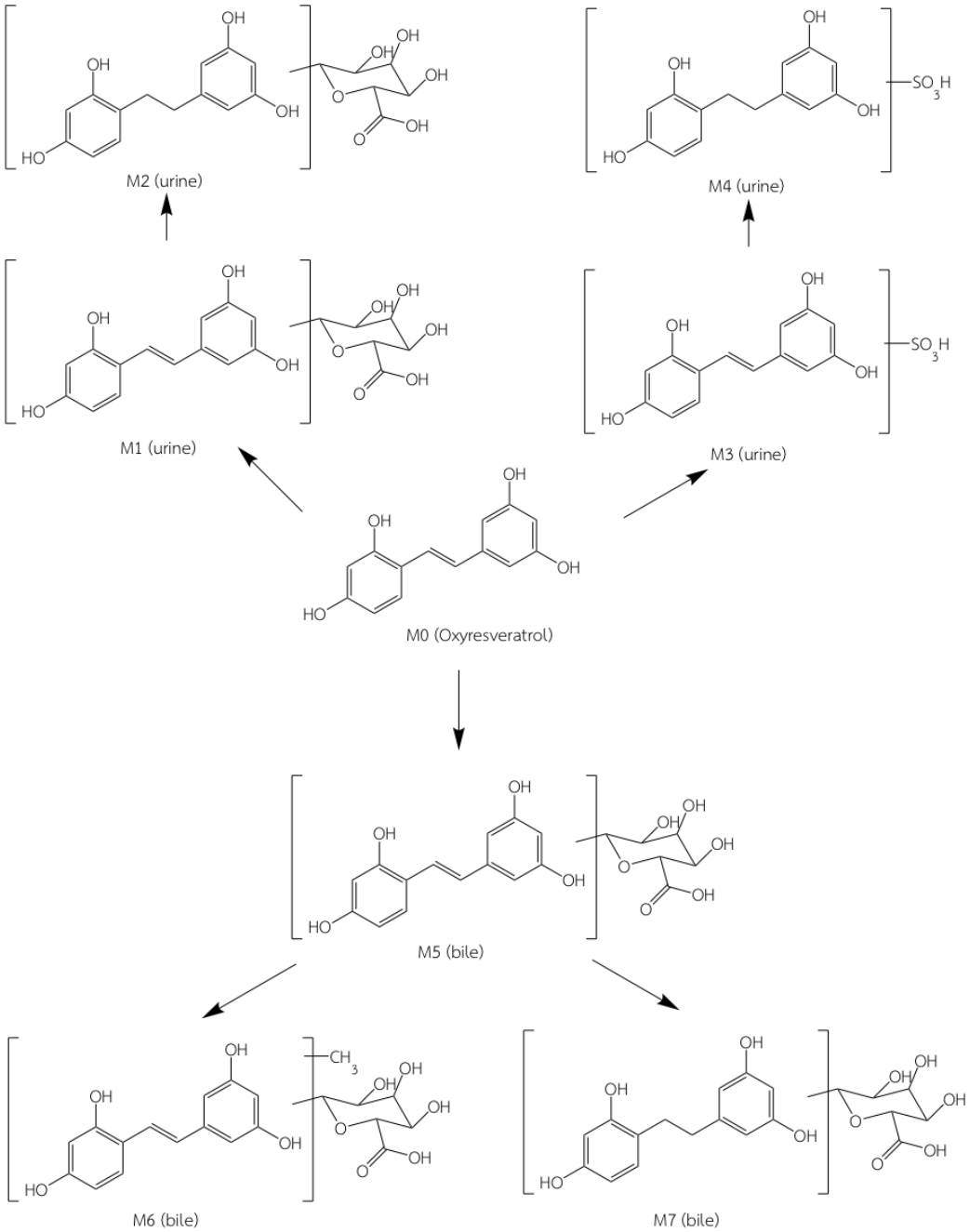

Figure 7 The metabolites pathways of oxyresveratrol in rat urine and bile sample after oral administration of 100 mg/kg oxyresveratrol (modified from [86]).

2.6 Caco-2 cells

Caco-2 cells originate from human colonic adenocarcinoma cell lines. Caco-2 monolayers are accepted as an *in vitro* model for drug transport studies as these cells have been shown to express most of the enzymatic, functional, and morphological characteristics of the intestinal mucosa [88, 89]. Caco-2 monolayers have been extensively used for years as a tool to test permeability, assess the oral absorption potential, and study the absorption mechanism of compounds [90]. Typically, 21-24 days post-confluence, fully differentiated Caco-2 cells form a monolayer with microvillus structures and many other biochemical and functional characteristics of small intestinal villus epithelium. The cell monolayers form tight junctions, express many brush border enzymes, some CYP isoenzymes, and phase II enzymes (such as glucuronidase, glutathione-S-transferases, and sulfotransferase) [91, 92]. The expression pattern of carboxylesterase (CES) in Caco-2 cell monolayer is completely different from that in the human small intestine but very similar to the human liver that expresses a much higher level of human carboxylesterase (hCES)-1 and lower level of hCE-2 [93].

In the transport experiment, Caco-2 cells are cultivated on permeable filters in which they represent the intestinal environment in that lumen is separated from the bloodstream by the intestinal epithelial monolayer (Figure 8). Transepithelial passage of molecules from the apical to the basolateral side of the monolayer can be easily measured in different experimental conditions, thus allowing discriminating factors involved in transport mechanisms. In the standard setting, pH 7.4 is applied on both sides of the monolayer. However, to mimic the mild acid condition of the small intestine or to study proton dependent transport mechanisms, an apical pH 6.5 should be used. pH 6.5 can be used in an apical compartment to represent the pH of the upper small intestine under fasted conditions. In contrast, a pH 7.4 can be used in the basolateral compartment to replicate the pH of blood in the body [91]. The integrity of Caco-2 cell monolayer can be determined by monitoring a transepithelial electrical resistance (TEER) > 500 $\Omega \cdot cm^2$ and phenol red transport < 0.1% of phenol [94].

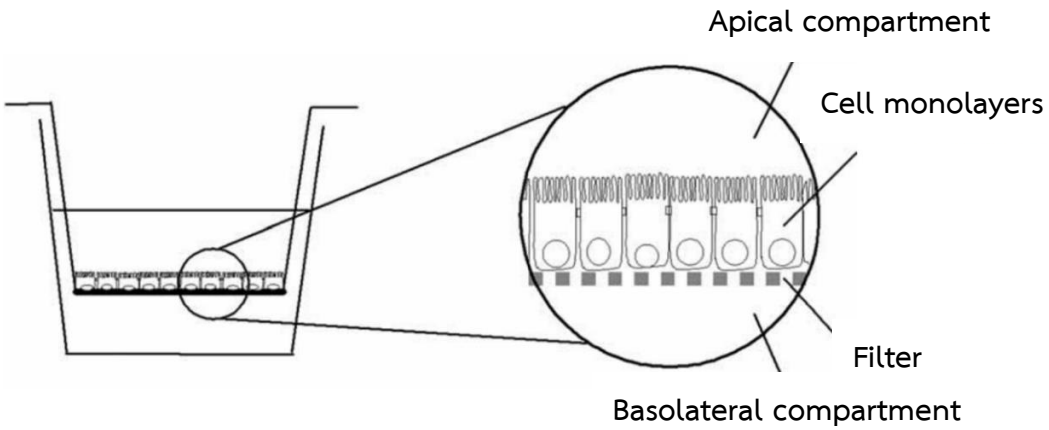

Figure 8 Diagram of the Caco-2 monolayer cultivated on permeable filter support. The test compound is placed on the apical or basolateral compartments [91].

Caco-2 monolayer experiments provide valuable information regarding (1) intestinal permeability, (2) transport mechanisms - paracellular, transcellular or active carrier, (3) role of intestinal metabolism, and (4) influence of p-glycoprotein efflux system [95]. Therefore, Caco-2 cell model experiments offer vital insight in the preliminary phase of compound discovery on intestinal permeability, transport, absorption through membranes, and overall potential bioavailability.

Passive diffusion can occur via the transcellular route (1) or the paracellular (2). Transcytosis (3) and carrier-mediated transport (4) are two additional absorptive pathways, the latter often relevant for the absorption of macromolecules. The efflux transporters in the apical membrane transport the drug in the exsorptive direction (5). A combination of these routes often defines the overall transepithelial transport rate of nutrients and drugs (Figure 9).

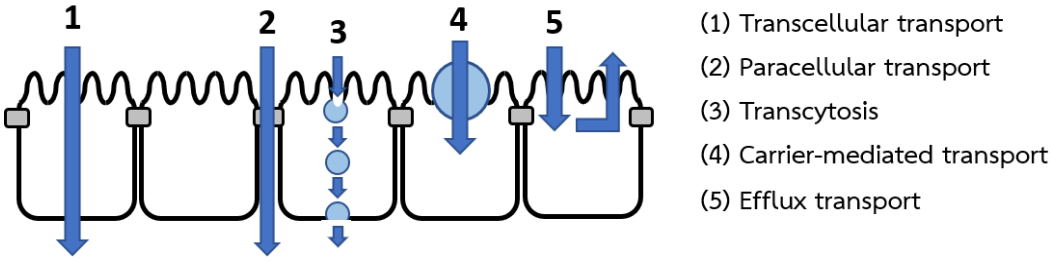

Figure 9 Pathways for drug absorption across an epithelial monolayer (modified from [95]).

2.7 Ester prodrugs

The concept of prodrug was introduced in 1958 by Adrien Albert to describe pharmacologically inactive derivatives, which then can be transformed into active metabolites *in vivo* after absorption [96]. For drug delivery, the most popular and convenient route is the oral route. The optimal physicochemical properties are well-established and include a limit on adequate lipophilicity, molecular size, and hydrogen bonding potential. These properties permit high transcellular absorption following oral administration. For drug targets, synthetic strategies can be created to balance the physicochemical properties required for high transcellular absorption and the structure-activity relationships (SAR) for the drug target. These include a requirement for polarity and groups that show high hydrogen-bonding potentials such as carboxylic acid (R-COOH) and alcohol (R-OH). In such cases, prodrug design strategies have been employed [97]**.** Prodrugs are derivatives of drugs that require only one to two chemical or enzymatic transformation steps to yield the active parent drug.

Prodrug strategies are most used to increase the permeability of compounds by masking the polar functional groups and hydrogen bonds with ester linkers to increase lipophilicity. The permeability by passive diffusion and the transporter-mediated process has been modulated by prodrug approaches. Oral delivery of ester prodrugs to the therapeutic target is confronted with many chemical, biochemical, and physiological barrier processes. In general, the highest oral bioavailability values that ester prodrugs can achieve clinically are 40-60%. This is owing to incomplete membrane permeation, P-glycoprotein (P-gp) efflux, hydrolysis in the GI lumen and intestinal cells, non-esterase metabolism in the liver, biliary excretion, and metabolism of the parent [97]. The rationale behind the prodrug design strategy is to improve oral absorption and aqueous solubility, enhance lipophilicity and active transport, and achieve site-selective delivery [97, 98] (Figure 10). Thus, the success of the prodrug approach must consider the balance of all these issues. The ideal ester prodrug should have the following properties [99]:

- No or weak activity against any pharmacological target
- High passive permeability

- Good chemical stability at physiological pHs
- Sufficient aqueous solubility
- Resistance to hydrolysis during absorption
- Hydrolyze to active (parent) drug rapidly and quantitatively after absorption
- The released promoiety has no toxicity or unwanted pharmacological effects

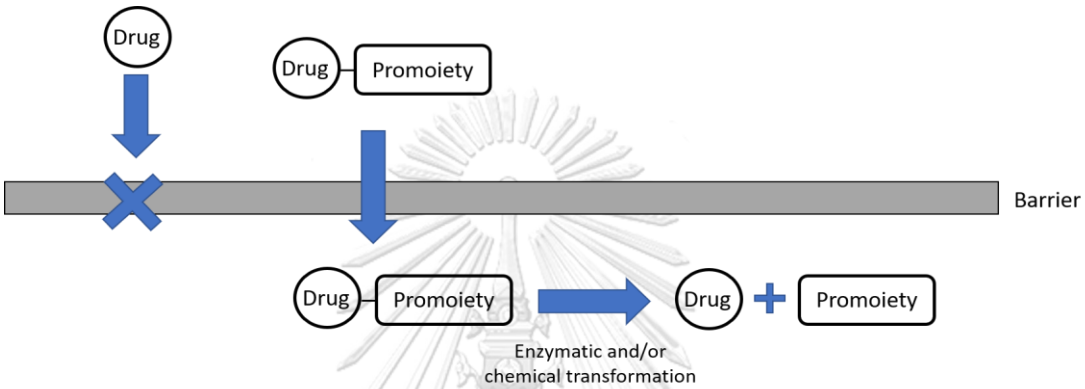

Figure 10 The concept of a prodrug (modified from [100]).

An increase in the lipophilicity of alcohols and phenols can often be achieved by preparing ester prodrugs using carboxylic acids. An ester bond is the most widely used chemical bond in linking the parent drug and the carrier. Esters are also the most common prodrugs used to improve the passive membrane permeability [97, 101]. In the body, the bond of an ester is readily hydrolyzed by esterases present in the blood, and other organs and tissues, including arylesterases, acetylcholinesterases, butyrylcholinesterases, carboxylesterases, and paraoxonases [102]. However, one significant challenge with prodrugs of an ester is the accurate prediction of pharmacokinetic disposition in humans, because of significant differences in specific carboxylesterase activities in preclinical species [103]. Beaumont *et al*. 2003 reported that ester prodrugs enhance oral absorption of predominantly poorly permeable and polar parent drugs [97]. In oral drug delivery systems, ester prodrugs are commonly used to enhance membrane permeation and transepithelial transport of drugs by increasing the lipophilicity of the parent compound, resulting in enhanced transmembrane transport by passive diffusion [101,

104]. Examples of ester prodrugs with enhanced permeability designed are listed in Table 2.

Table 2 Ester Prodrugs with improved permeability (modified from [105]).

Prodrugs	Limitations of Parent	Benefits of Prodrug
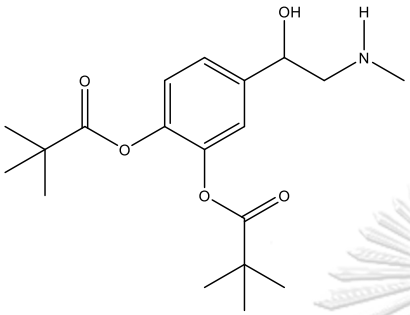 Dipivaloyl-epinephrine	log *P* = −0.04 Low corneal penetration	log *P* = 2.08 4- to 6-fold increase in corneal penetration
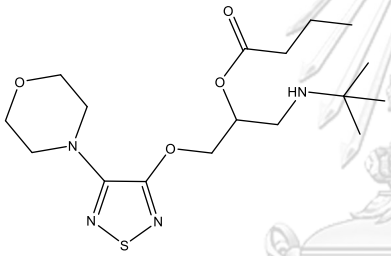 Butyryl-Timolol	Low dose oral exposure	High dose oral exposure, enable IV formulation
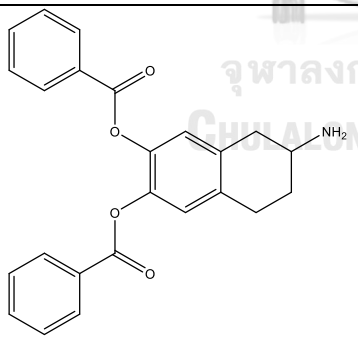 Dibenzoyl-ADTN	No central nervous system penetration	Reaches central nervous system

Recently, OXY has been attempting to improve permeability and, accordingly, the bioactivities of OXY by ester prodrugs. Chatsumpun *et al*. reported a diacetyl ester prodrug at position 3’ and 5’ of *i*-propyl-OXY (*i*-pr-OXY-DAc) with potent and selective cytotoxicity against HeLa cancer cells [106]. Tetraacetyl oxyresveratrol (OXY-TAc) was evaluated for anti-melanogenic activity and found to

be more stable than its parent OXY due to more resistance to oxidative discoloration. *In vitro*, OXY-TAc inhibited tyrosinase activity by a lesser extent than OXY, but it effectively inhibited cellular melanogenesis by reducing the melanin content of human epidermal melanocytes. These indicated the bioconversion of OXY-TAc prodrug to the parent OXY [107].

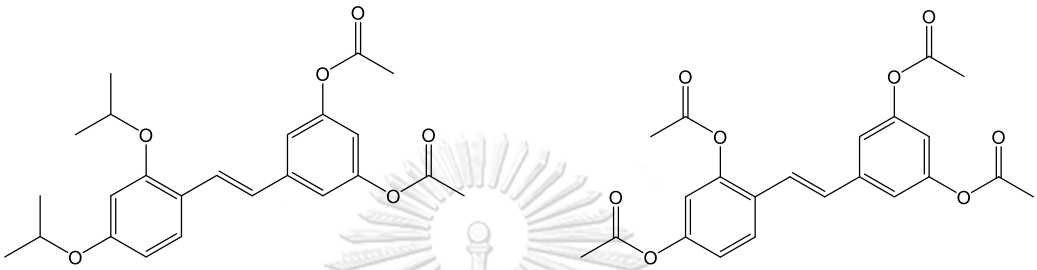

i-pr-OXY-DAc OXY-TAc.

Figure 11 Chemical structures of *i*-pr-OXY-DAc and OXY-TAc.

CHAPTER 3

RESEARCH METHODOLOGY

3.1 Cell lines, media, chemicals, and equipment

- Human colorectal adenocarcinoma; Caco-2, No. HTB37 (ATCC, Virginia, USA)
- RAW264.7 murine macrophage cell line #TIB-71) (ATCC, Maryland, USA)
- Dulbecco's Modified Eagle Medium #12800 (Gibco, Massachusetts, USA)
- Fetal bovine serum (FBS) #16000-044 (Gibco, Massachusetts, USA)
- L-Glutamine 200 mM (100x) #25030-081) (Gibco, Massachusetts, USA)
- Nonessential amino acids #11140-050 (Gibco, Massachusetts, USA)
- Penicillin-Streptomycin #15140-122 (Gibco, Massachusetts, USA)
- Sodium bicarbonate ($NaHCO_3$) (Gibco, Massachusetts, USA)
- Bicinchoninic Acid (BCA) Protein Assay Reagent A #23223 (Thermo Scientific, Rockford, USA)
- Bovine serum albumin (Sigma-Aldrich, Missouri, USA)
- 30% Acrylamide/Bis solution 29:1 #1610156 (Bio-Rad, California, USA)
- Trizma® base (Sigma-Aldrich, Missouri, USA)
- Glycine (Bio-Rad, California, USA)
- N-(1-naphthyl) ethylenediamine dihydrochloride (NED) (Sigma-Aldrich, Missouri, USA)
- Sulfanilamide (Sigma-Aldrich, Missouri, USA)
- Ammonium persulfate (Sigma-Aldrich, Missouri, USA)
- TEMED (Merck Millipore, Darmstadt, Germany)
- Blocking Powder (Bio-Rad, California, USA)
- 2,4,6-tri(2-pyridyl)-1,3,5-triazine (Sigma-Aldrich, Missouri, USA)
- Mouse IL-6 ELISA kit #431301 (Biolegend, California, USA)
- RIPA lysis buffer (Cell Signaling Technology, Boston, Massachusetts, USA)

- proteinase inhibitor (Roche Applied Science, Mannheim, Germany)
- phosphatase inhibitor (Roche Applied Science, Mannheim, Germany)
- β-actin Rabbit mAb (HRP Conjugate) #5125, (Cell Signaling, Massachusetts, USA)
- COX-2 Rabbit mAb #12282 (Cell Signaling, Massachusetts, USA)
- iNOS Rabbit mAb # 13120 (Cell Signaling, Massachusetts, USA)
- Anti-rabbit IgG HRP-linked Ab #7074 (Cell Signaling, Massachusetts, USA)
- Trans-well insert 6 well plates (Greiner Bio-one, St. Gallen, Switzerland)
- 37% Hydrochloric acid (Merck Millipore, Darmstadt, Germany)
- Sodium chloride (NaCl) (Sigma-Aldrich, Missouri, USA)
- Sodium hydroxide (Merck Millipore, Darmstadt, Germany)
- Western Blotting Reagent (Merck Millipore, Darmstadt, Germany)
- Nitrocellulose membranes (GE Healthcare Life Sciences, Buckinghamshire, UK)
- SuperSignal solution (Endogen Inc, Rockford, Illinois, USA)
- Laminar flow hood, Model: BV-126 (Thermo Scientific, Massachusetts, USA)
- CO_2 Incubator for cell culture (Thermo Scientific, Massachusetts, USA)
- Mini-PROTEAN® Tetra Cell, Mini Trans-Blot® Module, and PowerPac™ HC Power Supply #1658035 (Bio-Rad, California, USA)
- Vortex mixer, Model: Vortex-Genie 2 (Scientific Industries, New York, USA)
- pH meter, Model: SevenEasy™ (METTLER TOLEDO, Novate Milanese, Italy)
- Centrifuge #1706-01 Rotina 380R Benchtop (Hettich instrument, Massachusetts, USA)
- Nikon TMS Inverted Microscope (Nikon, Tokyo, Japan)
- Microplate reader (CLARIOstar, BMG LABTECH, Germany).
- 6, 24 and 96 well plates for cell culture (Corning, New York, USA)
- 75 T-flask for cell culture (Corning, New York, USA)

3.2 Methodology

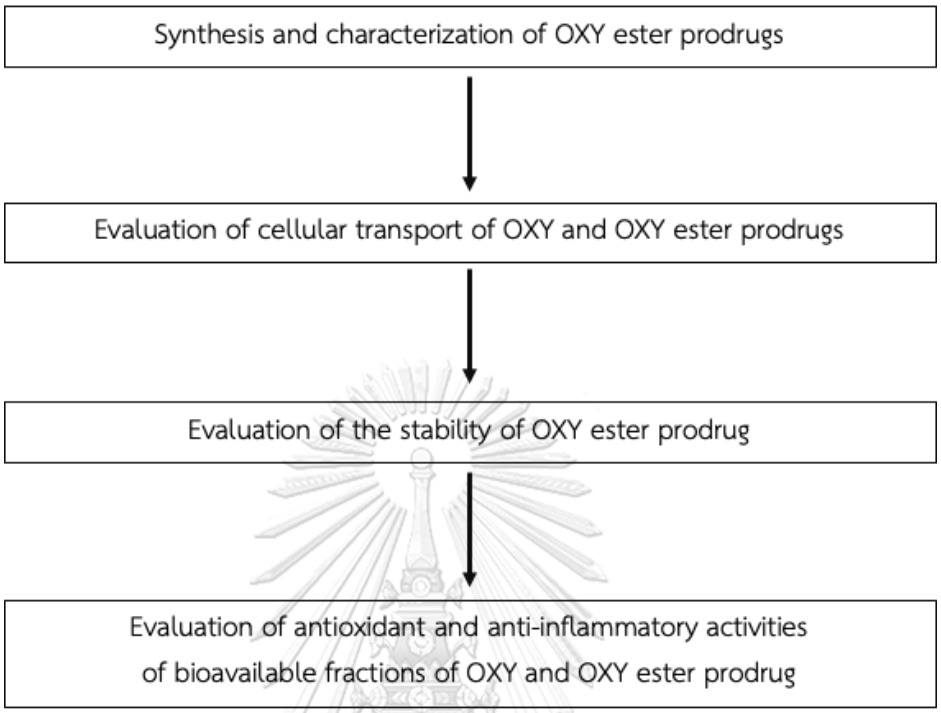

3.2.1 Synthesis of OXY ester prodrugs

Oxyresveratrol tetraacetate (OXY-TAc). OXY-TAc was synthesized by a slight modification of previously reported procedures [107]. OXY (1.0 g, 4.0 mmol) was dissolved in a mixture of pyridine (4 mL) and acetic anhydride (1.6 mL, 16.8 mmol, 4.2 eq) at room temperature and the reaction mixture was stirred under N_2 atmosphere for 24 h. Then, the mixture was quenched with saturated $NaHCO_3$ and extracted with ethyl acetate (3x10mL). The pooled ethyl acetate layer was washed with water and brine, dried over Na_2SO_4, filtered and concentrated under high vacuum to obtain the product. OXY-TAc was purified by flash chromatography on silica gel and eluted with 50% acetone in hexane. Evaporation of the solvent afforded the product.

Oxyresveratrol tetrapropionate (OXY-TPr). OXY-TPr was synthesized by a slight modification of previously reported procedures [107]. OXY (1.0 g, 4.0 mmol, 4.2 eq) was dissolved in a mixture of pyridine (4 mL) and propionic anhydride (2.1 mL, 16.8 mmol) at room temperature, and the reaction mixture was stirred

under N_2 atmosphere for 24 h. Then, the mixture was quenched with saturated $NaHCO_3$ and extracted with ethyl acetate (3x10mL). The pooled ethyl acetate layer was washed with water and brine, dried over Na_2SO_4, filtered, and concentrated under high vacuum to obtain the product. OXY-TPr was purified by flash chromatography on silica gel and eluted with 50% acetone in hexane. Evaporation of the solvent afforded the product.

Oxyresveratrol tetrabutyrate (OXY-TBu). OXY-TBu was synthesized by a slight modification of previously reported procedures [107]. OXY (1.0 g, 4.0 mmol) was dissolved in a mixture of pyridine (4 mL) and butyric anhydride (2.6 mL, 16.8 mmol, 4.2 eq) at room temperature, and the reaction mixture was stirred under N_2 atmosphere for 24 h. Then, the mixture was quenched with saturated $NaHCO_3$ and extracted with ethyl acetate (3x10mL). The pooled ethyl acetate layer was washed with water and brine, dried over Na_2SO_4, filtered, and concentrated under high vacuum to obtain the product. OXY-TBu was purified by flash chromatography on silica gel and eluted with 50% acetone in hexane. Evaporation of the solvent afforded the product.

3.2.2 Characterization of OXY ester prodrugs

^1H and ^{13}C NMR spectra were recorded on the Bruker NMR spectrometer, operating at 300 MHz for ^1H and 75 MHz for ^{13}C (Bruker Company, Fällanden, Switzerland). Mass spectra were measured by high-resolution electrospray ionization mass spectra (HR-ESI-MS) (Bruker Company, MA, USA).

3.2.3 The cytotoxic effect of OXY and OXY ester prodrugs on Caco-2 cells

Each of the OXY ester prodrugs was primarily screened for their antioxidant and anti-inflammatory activities with a bioavailable fraction (transported fraction of ester prodrug across Caco-2 monolayers). The ester prodrug with the highest cellular transport across Caco-2 monolayers was studied for stability and biological activities.

Caco-2 cells (human colon carcinoma cell line) can differentiate into monolayers that can simulate the structure and function to become human

intestinal-like epithelium *in vitro*. Therefore, Caco-2 cell monolayers have been widely used as a model to study *in vitro* intestinal absorption of drugs and nutrients [108, 109]. Evaluation of the transport of the OXY ester prodrugs was performed using Caco-2 cells (ATCC No. HTB37). The Caco-2 cells were cultured with complete medium containing 10% (v/v) heat-inactivated fetal bovine serum (FBS), 1% (v/v) nonessential amino acids, 1% (v/v) L-glutamine, 1% (v/v) penicillin-streptomycin (antibiotic), 0.2% (v/v) fungizone (antifungal) and serum-free media (DMEM).

The MTT (3-[4,5-dimethylthiazole-2-yl]-2,5-diphenyltetrazolium bromide) assay has been used to evaluate cell viability. The principle of the measurement is the viable cells, which survive exposure to compounds. These substances can induce apoptosis or necrosis. So, the assay is called the cytotoxicity assay. The viable cells can transform a yellow and water-soluble salt (MTT) to a purple and insoluble formazan crystal (Figure 12). The transformation of MTT to formazan was reduced by mitochondrial succinate dehydrogenase from viable cells [110].

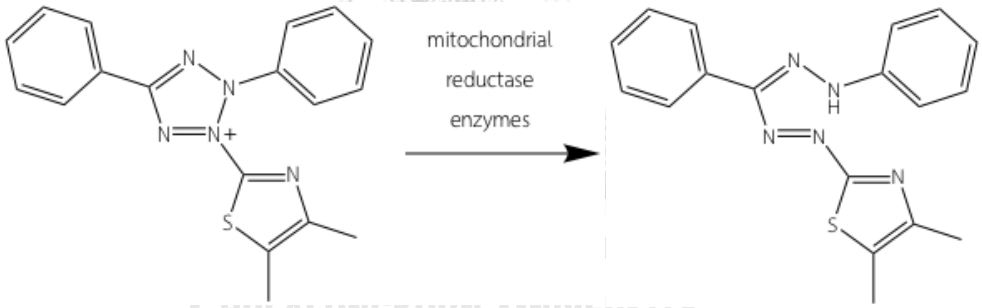

Figure 12 MTT assay. MTT was reduced in live cells by mitochondrial reductase results in the formation of insoluble formazan.

The Caco-2 cells were seeded in 96-well plates at a density of 1×10^4 cells/well in 200 µL complete medium and incubated in an atmosphere with 5% CO_2 and 95% relative humidity for 24 h at 37 °C. The cells were washed with DMEM after the medium was removed. The cells were treated with different concentrations (1, 10, 25, 50, and 100 µM) of OXY or OXY ester prodrug for 24 h. The cells treated with 0.5% DMSO were used as a control group. After treatment, 20 µL of MTT solution

(5 mg/mL) was added to each well and incubated in an atmosphere with 5% CO_2 and 95% relative humidity for 4 h at 37 °C. The medium was removed, and DMSO (200 µL) was added to dissolve the formazan crystals. The absorbance of formazan was measured at 540 nm by a microplate reader (SPECTROstar, BMG LABTECH, Germany). Four replicates of each experiment were performed. The following equation calculated the percent of cytotoxicity:

$$\%\text{Cell viability} = \frac{\text{Absorbance}_{\text{sample}}}{\text{Absorbance}_{\text{control}}} \text{x} 100$$

The concentrations of OXY and OXY ester prodrug that produced cell viability that was not significantly different from the control were chosen for further evaluation of cellular transport.

3.2.4 Cellular transport of OXY and OXY ester prodrugs

For the cellular transport experiment, Caco-2 cells from passage number 25-35 were seeded at a density of 4×10^4 cells/well in trans-well inserts of 6-well plates (diameter 24 mm, pore size 0.4 µm; ThinCerts™-TC Einsatze, Greiner Bio-One, Switzerland). The cells were cultured with 2 mL of DMEM supplemented with 15% FBS in both the apical and basolateral compartments at 37 °C in an atmosphere with 5% CO_2 and 95% relative humidity. The complete medium is changed every other day. After confluency, the serum content of the complete medium was switched from 15% FBS to 7.5% FBS. The experiments were performed 21-24 days after cells reached the confluence. The monolayer with a transepithelial electrical resistance (TEER) > 500 Ω·cm^2 and phenol red transport < 0.1% of phenol were considered suitable for use [94]. The monolayers were washed with the serum-free medium before the addition of 2 mL of serum-free medium pH 6.8 containing 0.5% DMSO, OXY, or OXY ester prodrug. The basolateral compartment was filled with 2 mL of phenol-red free and serum-free medium pH 7.4. The medium in the basolateral compartment after the sample treatment were collected at 15, 30, 60, 120, and 240 min. The experiments were performed in 4 replicates. The samples were blanketed with nitrogen gas and stored at -80°C for further experiments. The

apparent permeability coefficients (Papp, cm/s) of OXY and OXY ester prodrug were calculated according to the following equation:

$$P_{app} = \frac{dQ}{dt} \times \frac{V}{A \times C_0}$$

where dQ/dt is the permeability rate (μM/s), V is the volume of the basolateral chamber (2 cm^3), A is the surface area of the insert (4.524 cm^2), and C_0 is the initial concentration (μM) of the samples. The percent of transport was calculated according to the following equation:

$$\%\text{Transport} = \frac{\text{Concentration of transported compound}}{\text{Concentration of loaded compound}} x100$$

3.2.5 Extraction of OXY and OXY-TAc from bioavailable fractions for HPLC analysis

Briefly, 2 mL of each sample from the cellular transport experiment was transferred to a 15-mL centrifuge tube and mixed with an equal volume of 0.1 M potassium phosphate buffer (pH 7.1) containing 100 U of ß-glucuronidase and 0.1 U of sulfatase. The mixture was then lightly vortexed and was placed in a shaking water bath at 37 °C and incubated for 3h. After that, 1 mL of 1% sodium dodecyl sulfate (SDS) in ethanol was added to the mixture and subsequently vortexed for 1 min. A mixture was extracted twice with ethyl acetate at a ratio of 1:1, and then sonicated for 10 min, vortexed for 2 min and centrifuged (ROTINA 380 R, Germany) at 4000 × g for 10 min. The ethyl acetate layer was combined into a 10-mL vial. The combined layers were blow-dried with nitrogen gas and reconstituted the residue with a mobile phase prior to HPLC analysis. The HPLC analysis was performed using the Agilent 1290 UHPLC series (Agilent Technologies, CA, USA).

3.2.6 HPLC system and chromatographic condition

The HPLC analysis was performed using the Agilent 1290 Infinity II UHPLC system (Agilent Technologies, Palo Alto, CA, U.S.A.), equipped with an auto-sampler, a binary pump, a Multicolumn Thermostat, and a diode array detector (DAD) detector. A HALO C18 column (4.6 × 100 mm, 5 μm) was used for separation. The

mobile phases consisted of 0.1% formic acid as mobile phase A and methanol as mobile phase B. The gradient sequence was as follows: 40-46% B from 0 to 5 min, 46–48% B from 5 to 10 min, 48–48% B from 10 to 17 min, 48-52% B from 17 to 18 min, and 52–52% B from 18 to 23 min at a flow rate of 1 mL/min. Before use, the mobile phase was filtered and degassed. The injection volumes were 5 µL of the samples. The column and autosampler tray were maintained at 25 °C. The detection of OXY and OXY-TAc was monitored at 320 nm.

3.2.7 The stability of OXY-TAc in buffer solutions

The chemical stability of OXY ester prodrugs was carried out in HCl buffer pH 1.2, acetate buffer pH 4.5, phosphate buffer pH 6.8, and phosphate buffer pH 7.4, which mimic the pH of several biological fluids in the body. All buffer solutions were prepared as per USP [111]. Stock solutions of OXY ester prodrug were prepared in DMSO. The stability of the prodrug was initiated by adding 20 µL of OXY ester prodrug into 980 µL of buffer solutions to obtain a final concentration of 50 µM. The reactions were incubated at 37 °C. The amount of OXY ester prodrug was determined at 0, 0.5, 1, 2, 4, 8, 12, 18, and 24 h using an HPLC method. Experiments were performed in triplicate.

The apparent pseudo-first-order degradation rate constants of the test compounds were determined by plotting the natural logarithm of test compound concentration as a function of time. The slope of the plot is equal to the negative rate constant (k, min^{-1}). The degradation half-lives ($t_{1/2}$, min) were calculated by the equation:

$$t_{1/2} = 0.6932/k$$

3.2.8 The stability of OXY-TAc in simulated gastric fluid and simulated intestinal fluid

The simulated gastric and intestinal fluids were prepared according to USP specification [111] and performed using the previously studied [112]. For simulated gastric fluid (SGF), 2 g of sodium chloride and 3.2 g of pepsin (from porcine stomach mucosa) was dissolved in 7 mL of 0.2 N hydrochloric acid and a sufficient volume of water to make 1000 mL. The pH of SGF was adjusted to 1.2. For simulated intestinal fluid (SIF), 6.8 g of monobasic potassium phosphate was dissolved in 250 mL of water. To this, 77 mL of 0.2 N sodium hydroxide and 500 mL of water was added and mixed along with 10 g pancreatin (from the porcine pancreas). The SIF solution was adjusted to pH 6.8 ± 0.1 with either 0.2 N of sodium hydroxide or 0.2 N of hydrochloric acid and then diluted with water to 1000 mL.

The reactions were initiated by adding an appropriate amount of stock solutions of OXY ester prodrug into SGF and SIF to obtain a final concentration of 50 μM. The solutions were pipetted into glass tubes and placed in a 37 ^{o}C shaking water bath. The amount of OXY ester prodrug was determined at 5, 15, 30, 45, 60, 90, and 120 min for the gastric stability experiment and at 15, 30, 60, 120, 180, and 240 min for the intestinal stability experiment. Experiments were performed in triplicate. The amount of OXY ester prodrugs was determined at appropriate time intervals using an HPLC method.

The apparent pseudo-first-order degradation rate constants of the test compounds were determined by plotting the natural logarithm of test compound concentration as a function of time. The slope of the plot is equal to the negative rate constant (k, min^{-1}). The degradation half-lives ($t_{1/2}$, min) were calculated by the equation:

$$t_{1/2} = 0.6932/k$$

3.2.9 The stability of OXY-TAc in human plasma

The hydrolysis of OXY-TAc was investigated in human plasma (Innovative Research, MI, USA). Human blank plasma was pre-incubated at 37 °C for 10 min. The reaction was initiated by the addition of a stock solution of OXY-TAc into the pre-incubated plasma to obtain a final concentration at 50 μM. The sample was withdrawn at a different time. The reaction was quenched by mixing a 50 μL of the plasma sample at a different time with a 200 μL of acetonitrile containing 0.5 μM of resveratrol (RES; an internal standard). Subsequently, the samples were centrifuged at 4,000 rpm at 4 °C for 5 min. Then, the clear supernatants were transferred to HPLC vials and subjected to HPLC analysis. Experiments were performed in triplicates.

The apparent pseudo-first-order degradation rate constants of the test compounds were determined by plotting the natural logarithm of test compound concentration as a function of time. The slope of the plot is equal to the negative rate constant (k, min^{-1}). The degradation half-lives ($t_{1/2}$, min) were calculated by the equation:

$$t_{1/2} = 0.6932/k$$

3.2.10 Preparation of BF-OXY and BF-OXY-TAc for evaluation of antioxidant and anti-inflammatory activities

Caco-2 cells from passage number 25-35 were seeded at a density of 4×10^4 cells/well in trans-well inserts of 6-well plates (diameter 24 mm, pore size 0.4 μm; ThinCerts™-TC Einsatze, Greiner Bio-One, Switzerland). The cells were cultured with 2 mL of DMEM supplemented with 15% FBS in both the apical and basolateral compartments at 37 °C in an atmosphere with 5% CO_2 and 95% relative humidity. The complete medium is changed every other day. After confluency, the serum content of the complete medium was switched from 15% FBS to 7.5% FBS. The experiments were performed 21-24 days after cells reached the confluence. The monolayer with a TEER > 500 $\Omega\cdot cm^2$ and phenol red transport < 0.1% of phenol were considered suitable for use. The monolayers were washed with the serum-free medium before the addition of 2 mL of serum-free medium containing 0.5% DMSO,

OXY, or OXY ester prodrug. The basolateral compartment was filled with 2 mL of phenol-red free and serum-free medium. The medium in the basolateral compartment after the sample treatment was collected at 4 h. The experiments were performed in 4 replicates. The samples were blanketed with nitrogen gas and stored at -80℃ for the evaluation of antioxidant and anti-inflammatory activities.

3.2.11 Antioxidant activity of BF-OXY and BF-OXY-TAc

3.2.11.1 DPPH assay

The DPPH assay was carried out with some modification, according to Lu *et al*. [113]. The radical scavenging activity of the sample was determined using the stable free radical DPPH. The deep purple solution is scavenged by the antioxidants in the sample and turns to yellow.

The color changes from violet to yellow is proportional to the radical scavenging activity (RSA). A diluted sample at 50 µg/mL (22 µL) was added to wells in a 96-well plate followed by 200 µL of 150 µM DPPH in methanol. The plate was covered and left at room temperature in the dark for 30 min. Trolox (6-hydroxy-2,5,7,8-tetramethylchromane-2-carboxylic acid) is a vitamin E analogue and a known antioxidant. It was used as a standard [114]. Experiments were performed in triplicate. The solution was monitored at 517 nm using a microplate reader (CLARIOstar, Germany). The percent of radical scavenging activity (%RSA) was calculated using the following equation:

$$\%\ RSA = \frac{Absorbance_{sample} - Absorbance_{blank}}{Absorbance_{control}} x100$$

3.2.11.2 FRAP assay

The FRAP assay relies on the reduction by the antioxidants of the complex ferric ion-TPTZ (2,4,6-tri(2-pyridyl)-1,3,5-triazine). The binding of Fe^{2+} to the ligand creates a very intense navy-blue color. Trolox [115] was used as a reference. FRAP assay was carried out essentially as previously described [116] with slight modifications. In short, the FRAP reagent contains acetate buffer (300 mM, pH 3.6), ferric solutions (20mM $FeCl_3.6H_2O$), and TPTZ solution (10 mM) in 40 mM HCl at a

proportion of 84:8:8. An aqueous sample of 2 µL at various concentrations and 198 µL of FRAP reagent was mixed, and absorbance of 595 nm was recorded. Trolox was also tested as a standard antioxidant compound. Experiments were performed an in triplicate. The final results were shown as micromole Trolox equivalents per milliliter of a sample (µmol TE/mL). FRAP values were calculated using the following equation:

$$\text{FRAP values} = \frac{(A_{blank} - A_{sample})}{A_{blank}(in\ \mu mol\ Trolox\ equivalents(TE)mL^{-1})}$$

3.2.11.3 ORAC assay

The ORAC assay is one method that measures the antioxidant capacity of a substance. The ORAC method measures a fluorescent signal from a probe that is quenched in the presence of ROS. The presence of antioxidants, such as Trolox, antioxidants absorbs the generated ROS, allowing the fluorescent signal to against.

The ORAC assay was carried out and modified according to previous studies [117, 118]. The procedure uses a microplate reader (CLARIOstar, Germany) with black 96-well plates. The experiment was conducted at 37 °C under pH 7.4 conditions with a blank sample in parallel. The reaction was performed by thermal decomposition of 2,2′-azobis(2-amidino-propane)dihydrochloride (AAPH) in a 75 mM phosphate buffer pH 7.4 due to the sensitivity of FL to pH at 37 °C. Trolox is used as a standard antioxidant [114]. Fluorescein (FL) was used as the substrate. Peroxyl radical (ROO•) was generated using AAPH. The reacting mixture contained the sample (25 µL) or Trolox (25 µL), fluorescein in buffer pH 7.4 (150 µL) and AAPH (25 µL), while the blank was reacting mixture without sample or Trolox. Experiments were performed in triplicate. The analyzer had recorded the fluorescence of FL every minute after the addition of AAPH at the excitation and emission wavelengths of 485 and 530 nm, respectively. All fluorescent measurements are expressed relative to the initial reading. The final results were calculated using the differences of areas under the FL decay curves between the blank and a sample and were showed as

micromole Trolox equivalent per milliliter of a sample (μmol TE/mL). ORAC values were calculated using the following equation:

$$\text{ORAC values} = \frac{(A_{blank} - A_{sample})}{A_{blank}(in\ \mu mol\ Trolox\ equivalents(TE)mL^{-1})}$$

3.2.11.4 Intracellular ROS production of in LPS-stimulated RAW264.7

Intracellular ROS levels were evaluated by monitoring fluorescent signals generated from oxidized 2',7'-dichlorodihydrofluorescein diacetate (DCFH-DA) (Sigma, USA). Non-fluorescent DCFH-DA diffused into cells and was deacetylated by cellular esterase to form DCFH, which can be rapidly oxidized to the fluorescent DCF by cellular ROS (Figure 13) [119].

RAW264.7 (ATCC TIB-71) murine macrophage cell line was purchased from ATCC (Bethesda, MD, USA). The cells were grown in DMEM complemented by 10% heat-inactivated FBS, penicillin, and 100 μg/mL streptomycin at 37 °C in an atmosphere with 5% CO_2 and 95% relative humidity. RAW264.7 macrophage cells were seeded in 96-well black plates at 1 × 10^4 cells/well and in an atmosphere with 5% CO_2 and 95% relative humidity at 37 °C for 24 h. The cells were washed with phenol-red free and serum-free medium and pretreated with BF-OXY, BF-OXY-TAc, or 100 M Vitamin C (Vc) for 1 h. Then, the cells were induced with or without LPS (1 μg/mL) for 24 h. The cells were washed and added with 5 μM of DCFH-DA in a serum-free medium for 30 min. Cells were washed with PBS and added 200 μL of cold PBS. The fluorescent signal (the excitation wavelength at 485 nm and emission wavelength at 530 nm) in the supernatant was measured using a microplate reader (CLARIOstar, Germany).

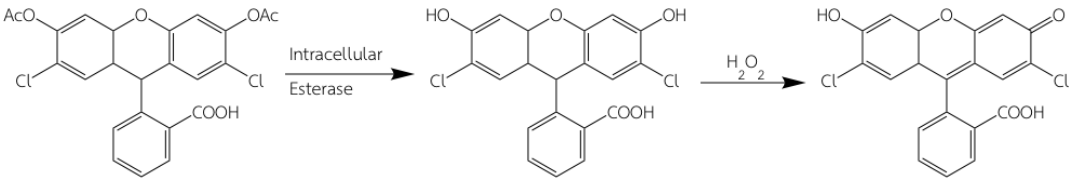

DCFH-DA (non-fluorescent) DCFH (non-fluorescent) DCF (fluorescent)

Figure 13 Detection of ROS level with DCFH-DA.

3.2.12 The cytotoxic effect on RAW264.7 macrophage cells

RAW264.7 macrophage cells were plated into 96-well plates at a density of $1x10^4$ cells/200 µL complete medium/well and incubated at 37 °C in a humidified atmosphere (95% air, 5% CO_2) for 24 h. The cells were washed with serum-free media. Two hundred microliters (200 µL) of the bioavailable fraction was added to each well. The cells were cultured at 37 °C in a humidified atmosphere (95% air, 5% CO_2) for 24 h. Then, MTT solution (5 mg/mL in PBS) was added to each well and incubated as above for 4 h. The culture media was removed before adding DMSO (200 µL) to ensure cell lysis and dissolving of formazan crystals. The absorbance of formazan was then measured at 540 nm. Experiments were performed in four replicates. The following equation calculated the percent of cytotoxicity

$$\%\ \text{Cell viability} = \frac{\text{Absorbance}_{\text{sample}}}{\text{Absorbance}_{\text{control}}} \text{x} 100$$

3.2.13 Anti-inflammatory effect of BF-OXY and BF-OXY-TAc

The RAW264.7 macrophage cells were seeded in 6-well plates at a density of 1.0×10^6 cells/well in the complete medium (DMEM contained 10% (v/v) heat-inactivated fetal bovine serum and 1% (v/v) penicillin-streptomycin) and incubated at 37 °C in a humidified atmosphere containing 5% CO_2 and 95% air for 24 h. After the medium was removed, the cells were washed with phenol-red free and serum-free medium and pretreated with BF-OXY, BF-OXY-TAc, or 100 µM indomethacin (Indo; positive control) for 1 h. Then, the cells were induced with or without LPS (1 µg/mL) for 24 h. The untreated cells were used as a control group.

The culture medium was collected for determination of NO and IL-6. The cells were evaluated for viability and protein production by MTT assay and Western blot analysis, respectively.

3.2.13.1 The production of NO in LPS-stimulated RAW264.7 macrophage cells

The production of NO on LPS-stimulated RAW264.7 macrophage cells was evaluated by measuring the nitrite concentration in the medium using the Griess reagent as previously described with some modifications (Figure 14) [120]. Briefly, 100 µL of BF-OXY or BF-OXY-TAc were incubated with 50 µL of 0.1% N-(1-naphthyl) ethylenediamine dihydrochloride (NED) and 50 µL of 1% sulfanilamide in 5% phosphoric acid at room temperature. The sample was measured at 520 nm using the microplate reader (CLARIOstar, Germany). Nitrite concentration was calculated by comparison with absorbance 520 nm of standard solutions of sodium nitrite prepared in serum-free medium.

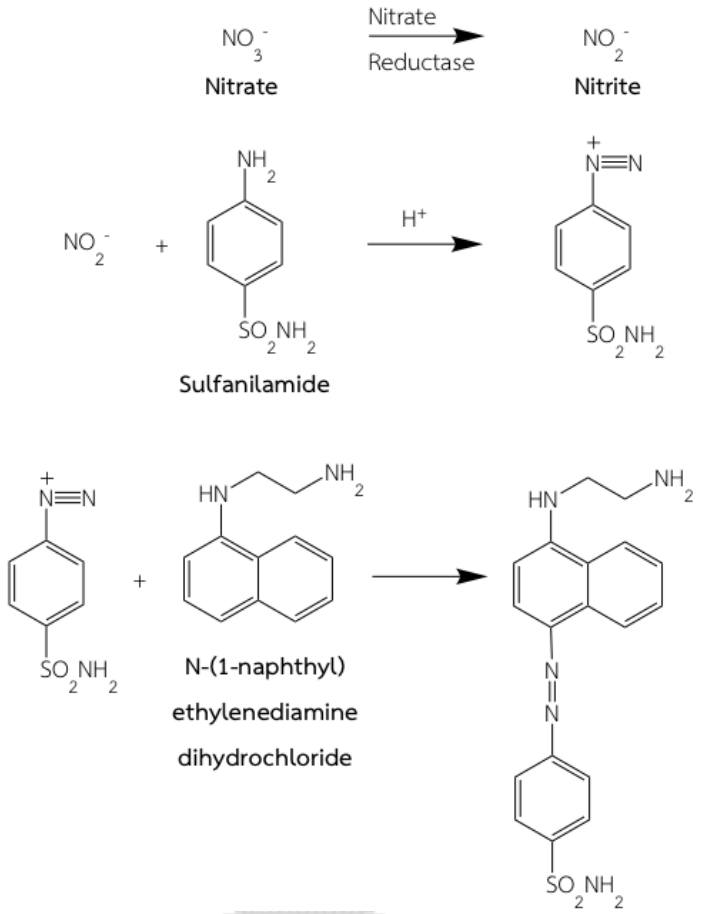

Figure 14 Nitric oxide determination by Griess assay.

3.2.13.2 The production of IL-6 in LPS-stimulated RAW264.7 macrophage cells

IL-6 produced by LPS-induced RAW264.7 macrophage cells was determined by a quantitative "sandwich" ELISA using paired antibodies purchased from Peprotech Inc (Rocky Hill, NJ, USA) as previously described. In brief, capture antibodies for IL-6 were coated in 96-well plates (NUNC, Denmark). After overnight incubation at 25°C, plates were blocked by incubation with 1% bovine serum albumin (BSA) in phosphate-buffered saline for 1 h. Culture medium or various concentrations of recombinant mouse IL-6 protein was incubated at 25°C for 2 h before adding biotinylated detecting antibodies to the wells. After 1 h at 25°C, the immune complex was detected by reacting with a streptavidin-horseradish-HRP-tetramethylbenzidine detection system (Endogen Inc., Rockford, IL, USA). Reactions were terminated by the addition of 2M H_2SO_4, and the absorbance was determined

at 450 nm using a microplate reader (CLARIOstar, German). Experiments were performed in triplicate. Concentrations of IL-6 in samples was calculated by comparing absorbance with the standard curve.

3.2.13.3 The expression of iNOS and COX-2 in LPS-stimulated RAW264.7 macrophage cells

The effect of BF-OXY and BF-OXY-TAc on iNOS and COX-2 expressions were determined by western blot analysis. RAW264.7 macrophage cells with passage number 5-15 were used. Cells were seeded in 6-well plates at a density of 1.0×10^6 cells/well in the complete medium (DMEM) containing 10% (v/v) heat-inactivated fetal bovine serum and 1% (v/v) penicillin-streptomycin. Then, the plate was incubated at 37 °C in a humidified air atmosphere containing 5% CO_2 for 24 h. The medium was removed, and the cells were washed with phenol-red free and serum-free medium and pretreated with BF-OXY, BF-OXY-TAc, or 100 μM indomethacin (Indo; positive control) for 1 h. Then, the cells were induced with or without LPS (1 μg/mL) for 24 h. The cells that were not treated with BF and not activated with LPS were used as the control group.

RAW264.7 macrophage cells in 6-well plates were collected after being pretreated with BF-OXY or BF-OXY-TAc for 1 h and induced with or without LPS (1 μg/mL) for 24 h. RIPA lysis buffer (Cell Signaling Technology, Boston, Massachusetts USA) was supplemented with a proteinase inhibitor (Roche Applied Science, Mannheim, Germany) and a phosphatase inhibitor (Roche Applied Science, Mannheim, Germany). Then the buffer was used to lyse the cells to collect the protein. The protein concentration was determined by BCA protein assay. Equal amounts (40 μg) of the protein samples were separated on 8% sodium dodecyl sulfate-polyacrylamide gel electrophoresis and transferred into a nitrocellulose membrane (GE Healthcare Life Sciences, Buckinghamshire, UK). The membrane was blocked with 5% nonfat dry milk in TBST (20 mM Tris-HCl, 140 mM NaCl, 0.1% (v/v) Tween-20) and incubated with primary antibody (iNOS and COX-2) in TBST containing 5% BSA at 4 °C overnight. After that, the membrane was washed with TBST and

incubated with the appropriate HRP-conjugated anti-rabbit IgG secondary antibody at room temperature for 2 h. All antibodies were purchased from Cell Signaling Technology (Massachusetts, USA). Then, the membrane was reacted with a SuperSignal solution (Endogen Inc, Rockford, IL, USA) for 2 min and detected with the ECL-Western blot system (Amersham Pharmacia, Braunschweig, Germany). The membrane was then stripped off the bound antibody and reprobed with anti-ß actin to confirm the equal loading of protein. The density of target bands was quantified by the Image J software (National Institutes of Health, Bethesda, MD, USA). The results were expressed as a relative band intensity ratio between iNOS, COX-2, and ß-actin for evaluating the anti-inflammatory effect of BF-OXY-TAc.

3.2.14 Statistical analysis

Statistical analyses were used to compare the results obtained in the replications and the data were expressed as the mean ± standard deviation (SD). All analysis was performed by GraphPad Prism software version 8.0 (GraphPad Software, San Diego, CA).

CHAPTER 4

RESULTS

4.1 Synthesis and structure elucidation of OXY ester prodrugs

The hydroxy groups of OXY at C-2 and C-4 positions of ring A were more reactive than hydroxy groups on ring B as a result of the resonance effect. Since the hydroxy groups on ring A can conjugation with olefinic bonds, ring B cannot react. The steric effect made the hydroxy group C-4 more reactive than the hydroxy group C-2 [106]. Esterification of alcohols using acid anhydrides in pyridine has been known and extensively used by organic chemists for nearly 100 years [121]. Esterification of OXY is an acylation procedure using acid anhydride as acylating agents. In this case of the esterification in pyridine, pyridine not only acts as the solvent but also acts as a basic catalyst by forming a reactive intermediate driving the reaction forward. The ester prodrugs of OXY were synthesized by the single-step protocol by esterification of phenolic hydroxyl groups of OXY bearing carboxyl groups of acid anhydride; hence, enhanced lipophilicity can be achieved. OXY ester prodrugs were synthesized from OXY following well established synthetic procedures from the literature. The OXY ester prodrugs were synthesized from acid anhydride to give OXY ester prodrugs. The overall yield of the prodrug was 26-32%. All the OXY ester prodrugs were structurally corroborated through ^{1}H and ^{13}C NMR and HRMS spectral data. Mass spectra showed a single molecular ion peak for all the prodrugs, and ^{1}H and ^{13}C NMR spectra were in complete agreement with the compound structure.

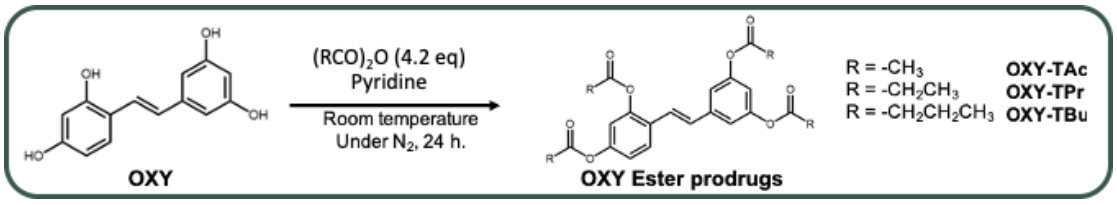

Figure 15 Synthesis of OXY ester prodrugs.

OXY-TAc (0.43 g, 26%). ^{1}H NMR (300 MHz, DMSO-d_6) (Appendix A; Figure 31), δ (ppm): 7.85 (d, *J* = 8.6 Hz, 1H), 7.35 (d, *J* = 2.1 Hz, 2H), 7.27 (d, *J* = 16.4 Hz, 1H), 7.20 (d, *J* = 16.6 Hz, 1H), 7.12 (dd, *J* = 8.6, 2.4 Hz, 1H), 7.06 (d, *J* = 2.3 Hz, 1H), 6.94 (t, *J* = 2.1 Hz, 1H), 2.39 (s, 3H), 2.29 (d, *J* = 3.2 Hz, 9H). ^{13}C NMR (75 MHz, DMSO-d_6) (Appendix A; Figure 32), δ (ppm): 172.4, 154.1, 150.4, 141.6, 129.7, 127.6, 124.8, 120.5, 118.0, 117.5, 116.0, 21.3. High-resolution MS (HRMS) calculated for $C_{22}H_{20}O_8Na$ $(M+Na)^+$ (Appendix A; Figure 33): 435.1056; found: 435.1041.

OXY-TPr (0.61 g, 32%). ^{1}H NMR (300 MHz, DMSO-d_6) (Appendix A; Figure 34), δ (ppm): 7.84 (d, *J* = 8.8 Hz, 1H), 7.32 (d, *J* = 2.2 Hz, 2H), 7.26 (d, *J* = 16.5 Hz, 1H), 7.19 (d, *J* = 16.4 Hz, 1H), 7.12 (dd, *J* = 8.6, 2.4 Hz, 1H), 7.05 (d, *J* = 2.4 Hz, 1H), 6.94 (t, *J* = 2.1 Hz, 1H), 2.74 (q, *J* = 7.5 Hz, 2H), 2.62 (qd, *J* = 7.5, 2.6 Hz, 6H), 1.15 (tt, *J* = 7.5, 3.6 Hz, 12H). ^{13}C NMR (75 MHz, DMSO-d_6) (Appendix A; Figure 35), δ (ppm): 172.9, 157.9, 151.7, 150.2, 149.5, 139.5, 129.6, 127.6, 127.3, 123.3, 120.4, 117.9, 117.4, 115.9, 27.4, 9.3. HRMS calculated for $C_{26}H_{28}O_8Na$ $(M+Na)^+$ (Appendix A; Figure 36): 491.1682; found: 491.1701.

OXY-TBu (0.65 g, 31%). ^{1}H NMR (300 MHz, DMSO-d_6), δ (ppm) (Appendix A; Figure 37): 7.85 (d, J = 8.7 Hz, 1H), 7.32 – 7.24 (d, J = 16.5 Hz, 1H), 7.28 (d, J = 17.1 Hz, 2H), 7.16 (d, J = 17.1 Hz, 1H), 7.14 – 7.08 (m, 1H), 7.04 (d, J = 2.4 Hz, 1H), 6.93 (t, J = 2.0 Hz, 1H), 2.69 (t, J = 7.2 Hz, 2H), 2.58 (td, J = 7.3, 2.1 Hz, 6H), 1.69 (pd, J = 7.0, 2.5 Hz, 8H), 0.98 (td, J = 7.4, 3.1 Hz, 12H). ^{13}C NMR (75 MHz, DMSO-d_6) (Appendix A; Figure 38), δ (ppm): 172.0, 171.9, 151.7, 150.8, 148.8, 139.5, 129.6, 127.6, 127.3, 123.2, 120.5, 117.8, 117.4, 115.9, 35.7, 18.4, 18.3, 13.8. HRMS (Appendix A; Figure 39) calculated for $C_{30}H_{36}O_8Na$ $(M+Na)^+$: 547.2308; found: 547.2315.

4.2 Transport study of OXY ester prodrugs

4.2.1 The cytotoxic effect of OXY ester prodrugs on Caco-2 cells

The cell viability of Caco-2 cells was significantly reduced by OXY and OXY ester prodrugs at 100 μM after 24 h ($p < 0.05$). The concentration of ester prodrug prodrugs at 1-50 μM produced no toxicity and evoked no significant change in cell viability ($p < 0.05$). The highest concentration at which ester prodrugs could not significantly affect cell viability was 50 μM ($p < 0.05$). Therefore, 50 μM of the concentration was chosen in this study (Figure 16).

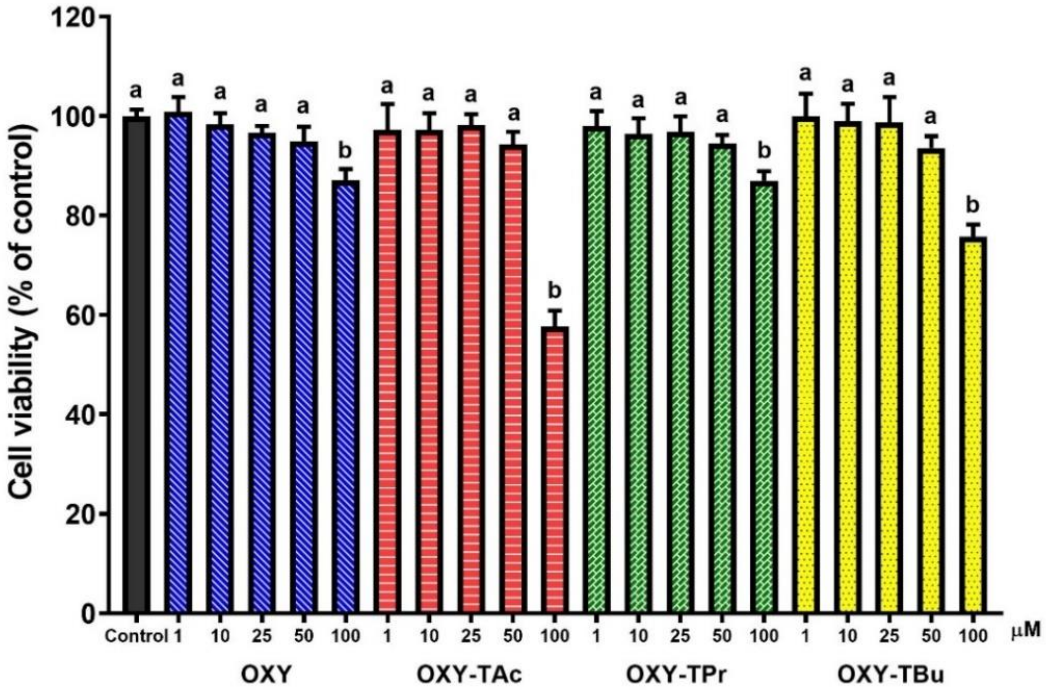

Figure 16 The viability of Caco-2 cells after 24 h exposure in OXY and OXY ester prodrugs (1-100 μM). The data are expressed as the mean ± SD for the four independent experiments. Statistically significant differences between control and treatment were determined using one-way ANOVA followed by Dunnett's multiple comparisons test. Different letters for each column correspond to significantly different values ($p < 0.05$).

4.2.2 The cellular transport of OXY ester prodrugs across Caco-2 monolayers

Because the transit time of an oral dose of the drug through the intestine is 180-240 min [122], the cellular transport studies were conducted for 240 min. The result of the transport study for OXY and their ester prodrugs across Caco-2 cell monolayers in the absorptive (an apical to a basolateral compartment) direction is presented in 17. The transport profiles of OXY and OXY ester prodrugs across monolayers at different time points (0-240 min) showed a consistent trend, the transport accumulation of ester prodrugs increased with time. Transcellular absorption from the apical to a basolateral compartment was observed at 50 μM. When either OXY or their ester prodrugs were loaded on the apical compartment, they were detected on the opposite side at the first time pull of 30 min and throughout the 4 h incubation period. Lipophilicity and permeability are expressed by log P-value and apparent permeability coefficient (P_{app}), respectively. Calculated log P (clog P), P_{app} values, and % transport of the OXY and OXY ester prodrugs were calculated, as shown in Table 3. OXY and three ester prodrugs exhibit a moderate permeability (2-10 x 10^{-6} cm/s) across Caco-2 cell monolayers. OXY and three ester prodrugs showed a linear transport across Caco-2 cell monolayers for 240 min, as shown in Figure 17. A cumulative apical to basolateral permeation of 2.71 ± 0.30 μM, 7.49 ± 0.56 μM, 4.83 ± 0.32 μM, and 3.51 ± 0.20 μM was observed for OXY, OXY-TAc, OXY-TPr, and OXY-TBu, respectively. These numbers translate to 5.42 ± 0.60%, 14.98 ± 1.11%, 9.66 ± 0.63%, and 7.01 ± 0.40% permeation for OXY, OXY-TAc, OXY-TPr, and OXY-TBu, respectively. Calculated P_{app} for OXY ester prodrugs were in the range of 2.17±0.16 (x10^{-6}) to 4.25±0.43 (x10^{-6}) cm/s, while calculated P_{app} for OXY was 1.44 ± 0.17 (x10^{-6}) cm/s (Table 3). Enhanced permeability was achieved with the majority of OXY ester prodrugs investigated in this study. OXY-TAc showed the maximum improvement in permeability among all ester prodrugs. %Transport of OXY-TAc was 2.76-fold higher than that of the OXY after 4 h. A slight increase (1.78 to 1.29-fold) in %transport was observed for OXY-TPr and OXY-TBu, respectively. OXY-TAc was further selected to study their stability, antioxidant, and anti-inflammatory activities.

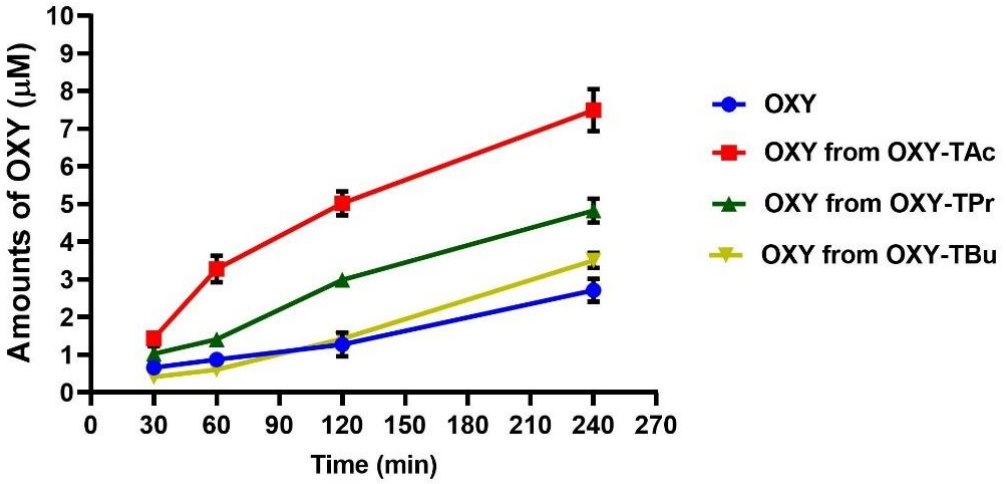

Figure 17 Time course of transport of OXY derived from OXY or OXY ester prodrugs across the Caco-2 cell monolayers. The concentration of each compound at selected timepoints was measured using HPLC. The data are expressed as the mean ± SD for the four independent experiments.

Table 3 Clog P, P_{app} values, and % transport of OXY and three OXY ester prodrugs.

Compounds	clog P	P_{app} values ($\times 10^{-6}$ cm/s)	%Transport in 4 h
OXY	2.06	1.44 ± 0.17^{a}	5.42 ± 0.60^{a}
OXY-TAc	3.52	4.25 ± 0.43^{b}	14.98 ± 1.11^{b}
OXY-TPr	5.15	2.67 ± 0.19^{c}	9.66 ± 0.63^{c}
OXY-TBu	6.32	2.17 ± 0.16^{d}	7.01 ± 0.40^{d}

The clog P is the calculated 1-octanol–water partition coefficient from http://www.vcclab.org/lab/alogps/. P_{app} values are expressed as the means ± SD for the four independent experiments. Statistical significance was performed using one-way ANOVA followed by Tukey's multiple comparison test. Different superscripts for each row correspond to significantly different values ($p < 0.05$).

4.3 The stability of OXY-TAc in various pH buffers, SGF, SIF, and human plasma

In vitro chemical hydrolysis of OXY-TAc was studied in various pH buffers (Figure 18). The half-lives of OXY-TAc in various pH buffers at 37 °C are shown in Table 4. The amount of OXY-TAc in buffer solutions pH 1.2, 6.8, and 7.4 decreased in the time-dependent. OXY-TAc was degraded to the extent of 92.3% in HCl buffer at pH 1.2. However, OXY-TAc was susceptible to degradation with 100% and 96.9% after 24 h in phosphate buffer pH 6.8 and 7.4, respectively.

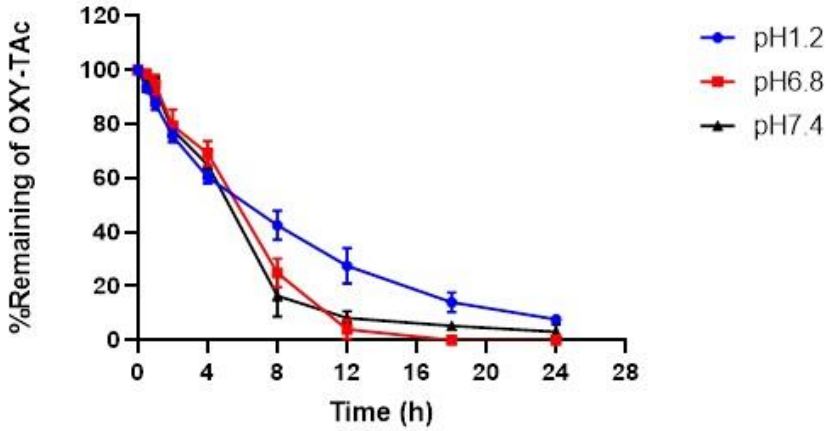

Figure 18 Time course of *in vitro* hydrolysis of OXY-TAc remaining in various buffer solutions at 37 °C.

In an *in vitro* hydrolysis pattern of OXY-TAc was studied in SGF and SIF at 37 °C. The half-lives of OXY-TAc in SGF and SIF at 37 °C were shown in Table 4. The % remaining of OXY-TAc is depicted in Figure 19. The amount of OXY-TAc in SGF and SIF decreased in the time-dependent. OXY-TAc was hydrolyzed up to 44.8% after 2 h. When OXY-TAc stock solutions were incubated in SIF, OXY-TAc was unstable, and the hydrolysis was 89.5%, after 2 h. Results revealed that OXY-TAc was unstable in SGF and SIF.

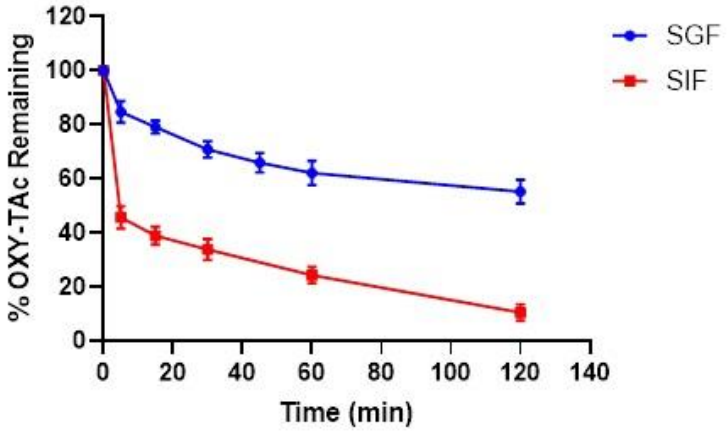

Figure 19 Time course of *in vitro* hydrolysis of OXY-TAc remaining in simulated gastric fluid (SGF) with pepsin and simulated intestinal fluid (SIF) at 37 °C.

Human stability assay also aims to test the functional group bioconversion rate in the circulation. The half-lives of OXY-TAc in human plasma at 37 °C are shown in Table 4. The hydrolysis rate of OXY-TAc in human plasma was higher than the corresponding rate in buffers, SGF, and SIF. OXY-TAc was completely hydrolyzed in human plasma after 60 s (Figure 20).

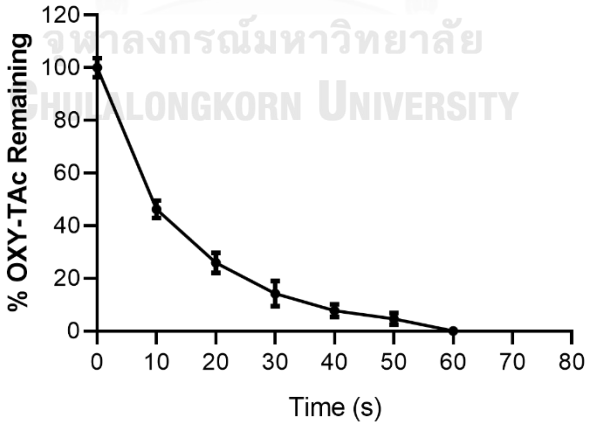

Figure 20 Time course of *in vitro* hydrolysis of OXY-TAc remaining in human plasma at 37 °C.

The *in vitro* hydrolysis pattern of OXY-TAc in buffer solutions, SGF, SIF, and human plasma had pseudo-first-order characteristics. Degradation kinetics were fitted

to the natural logarithm of OXY-TAc concentration vs. time data by non-linear regression using GraphPad Prism (version 8.0, San Diego, CA) software. The pseudo-first-order rate constants (k) and the estimated half-lives ($t_{1/2}$) obtained from the linear regression of pseudo-first-order plots of compound %OXY-TAc remaining vs. time are summarized in Table 4.

Table 4 Kinetic data for hydrolysis of OXY-TAc at 37 °C

Systems	k (min^{-1})	$t_{1/2}$ (min)	R^2
Hydrochloric acid buffer pH 1.2	7.03	355.2	0.9906
Phosphate buffer pH 6.8	8.02	311.0	0.9757
Phosphate buffer pH 7.4	9.61	259.8	0.9717
SGF	0.0350	19.83	0.9288
SIF	0.2272	3.05	0.9025
Human plasma	0.0012	0.1603	0.9908

4.4 Antioxidant effect of BF-OXY and BF-OXY-TAc

4.4.1 *In vitro* antioxidant activity of BF-OXY and BF-OXY-TAc

To assess *in vitro* antioxidant activity of BF-OXY and BF-OXY-TAc from the Caco-2 experiment was carried out by three different assays, namely, DPPH, FRAP, and ORAC assays.

The DPPH radical scavenging test is a easy and economical experimental platform where antioxidants are used to prevent oxidation products. Antioxidants change the color of the stable DPPH radical from purple to light yellow diphenyl-picrylhydrazine. As shown in Table 5, BF-OXY and BF-OXY-TAc exhibited radical scavenging ability and scavenged 4.95 ± 1.87% and 16.31 ± 1.34% of the DPPH free radical, respectively. It was shown that BF-OXY-TAc has a higher antioxidant activity than BF-OXY.

Next, the FRAP assay was used to assess whether BF-OXY-TAc and BF-OXY-TAc has an electron-donating capacity. The FRAP method is a pure electron transfer assay in which ferric ions are reduced by antioxidants that are detected by a

complex formation with the TPTZ probe. The color of the test solutions has changed from yellow to various shades of green and blue, depending on the reducing power of antioxidants [115]. As shown in Table 5, BF-OXY-TAc and BF-OXY-TAc has a FRAP value of 46.27 ± 0.95 and 51.15 ± 1.22 μmol TE/mL. FRAP value of BF-OXY-TAc was higher than BF-OXY, and these results indicated that BF-OXY-TAc showed an appreciably higher reduction capacity than BF-OXY.

The ORAC assay uses an AAPH-induced peroxyl radical that mimics lipid peroxyl radicals formed by the lipid peroxidation chain reaction *in vivo*. Inhibition of peroxyl radical-induced oxidation of the fluorescent probe by antioxidants was continually monitored, and the protective effect of an antioxidant was expressed by ORAC values [123]. As shown in Table 5, BF-OXY-TAc and BF-OXY-TAc has an ORAC value of 22.33 ± 1.92 and 42.14 ± 3.08 μmol TE/mL. ORAC value of BF-OXY-TAc was higher than BF-OXY, and these results indicated that BF-OXY-TAc was higher antioxidant activity than BF-OXY.

Table 5 Antioxidant properties of BF-OXY and BF-OXY-TAc.

Compound	DPPH (%RSA)	FRAP (μmol TE/mL)	ORAC (μmol TE/mL)
BF-OXY	4.95 ± 1.87[a]	46.27 ± 0.95[a]	22.33 ± 1.92[a]
BF-OXY-TAc	16.31 ± 1.34[b]	51.15 ± 1.22[b]	42.14 ± 3.08[b]

Trolox was used as a positive control. The data are expressed as the mean ± SD for the three independent experiments. Statistical significance for the comparison between treatment groups was assessed using an unpaired Student's t-test. Different letters for each row correspond to significantly different values ($p < 0.05$).

4.4.2 Antioxidant effect of BF-OXY and BF-OXY-TAc on intracellular ROS production in LPS-stimulated RAW264.7 macrophage cells

In macrophage cells stimulated with LPS, the intracellular ROS level in macrophages increased rapidly, causing oxidative stress. The antioxidant activity of BF-OXY-TAc was evaluated by examining the intracellular ROS generation.

RAW264.7 macrophage cells were pretreated with BF-OXY, BF-OXY-TAc, or 100 μM Vitamin C (Vc) for 1 h, then induced with or without LPS for 24 h and intracellular ROS production was measured by the DCFH-DA assay. The cells were incubated with BF control as a control. The results showed that RAW264.7 macrophage cells were induced with LPS significantly increased intracellular ROS production compared to the control ($p < 0.05$). Vc, an antioxidant, is capable of significantly decreasing the LPS-induced intracellular levels of ROS ($p < 0.05$). The regulatory effect of BF-OXY and BF-OXY-TAc on intracellular ROS production in LPS-induced RAW264.7 macrophage cells was shown in Figure 21. Intracellular ROS was increased by LPS stimulation. BF-OXY or BF-OXY-TAc alone did not affect intracellular ROS production but significantly decreased LPS-induced intracellular ROS production in RAW264.7 macrophage cells by compared with LPS alone, and the decrease was observed in BF-OXY and BF-OXY-TAc by 11% and 30%, respectively ($p < 0.05$). Results of the MTT assay showed no significant difference in cell viability was observed for RAW264.7 macrophage cells when pretreated with BF-OXY, BF-OXY-TAc, or Vc before induced with/without LPS as compared to the control (Figure 22). These results also clearly indicate that BF-OXY-TAc and BF-OXY-TAc can suppress the intracellular ROS generation induced by LPS without showing any cytotoxicity. Moreover, BF-OXY-TAc is a stronger decrease in intracellular ROS induction than BF-OXY.

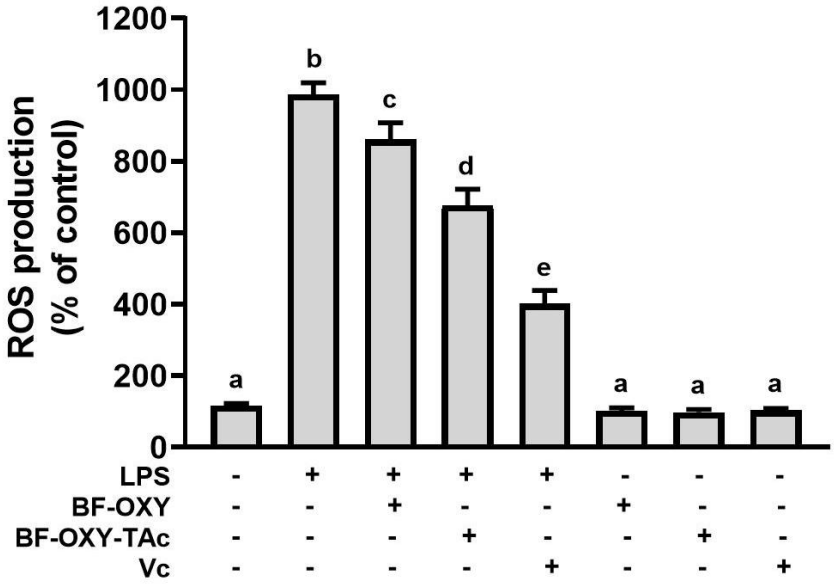

Figure 21 The effects of BF-OXY and BF-OXY-TAc on intracellular ROS production in LPS-stimulated RAW264.7 macrophage cells. The data are expressed as the mean ± SD. Statistical significance was performed using one-way ANOVA followed by Tukey's multiple comparison test. Different letters for each column correspond to significantly different values ($p < 0.05$).

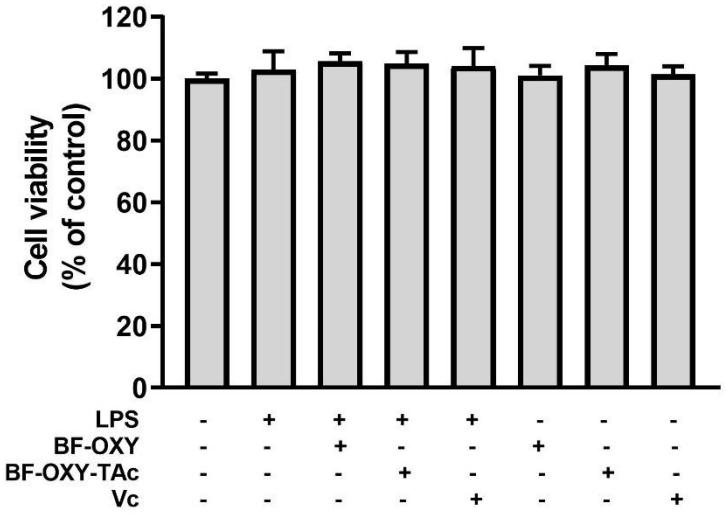

Figure 22 The effects of BF-OXY and BF-OXY-TAc on cell viability in LPS-stimulated RAW264.7 macrophage cells. Statistical significance was performed using one-way ANOVA followed by Dunnett's multiple comparisons test. The data are expressed as the mean ± SD for the four independent experiments.

4.5 Anti-inflammatory effect of BF-OXY and BF-OXY-TAc

4.5.1 Anti-inflammatory effect of BF-OXY and BF-OXY-TAc on NO and IL-6 production of in LPS-stimulated RAW264.7 macrophage cells

The anti-inflammatory effect of BF-OXY and BF-OXY-TAc was evaluated in RAW264.7 macrophage cells with inflammation induced by LPS. The cells were seeded and incubated with BF-OXY, BF-OXY-TAc, or 100 μM indomethacin (Indo; positive control) for 1 h and then induced with or without 1 μg/mL LPS for 24 h. NO and IL-6 productions were analyzed using the Griess assay and ELISA analysis. The cells were incubated with vehicle alone as a control. Incubation of RAW264.7 macrophage cells with LPS significantly increased NO and IL-6 production levels compared to the control ($p < 0.05$, Figures 23 and 24). Indo, a nonsteroidal anti-inflammatory drug (NSAID), is capable of significantly decrease the NO and IL-6 production levels induced by LPS ($p < 0.05$). Pretreatment of RAW264.7 macrophage cells with BF-OXY or BF-OXY-TAc before LPS exposure significantly decreased the induction of NO and IL-6 production ($p < 0.05$). The decrease of NO and IL-6 production was observed in BF-OXY and BF-OXY-TAc by compared with LPS alone. No significant changes were observed in the cell viability of each treatment ($p < 0.05$, Figure 25). BF-OXY significantly decreased NO and IL-6 production from LPS treated RAW264.7 macrophage cells by 13% and 17%, respectively ($p < 0.05$). BF-OXY-TAc significantly decreased NO and IL-6 production from LPS treated RAW264.7 macrophage cells by 32% and 30%, respectively ($p < 0.05$, Figures 23 and 24). These results also clearly indicate that BF-OXY-TAc is a stronger decrease of both NO and IL-6 production levels than BF-OXY without noticeable cell damage in RAW264.7 macrophage cells.

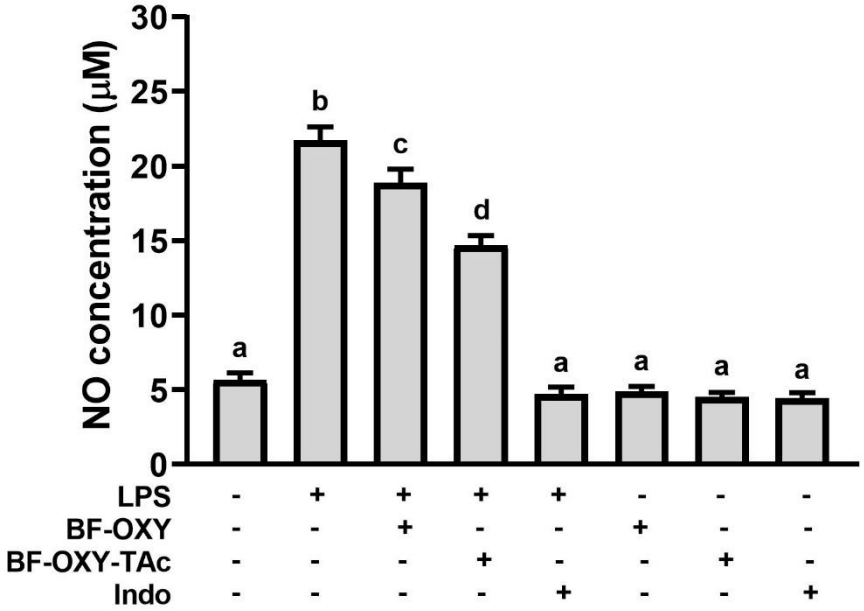

Figure 23 The effects of BF-OXY and BF-OXY-TAc on NO production in LPS-stimulated RAW264.7 macrophage cells. The data are expressed as the mean ± SD for the four independent experiments. Statistical significance was performed using one-way ANOVA followed by Tukey's multiple comparison test. Different letters for each column correspond to significantly different values ($p < 0.05$).

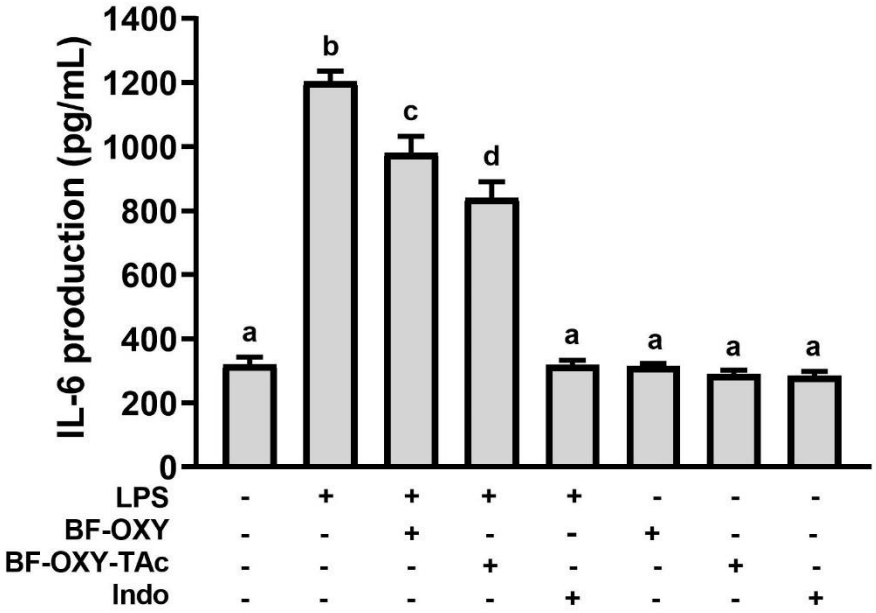

Figure 24 The effects of BF-OXY and BF-OXY-TAc on IL-6 production in LPS-stimulated RAW264.7 macrophage cells. The data are expressed as the mean ± SD for the four independent experiments. Statistical significance was performed using one-way ANOVA followed by Tukey's multiple comparison test. Different letters for each column correspond to significantly different values ($p < 0.05$).

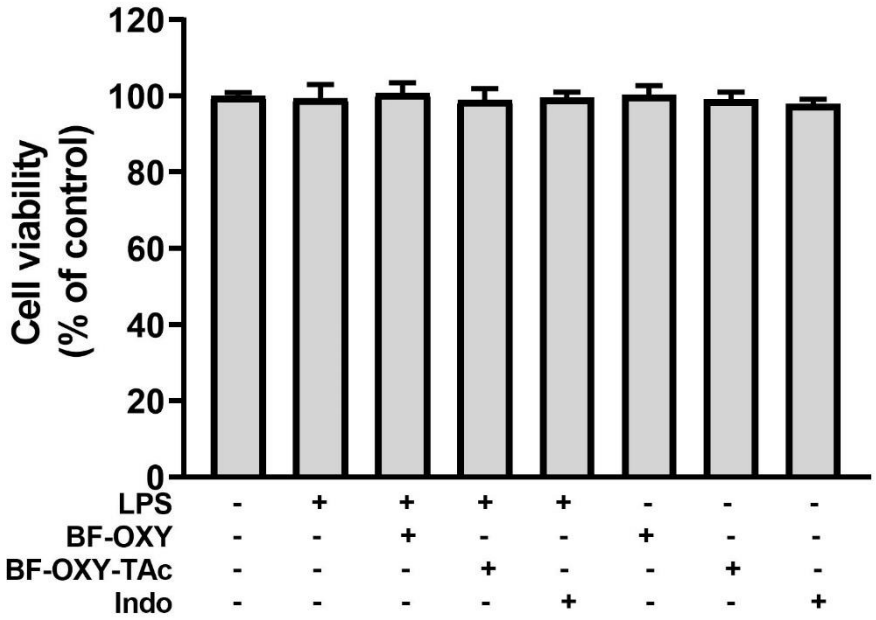

Figure 25 The effects of BF-OXY and BF-OXY-TAc on cell viability in LPS-stimulated RAW264.7 macrophage cells. The results are expressed in terms of the control percentages. Statistical significance was performed using one-way ANOVA followed by Dunnett's multiple comparisons test. The data are expressed in terms of the mean ± SD for the four independent experiments.

4.5.2 Anti-inflammatory effect of BF-OXY and BF-OXY-TAc iNOS and COX-2 expression in LPS-stimulated RAW264.7 macrophage cells

The expression of iNOS and COX-2 protein levels was examined on LPS-induced RAW264.7 macrophage cells by Western blot analysis. The cells were incubated with vehicle alone as a control. The inflammatory mediators, iNOS and COX-2, reflect the states of inflammations and are often used to estimate the severities of the inflammation. Both iNOS and COX-2 protein levels in RAW264.7 macrophage cells increased markedly after 24 h of LPS (1 μg/mL) induction, and the values were about 3.1 and 3.3-fold higher than that of the control, respectively, as shown in Figures 26 and 27. When cells were pretreated with BF-OXY or BF-OXY-TAc before the cells were exposed with LPS resulted in a considerable decrease in both iNOS and COX-2 expression levels in the LPS-induced RAW264.7 macrophage cells by western blot, as compared with LPS alone (Figures 26 and 27). The BF-OXY significantly decreased iNOS and COX-2 expression levels production from LPS treated RAW264.7 macrophage cells by 63% and 57%, respectively ($p < 0.05$). BF-OXY-TAc significantly decreased iNOS and COX-2 expression levels from LPS treated RAW264.7 macrophage cells by 92% and 74%, respectively ($p < 0.05$). The results also clearly showed that BF-OXY-TAc is a stronger decrease of both iNOS and COX-2 expression levels than BF-OXY on LPS-induced RAW264.7 macrophage cells. These results suggest that BF-OXY-TAc can prevent LPS-induced inflammation in RAW264.7 macrophage cells.

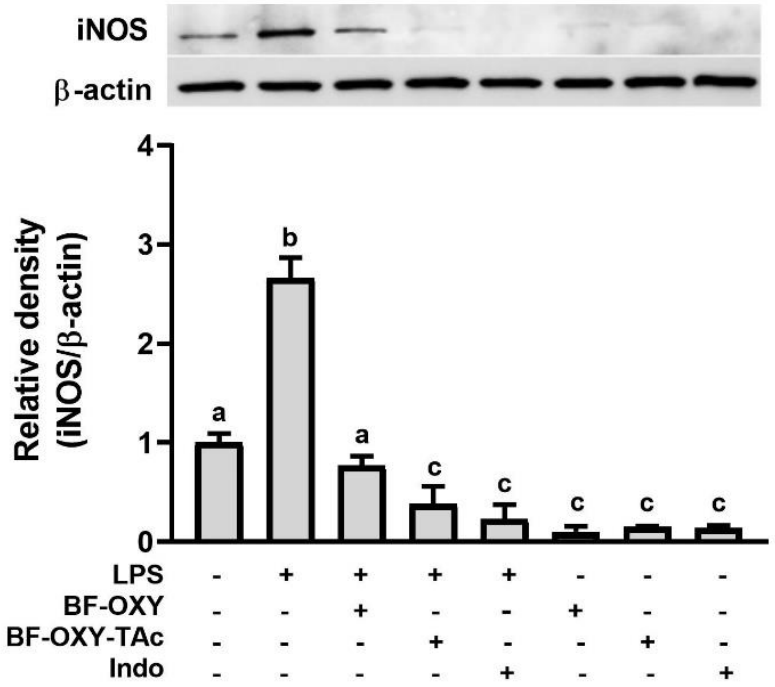

Figure 26 The effects of BF-OXY and BF-OXY-TAc on iNOS protein expression levels in LPS-stimulated RAW264.7 macrophage cells. The data are expressed in terms of the mean ± SD for the four independent experiments. Statistical significance was performed using one-way ANOVA followed by Tukey's multiple comparison test. Different letters for each column correspond to significantly different values ($p < 0.05$).

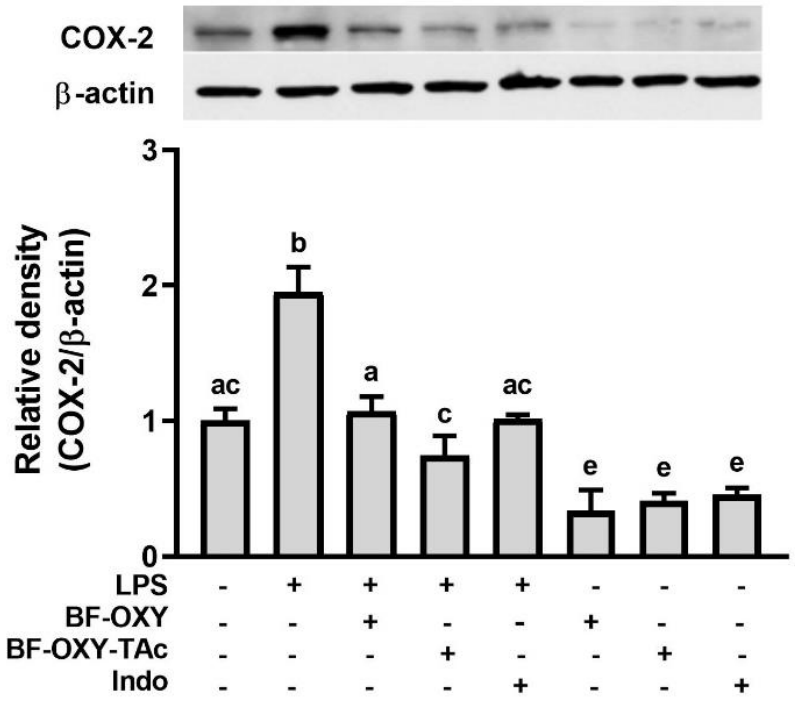

Figure 27 The effects of BF-OXY and BF-OXY-TAc on COX-2 protein expression levels in LPS-stimulated RAW264.7 macrophage cells. The data are expressed in terms of the mean ± SD for the three independent experiments. Statistical significance was performed using one-way ANOVA followed by Tukey's multiple comparison test. Different letters for each column correspond to significantly different values ($p < 0.05$).

CHAPTER 5
DISCUSSION AND CONCLUSION

.

A total of three OXY ester prodrugs, OXY-TAc, OXY-TPr, and OXY-TBu, of different chain lengths, were designed to enhance the lipophilicity, and thus the membrane permeability [28]. The OXY and three OXY ester prodrugs did not decrease cell viability at 1-50 μM; therefore, OXY and their ester prodrugs at 50 μM were used for the transport study. Transport was monitored for a period of 240 min because the transit time of the small intestine is generally 180-240 min [122].

Metabolism in Caco-2 cells involved glucuronidation and sulfation [124]. The transport of oxyresveratrol through Caco-2 cell monolayers can conjugate in glucuronide and sulfate forms. Therefore, to quantify free oxyresveratrol can be performed by deglucuronidation and desulfation of oxyresveratrol conjugations with glucuronidase and sulfatase enzymes [125]. As a result, the amounts of OXY were detected in the samples of the basolateral compartment of all ester prodrugs. The ester prodrugs were not detected in the basolateral compartment. These results indicate that the ester bonds of prodrugs were cleaved, OXY ester prodrugs were hydrolyzed, and OXY was liberated. The ester linkage in OXY ester prodrugs can be hydrolyzed to OXY by esterases. Caco-2 cells were reported to have sufficient carboxylesterases (CESs) [126]. P_{app} value of OXY is 1.44 ± 0.17 x 10^{-6} cm/s. This value is consistent with those reported previously [24]. A recent study provided some updated guidance on how permeability values could be correlated with human oral absorption: low permeability (0-20% human fraction absorbed (F_a)) is correlated to P_{app} values of <1-2 × 10^{-6} cm/s; moderate permeability (20-80% F_a) to P_{app} values of 2-10 × 10^{-6} cm/s; and high permeability (80-100% F_a) to P_{app} > 10 × 10^{-6} cm/s [127]. Comparing OXY, OXY-TAc, OXY-TPr, and OXY-TBu, a trend is observed. Three OXY ester prodrugs, OXY-TAc, OXY-TPr, and OXY-TBu, are moderate permeability, whereas OXY is low permeability. The difference in the transport through Caco-2 cell monolayers among the ester prodrugs was due to different chain lengths. In this study, the trend for permeabilities of ester prodrugs with a given chain

length was on the order of OXY-TAc > OXY-TPr > OXY-TBu. The degree of the amount OXY from OXY-TAc, OXY-TPr, and OXY-TBu on the basolateral compartment was 1.29 to 2.76-fold greater than that of the OXY after 4h.

Compound with a molecular weight that should be higher than 500 g/mol has been predicted to have poor absorption or permeation [31]. The molecular weight of OXY-TAc (412.39 g/mol) and OXY-TPr (468.50 g/mol) are lower than 500 g/mol. In contrast, the molecular weight of OXY-TBu (524.61 g/mol) exceeds 500 g/mol. Additionally, the permeation of drugs is decided by their logP. The log P value of the compound was a well-established measure of the lipophilicity of the compound. Higher logP values are higher lipophilicity [31]. High lipophilicities and high log P values may cause responsible for poor absorption or permeation. In addition, the clog P values of OXY-TAc, OXY-TPr, and OXY-TBu are 3.25, 5.15, and 6.32, respectively. Compounds with log P values that must not be greater than 5 have been shown to have ideal lipophilicity to permeate biological membranes. Further, compounds with logP greater than 5 have been predicted to have poor intestinal absorption [128, 129]. The results of the permeation of OXY-TAc, OXY-TPr, and OXY-TBu were better than that of OXY in Caco-2 cell monolayers due to the increase in lipophilicity to facilitate passive diffusion through the monolayer [130]. Based on this theory, OXY-TAc is expected to have the highest permeability among three ester prodrugs, which is in accordance with observations.

The results of chemical stability studies showed that OXY-TAc had different stabilities in the buffer solutions of various pH at 37 ^{o}C. Hydrolysis of OXY-TAc was observed at pH 1.2 and 6.8, yielding apparent half-lives 5.9 h and 5.1 h, respectively. The stability of OXY-TAc was evaluated in SGF and SIF. OXY-TAc was readily hydrolyzed in SGF and SIF with apparent half-lives of 19.83 and 3.05 min, respectively. In SGF with pepsin and SIF with pancreatin, OXY-TAc underwent dramatically rapid hydrolysis, suggesting that the ester bond was unstable in the hydrolysis of pepsin and pancreatin enzymes [131]. Additionally, the $t_{1/2}$ value of OXY-TAc in the plasma was much shorter than those in the simulated gastrointestinal fluids and various pH buffer solutions. These results indicated that OXY-TAc could

release the parent drug easily in the systematic circulation, which may increase the oral bioavailability of OXY.

The evaluation of antioxidant activities of BF-OXY and BF-OXY-TAc from the transport study at 4 h was carried out using three different assays (DPPH, FRAP, and ORAC assays). In DPPH assay, BF-OXY-TAc exhibited more effective radical scavenging activity than BF-OXY, indicating that the presence of OXY amount from transport studies in the Caco-2 cell monolayers had made a significant difference, possibly due to the ability to donate hydrogen atoms. FRAP value was used as an important indicator of the antioxidant capacity with regard to reducing ferric ions to ferrous ions [132]. The trend for reducing activities was similar to the DPPH method. The ORAC assay is based on the hydrogen atom transfer mechanism [132]. In this study, the ORAC value of OXY-TAc was higher than OXY-BF, suggesting that BF-OXY-TAC exhibited higher antioxidant activity in the *in vitro* assay methods and could possibly follow the hydrogen atom transfer mechanism than OXY-BF. The *in vitro* antioxidant activity with different assay detected in BF-OXY-TAc was significantly higher than that of BF-OXY. This result was in agreement with the higher amount of free OXY detected in the basolateral compartment for OXY-TAc. Thus, OXY presented in the BF could be responsible for its antioxidant activity. A similar trend is also observed in the present study, but the values are differed [133].

In this study, the results demonstrated that BF-OXY and BF-OXY-TAc reduced the intracellular ROS levels under LPS-stimulated oxidative stress environment. The reduction of the ROS level of BF-OXY-TAc was similar to that of Vitamin C. The reduction of intracellular ROS level induced by LPS after pretreatment with BF-OXY and BF-OXY-TAc indicates its antioxidant potential. The effect of BF-OXY and BF-OXY-TAc on the ROS production was in accordance with that of the antioxidant activity, suggesting that there was a direct relationship between the antioxidant activity and the protective effect against LPS-simulated oxidative stress in RAW264.7 macrophage cells. The result showed that BF-OXY-TAc reduces ROS production in agreement with Carlos *et al.* [134], who demonstrated that OXY decreases ROS levels in macrophage cells that were induced with oxidative stress conditions.

This study was the first to investigate the anti-inflammatory activity of BF-OXY-TAc in LPS-stimulated RAW264.7 macrophage cells. Throughout the investigation, it could be seen that the LPS (1 μg/mL) stimulation significantly induced the generation of NO production as well as the expressions of iNOS and COX-2. The OXY has been shown to reduce NO production and the expression of iNOS and COX-2 [3, 73]. Similarly, the present study showed that BF-OXY and BF-OXY-TAc could significantly inhibit LPS-simulated generation of NO production and expression of iNOS and COX-2 in RAW264.7 macrophage cells. The BF-OXY and BF-OXY-TAc inhibited NO via the downregulation of iNOS expression. BF-OXY-TAc exhibited a stronger inhibitory effect toward iNOS and COX-2 expressions than BF-OXY.

In addition to the inhibitory effect on pro-inflammatory enzymes, the anti-inflammatory activity of BF-OXY-TAc was consistent with the results of its effects on IL-6 (pro-inflammatory cytokines) in LPS-stimulated RAW264.7 macrophage cells. The secretion of IL-6 was increased in the medium of LPS-treated cells. BF-OXY and BF-OXY-TAc reduced the production of IL-6 in LPS-stimulated RAW264.7 macrophage cells. BF-OXY-TAc showed a higher decrease of IL-6 secretion level than BF-OXY. Moreover, the MTT assay showed that BF-OXY and BF-OXY-TAc were not cytotoxic but significantly reduced the secretion of IL-6. These results indicate that BF of OXY-TAc effectively improved inflammatory conditions, as it can suppress the overproduction of inflammatory mediators by activated macrophages. However, none of these studies measured the inhibition in the of NO and IL-6 productions and iNOS and COX-2 protein expressions by OXY-TAc after absorption processes.

In conclusion, enhancing the lipophilicity of OXY by esterification could increase the transport of OXY across Caco-2 cell monolayers. OXY-TAc showed the highest transport of three ester prodrugs across the Caco-2 cell monolayers. BF-OXY-TAC has a stronger antioxidant activity than BF-OXY and has the potential to prevent LPS-induced oxidative stress and inflammation damage in RAW264.7 macrophage cells through a decrease in the production of ROS, NO, and IL-6 as well as the expression of inflammatory enzymes such as iNOS and COX-2. The enhancement of antioxidant and anti-inflammatory activities could be derived from the higher

permeation, which in turn might be derived from an improvement in the lipophilicity of OXY. Therefore, OXY content in the basolateral compartment could play an important role in the antioxidant and anti-inflammatory activities found.

Further study is to determine the prevention of rheumatoid arthritis, which is joint inflammation with OXY-TAc [135]. OXY was active against oxidative stress and inflammation in rats. It was possible to reduce IL-6 production and iNOS and COX-2 expression [136], which is consistent with this study. The pharmacokinetics of oxyresveratrol was studied in rats by administering OXY 10 mg/kg [137], which did not show toxicity to rats. Therefore, OXY-TAc will be used 17 mg/kg in this model, which is an equivalent concentration with OXY.

APPENDIX

APPENDIX A

^{1}H NMR, ^{13}C NMR, AND MASS SPECTRA

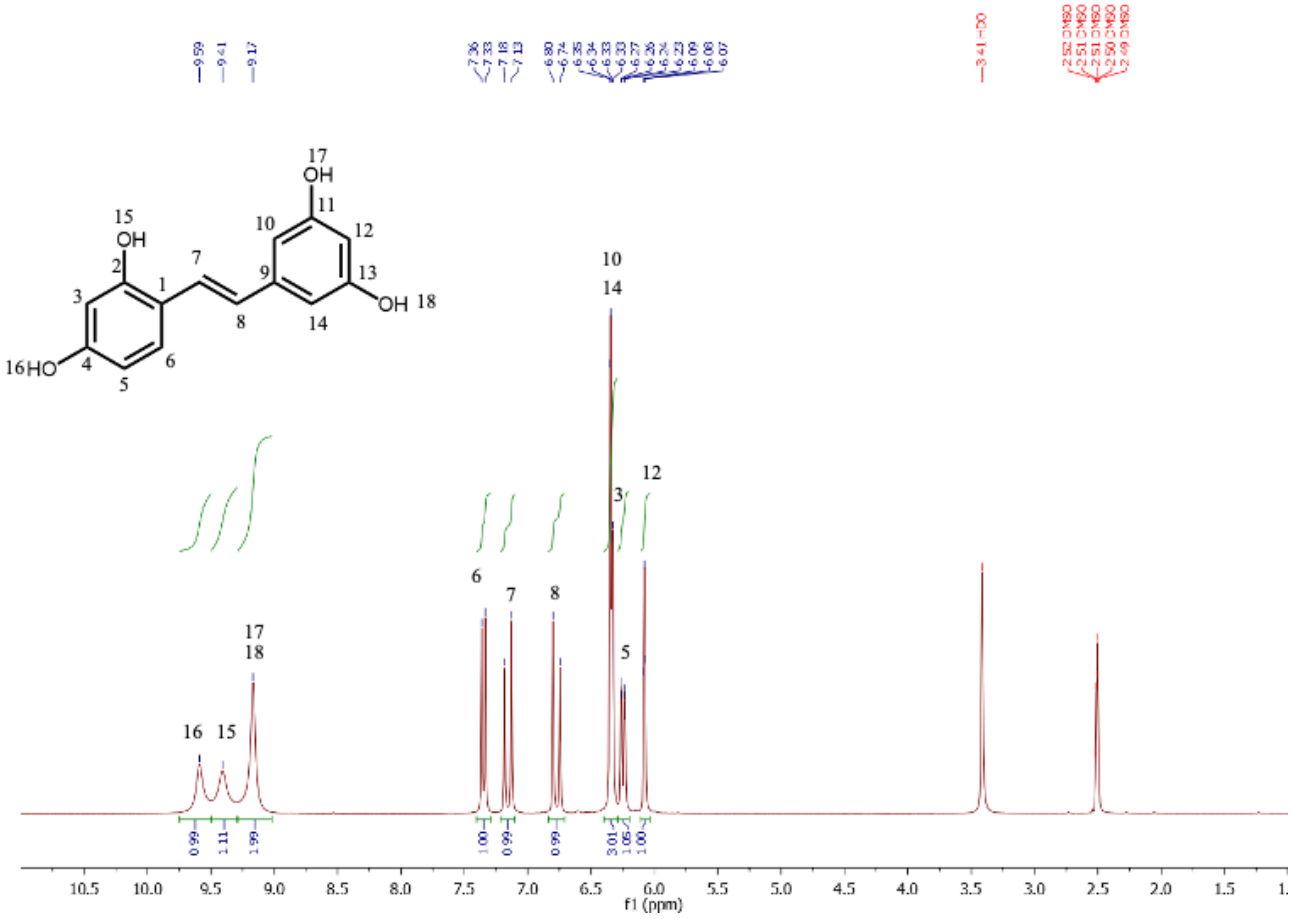

Figure 28 ^{1}H NMR spectrum of OXY in DMSO-d_6.

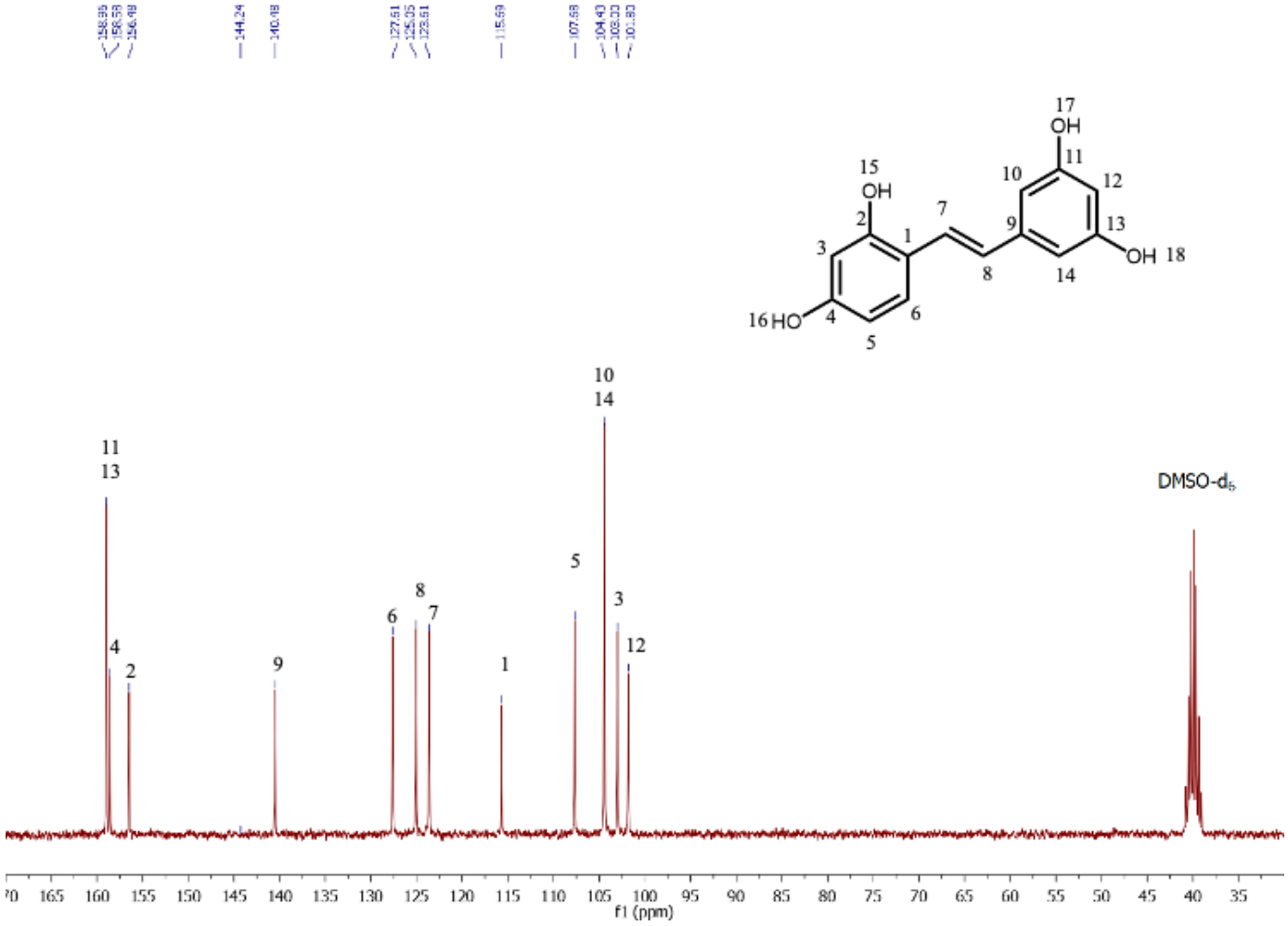

Figure 29 ^{13}C NMR spectrum of OXY in DMSO-d_6.

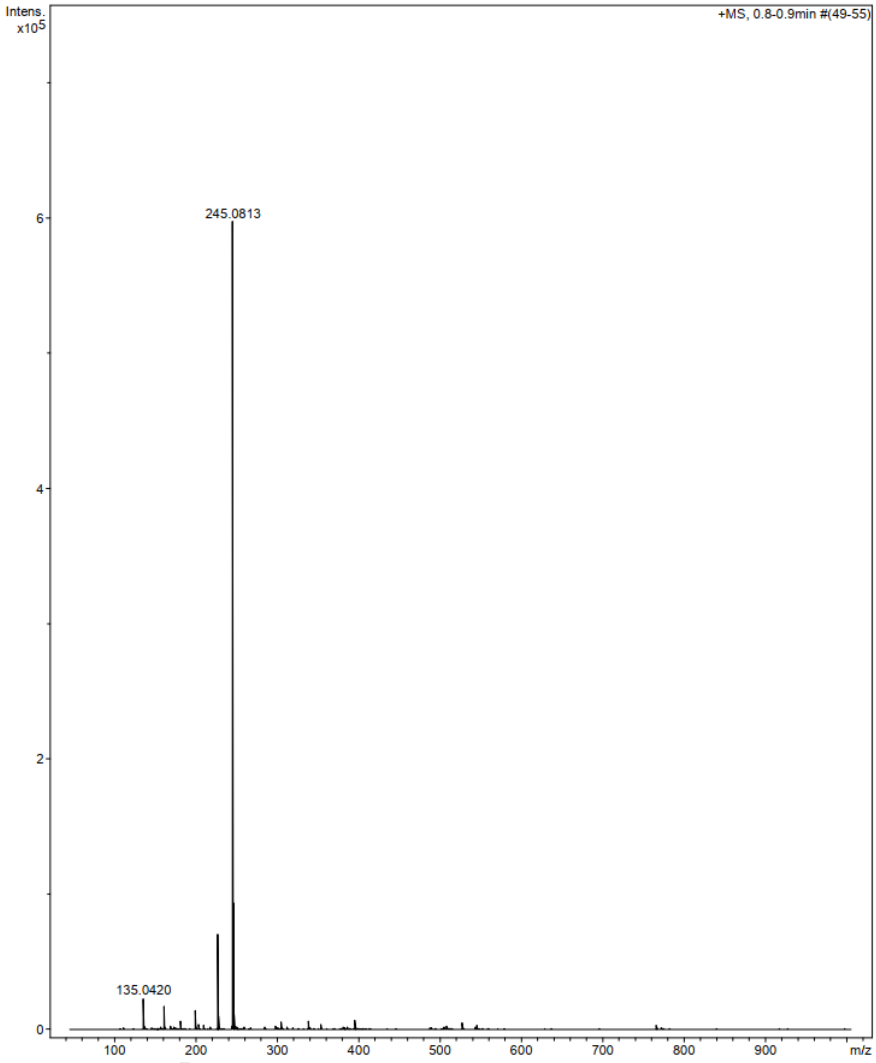

Figure 30 Mass spectrum of OXY.

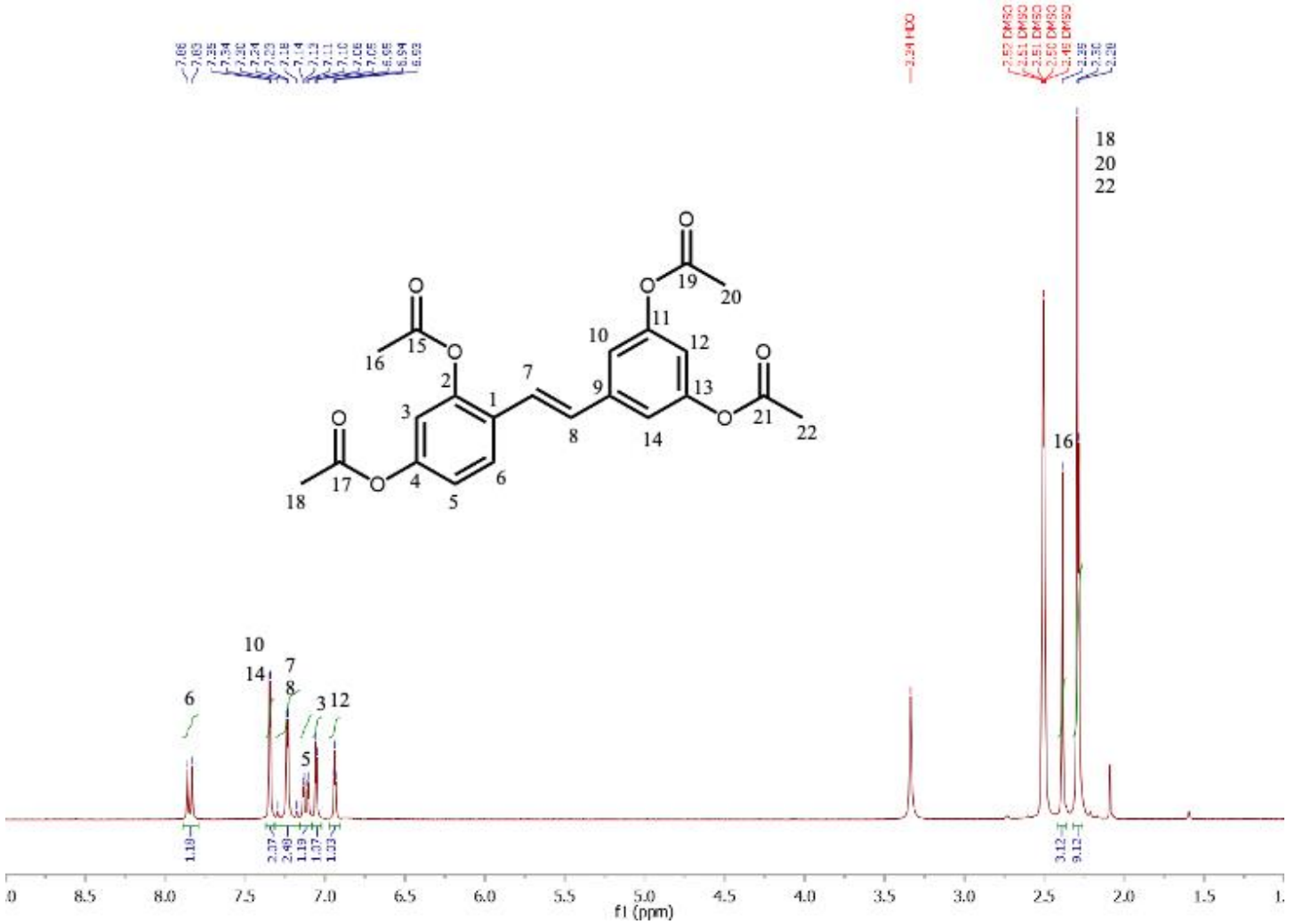

Figure 31 ^{1}H NMR spectrum of OXY-TAc in DMSO-d_6.

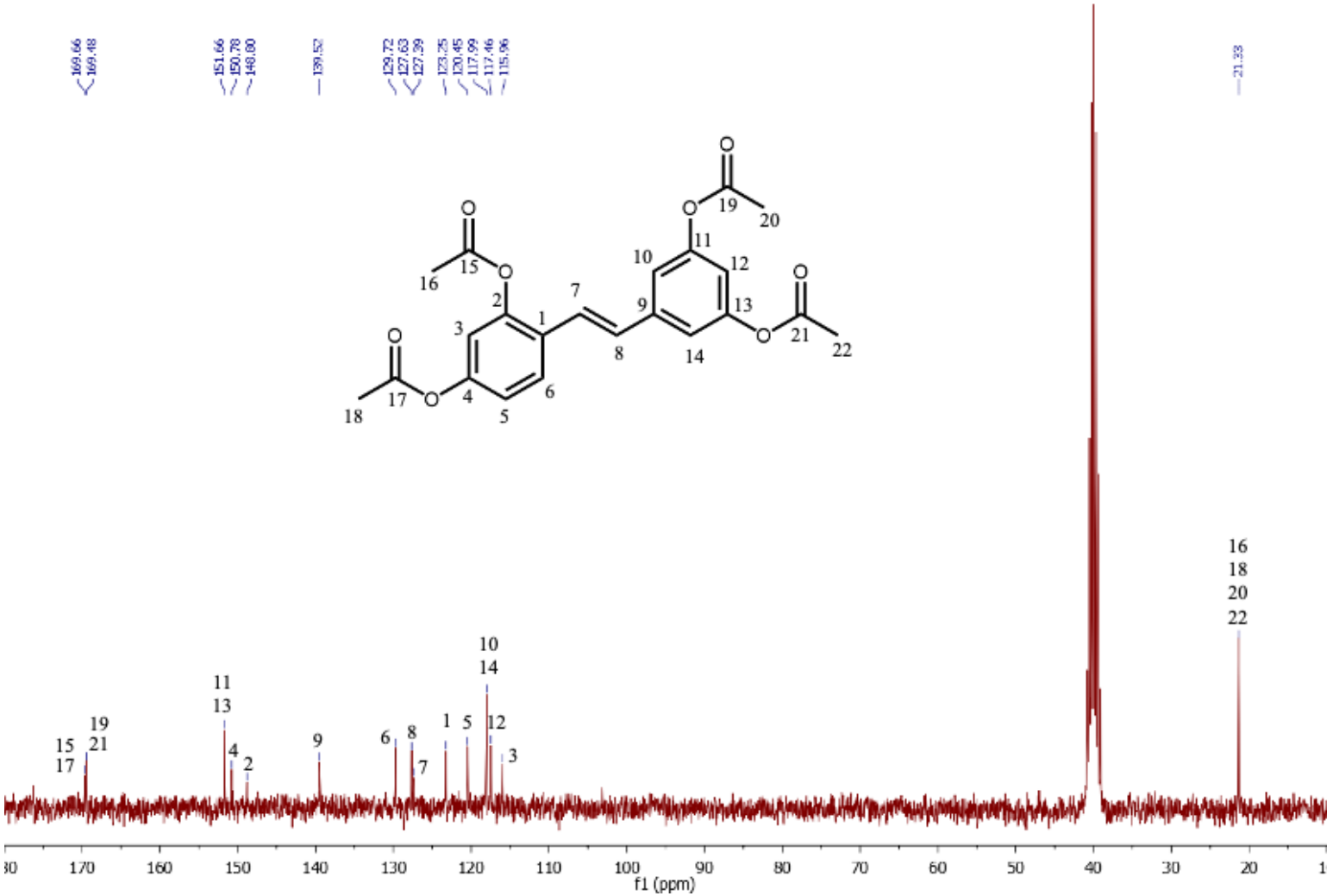

Figure 32 ^{13}C NMR spectrum of OXY-TAc in DMSO-d_6.

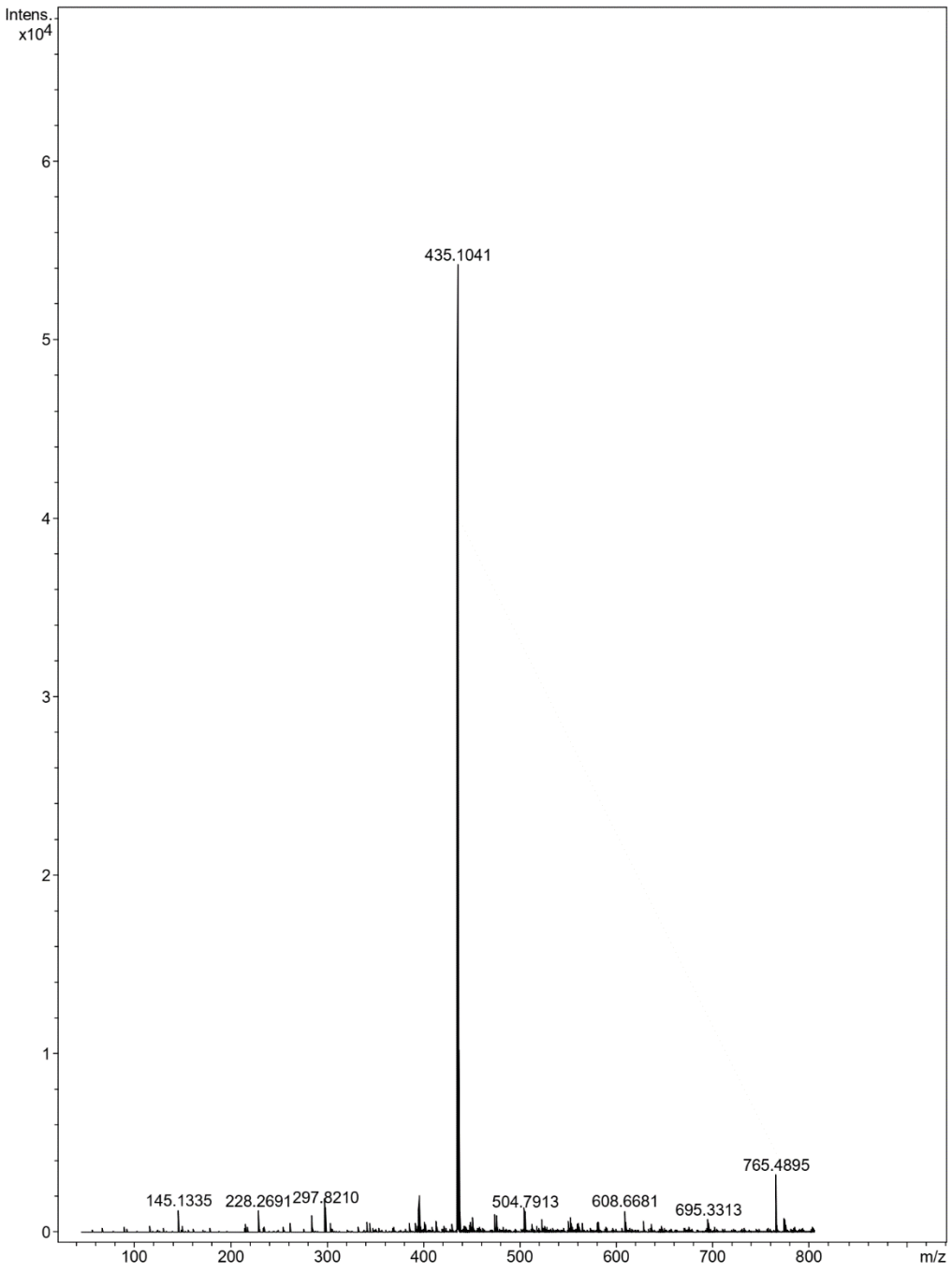

Figure 33 Mass spectrum of OXY-TAc.

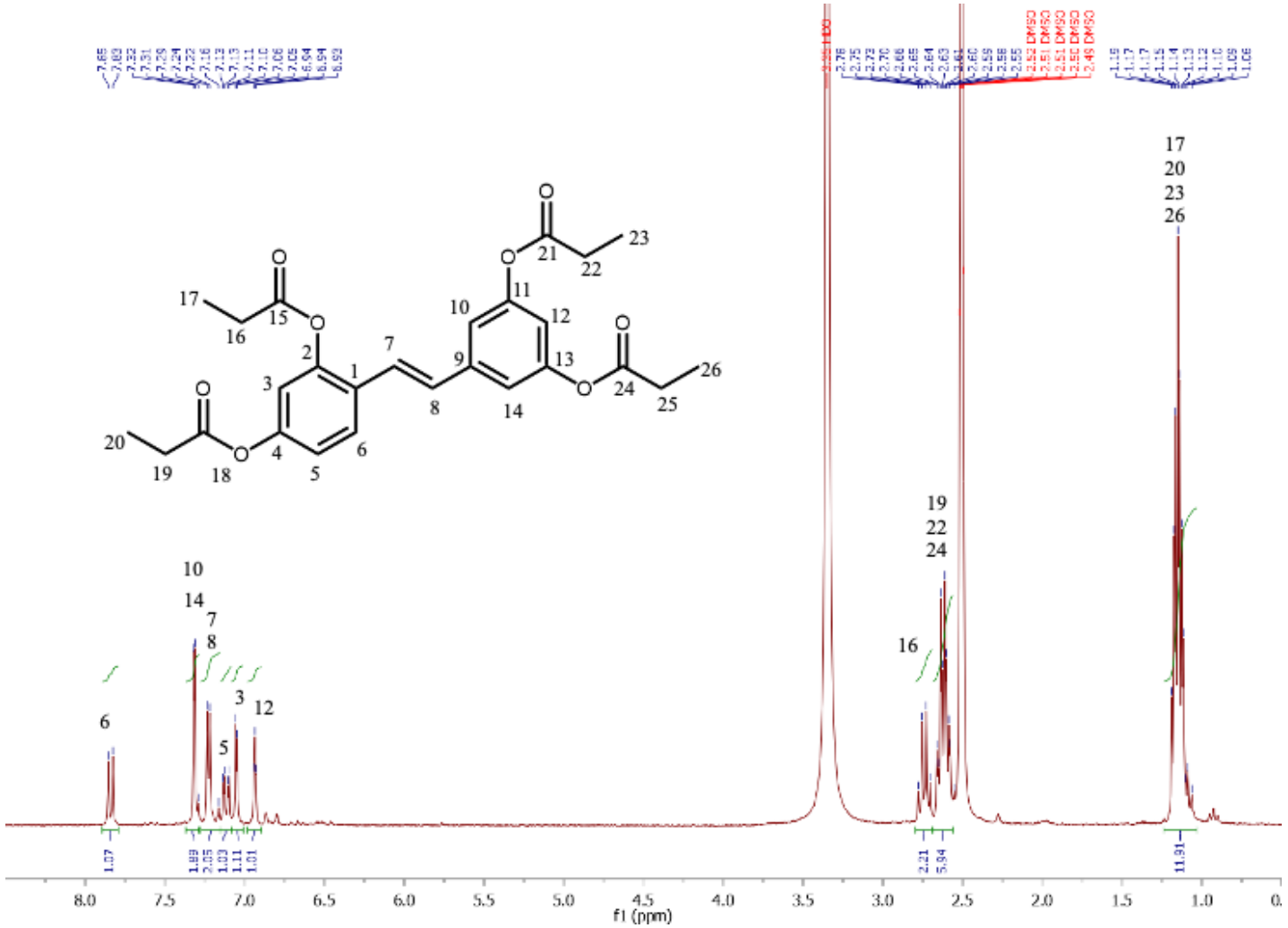

Figure 34 ^{1}H NMR spectrum of OXY-TPr in DMSO-d_6.

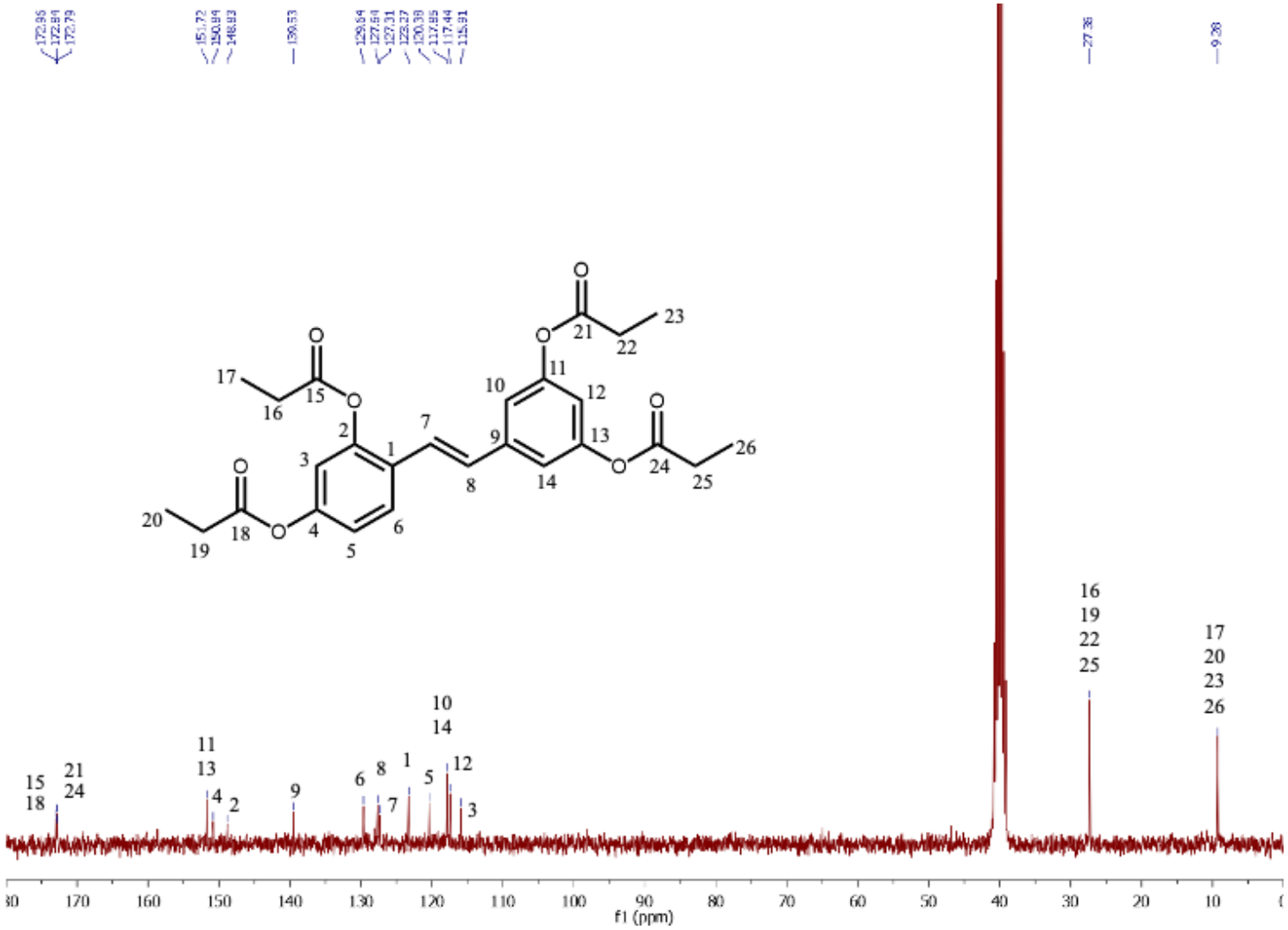

Figure 35 ^{13}C NMR spectrum of OXY-TPr in DMSO-d_6.

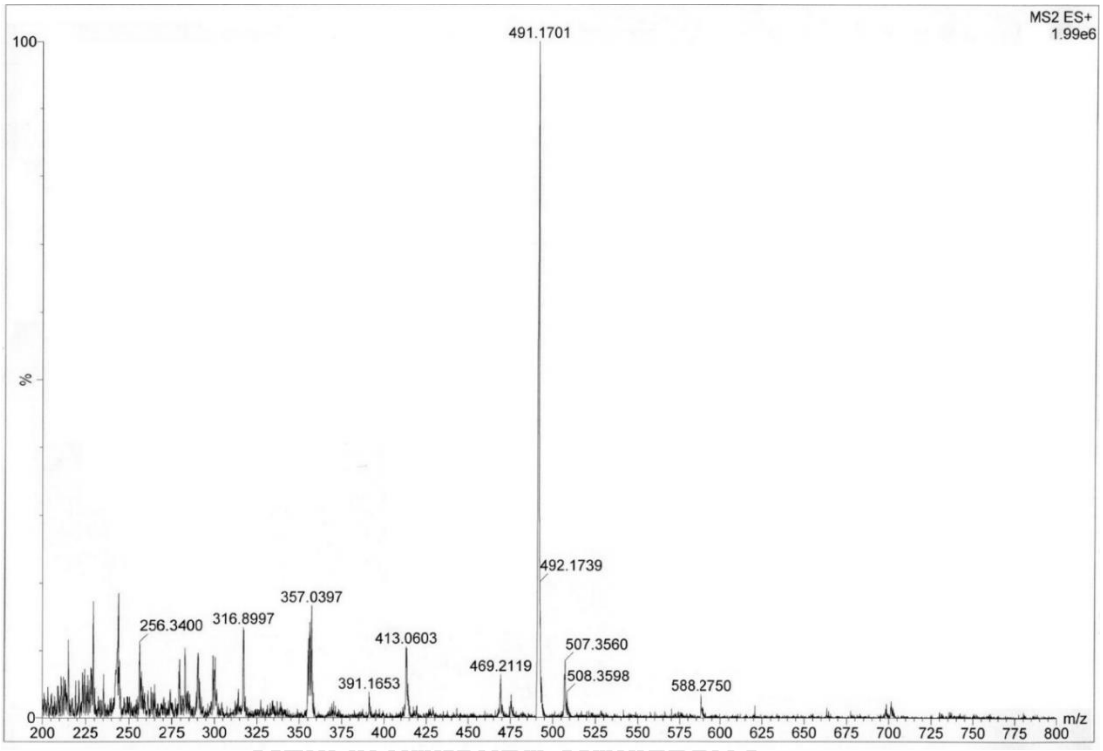

Figure 36 Mass spectrum of OXY-TPr.

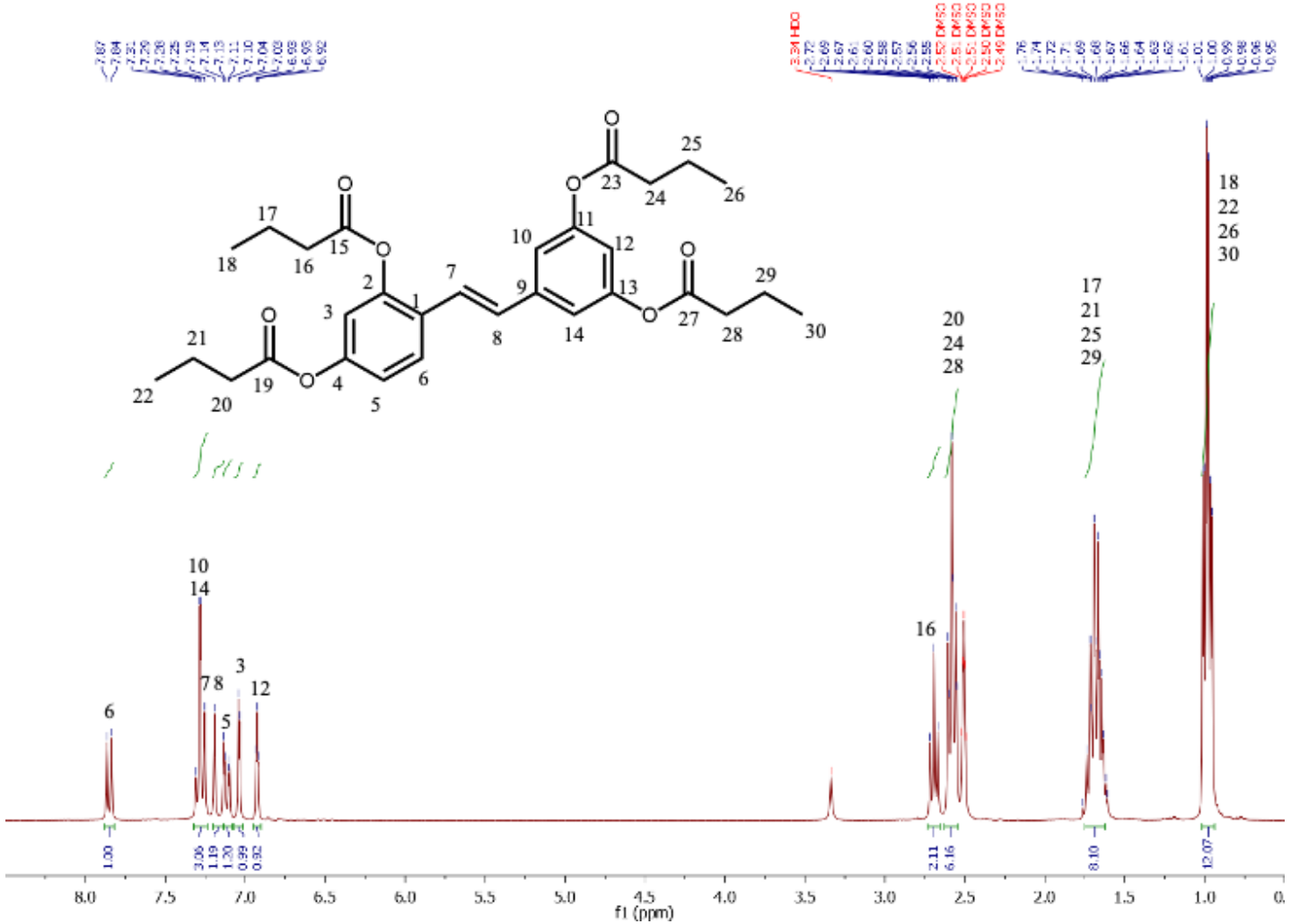

Figure 37 ^{1}H NMR spectrum of OXY-TBu in DMSO-d_6.

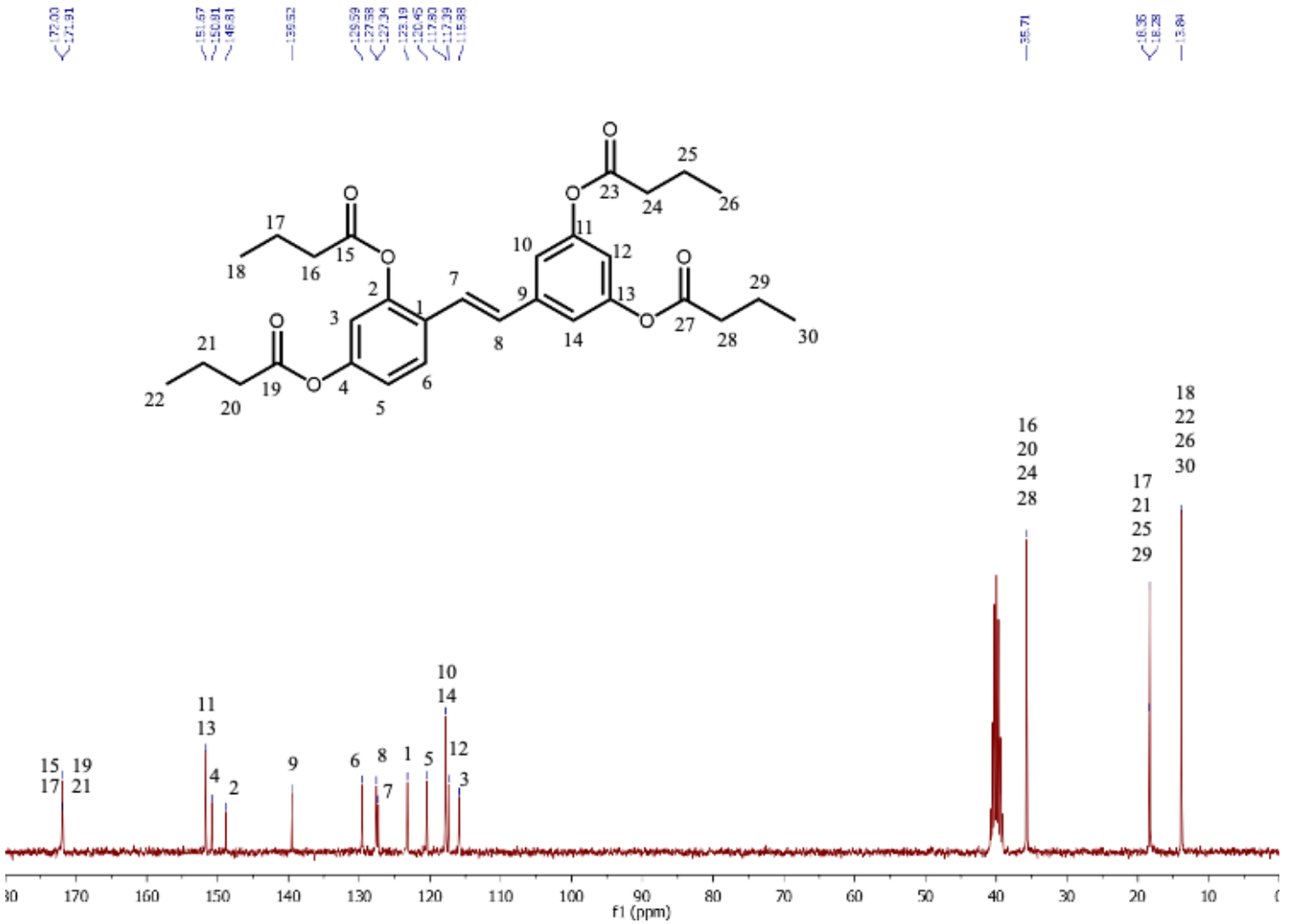

Figure 38 ^{13}C NMR spectrum of OXY-TBu in DMSO-d_6.

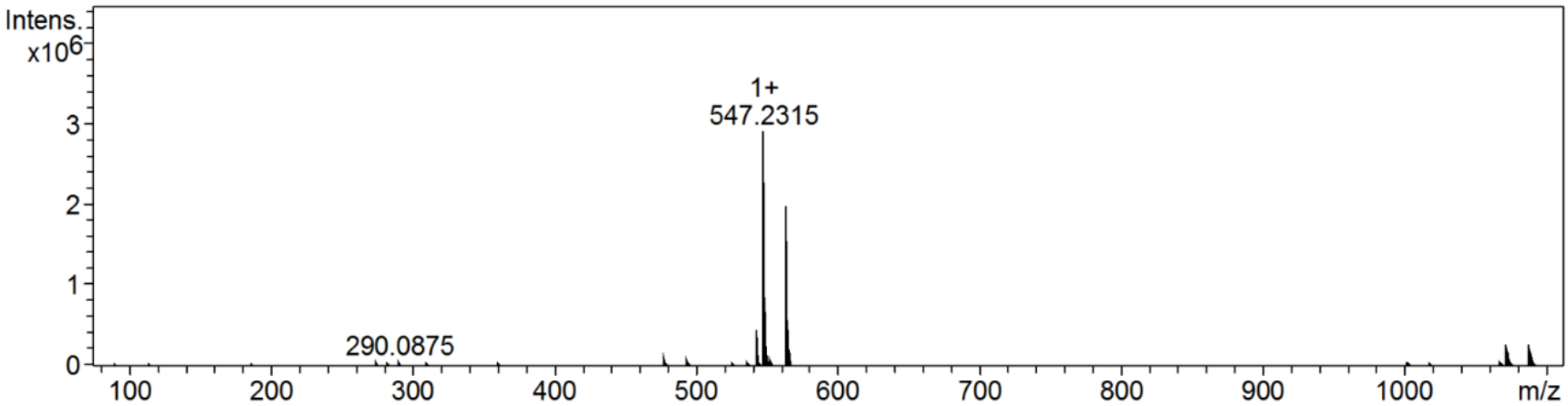

Figure 39 Mass spectrum of OXY-TBu.

APPENDIX B

HPLC CHROMATOGRAMS

Figure 40 HPLC chromatogram of OXY standard with retention time at 2.0 min. The detection was measured at 320 nm.

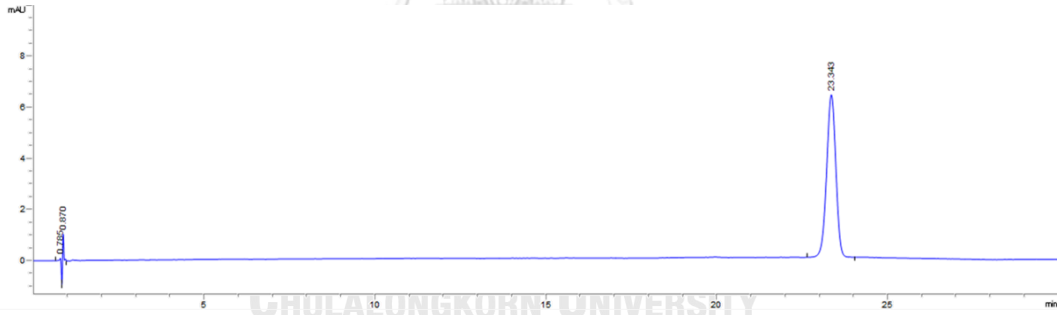

Figure 41 HPLC chromatogram of OXY-TAc standard with retention time at 23.3 min. The detection was measured at 320 nm.

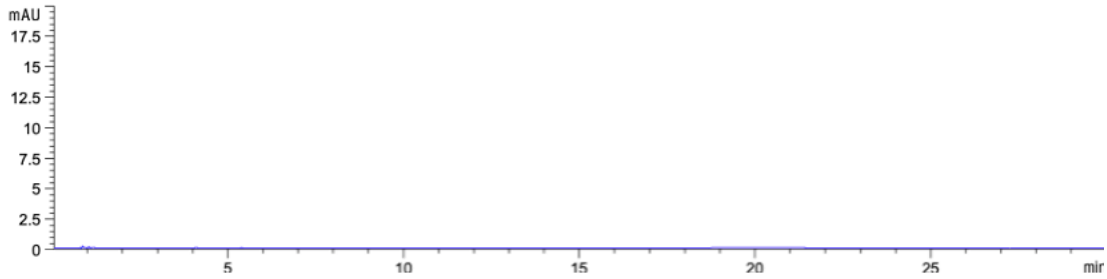

Figure 42 HPLC chromatograms of OXY transport across Caco-2 cell monolayers. The sample was taken after 0 min incubation from basolateral compartment at 37 °C. The detection was measured at 320 nm.

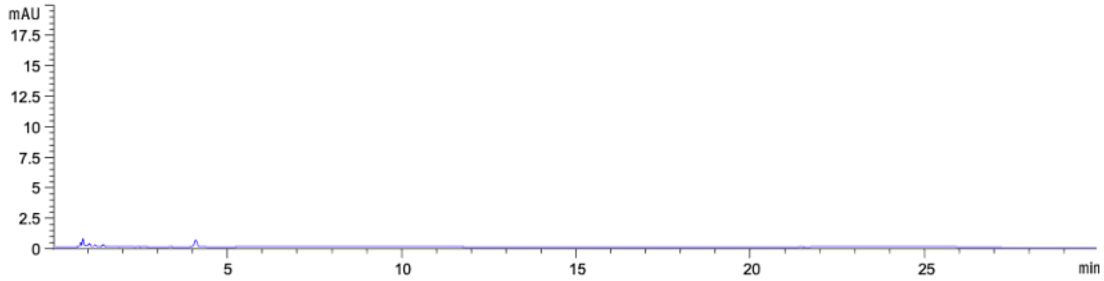

Figure 43 HPLC chromatograms of OXY transport across Caco-2 cell monolayers. The sample was taken after 15 min incubation from basolateral compartment at 37 °C. The detection was measured at 320 nm.

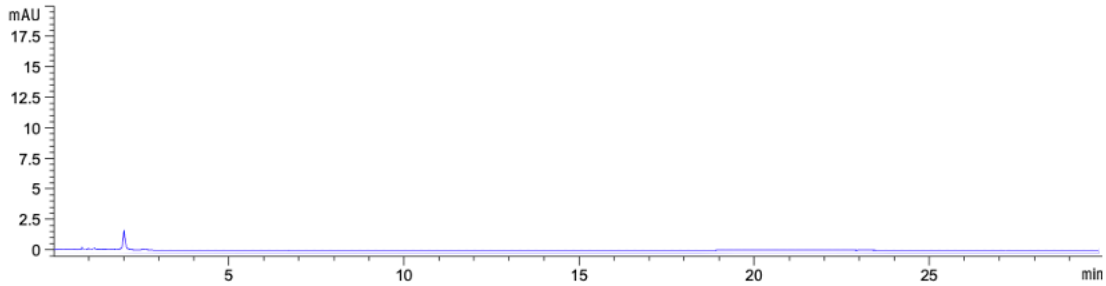

Figure 44 HPLC chromatograms of OXY transport across Caco-2 cell monolayers with retention time at 2.1 min. The sample was taken after 30 min incubation from basolateral compartment at 37 °C. The detection was measured at 320 nm.

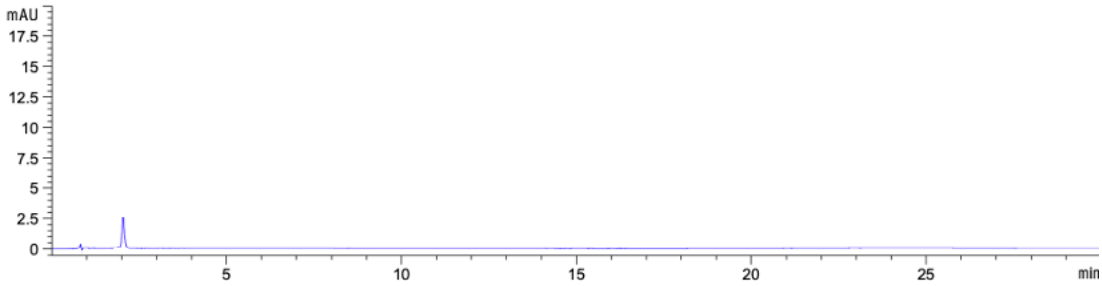

Figure 45 HPLC chromatograms of OXY transport across Caco-2 cell monolayers with retention time at 2.1 min. The sample was taken after 60 min incubation from basolateral compartment at 37 °C. The detection was measured at 320 nm.

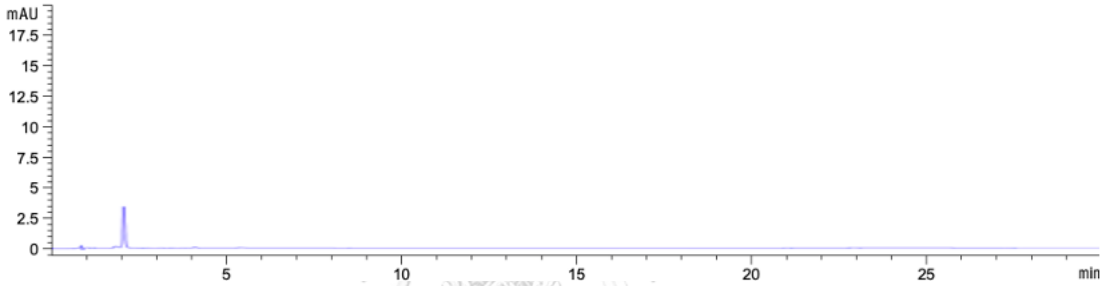

Figure 46 HPLC chromatograms of OXY transport across Caco-2 cell monolayers with retention time at 2.1 min. The sample was taken after 120 min incubation from basolateral compartment at 37 °C. The detection was measured at 320 nm.

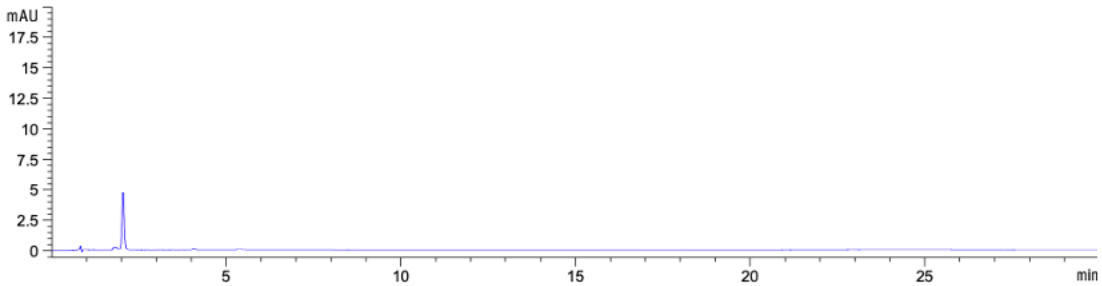

Figure 47 HPLC chromatograms of OXY transport across Caco-2 cell monolayers with retention time at 2.1 min. The sample was taken after 240 min incubation from basolateral compartment at 37 °C. The detection was measured at 320 nm.

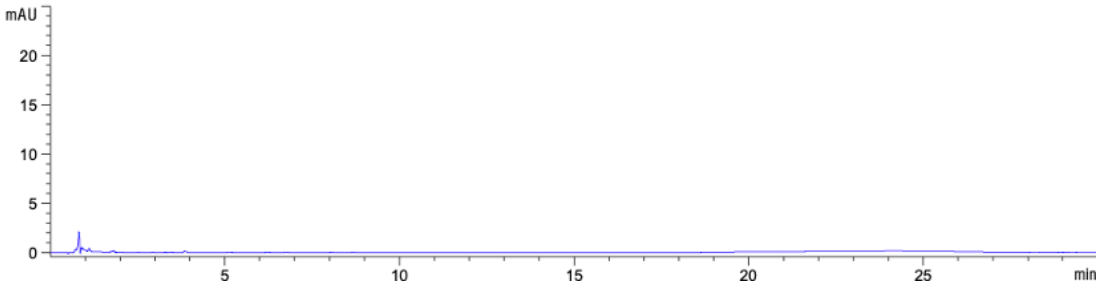

Figure 48 HPLC chromatograms of OXY-TAc transport across Caco-2 cell monolayers. The sample was taken after 0 min incubation from basolateral compartment at 37 °C. The detection was measured at 320 nm.

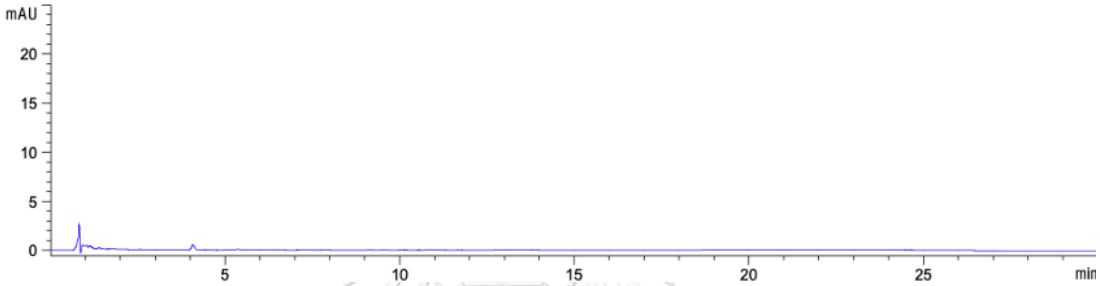

Figure 49 HPLC chromatograms of OXY-TAc transport across Caco-2 cell monolayers. The sample was taken after 15 min incubation from basolateral compartment at 37 °C. The detection was measured at 320 nm.

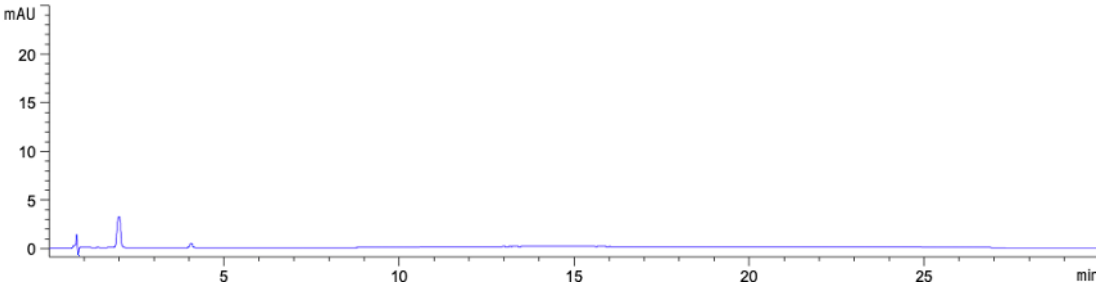

Figure 50 HPLC chromatograms of OXY-TAc transport across Caco-2 cell monolayers with retention time at 2.1 min. The sample was taken after 30 min incubation from basolateral compartment at 37 °C. The detection was measured at 320 nm.

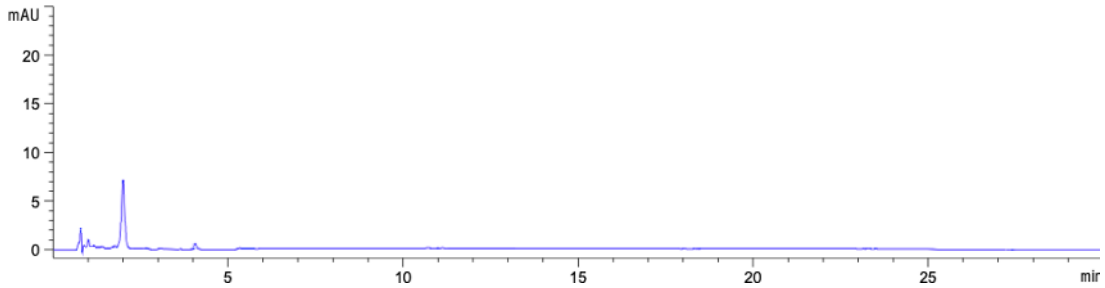

Figure 51 HPLC chromatograms of OXY-TAc transport across Caco-2 cell monolayers with retention time at 2.1 min. The sample was taken after 60 min incubation from basolateral compartment at 37 °C. The detection was measured at 320 nm.

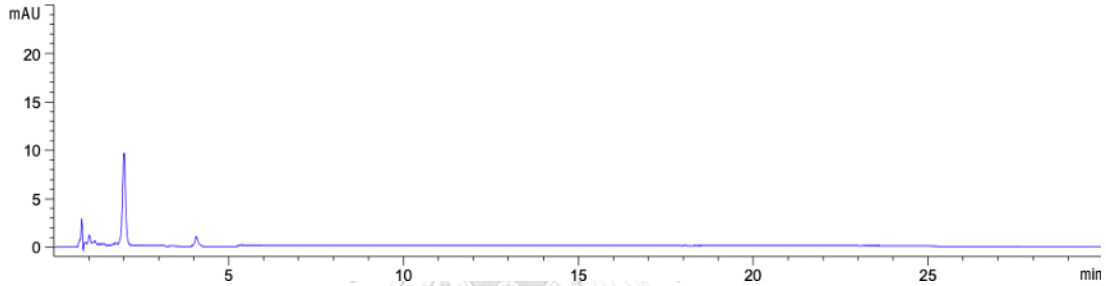

Figure 52 HPLC chromatograms of OXY-TAc transport across Caco-2 cell monolayers with retention time at 2.1 min. The sample was taken after 120 min incubation from basolateral compartment at 37 °C. The detection was measured at 320 nm.

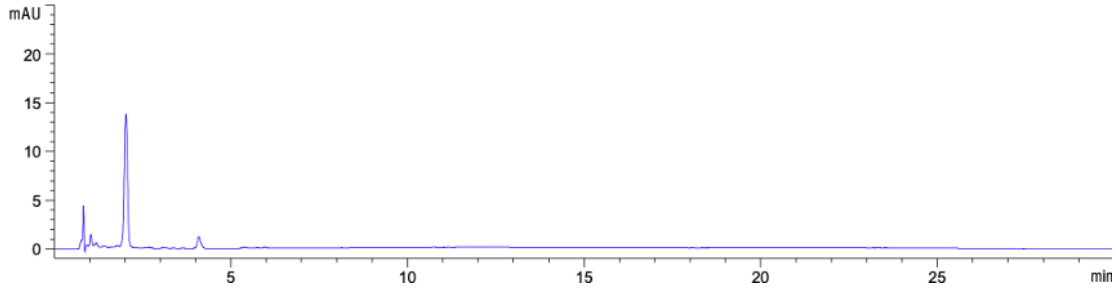

Figure 53 HPLC chromatograms of OXY-TAc transport across Caco-2 cell monolayers with retention time at 2.1 min. The sample was taken after 240 min incubation from basolateral compartment at 37 °C. The detection was measured at 320 nm.

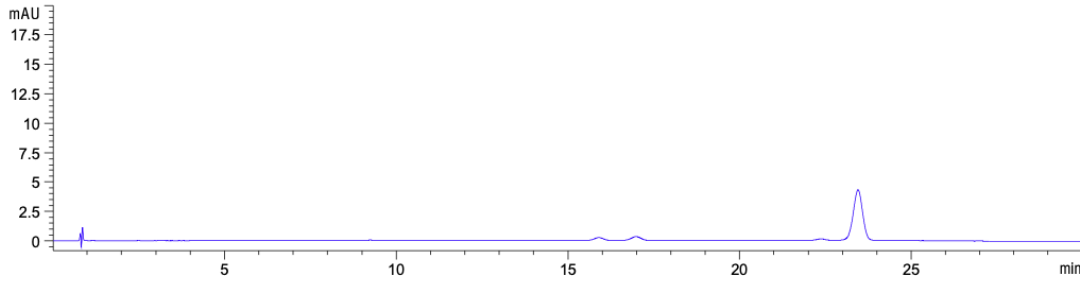

Figure 54 HPLC chromatograms of OXY-TAc with retention time at 23.4 min. The sample was taken after 1 h incubation in hydrochloric acid buffer pH 1.2 at 37 °C. The detection was measured at 320 nm.

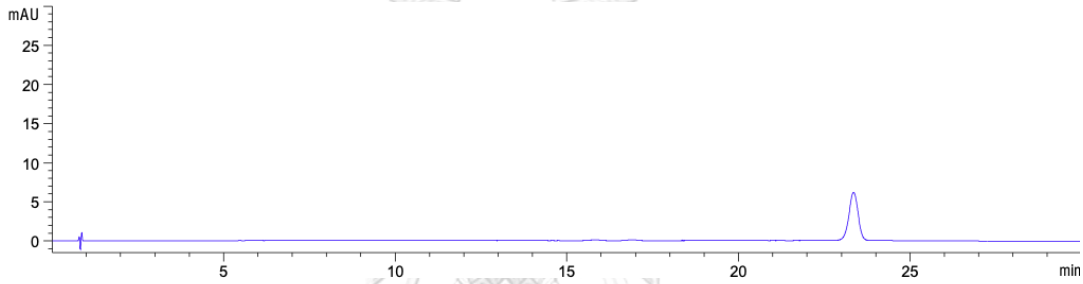

Figure 55 HPLC chromatograms of OXY-TAc with retention time at 23.4 min. The sample was taken after 1 h incubation in phosphate buffer pH 6.8 at 37 °C. The detection was measured at 320 nm.

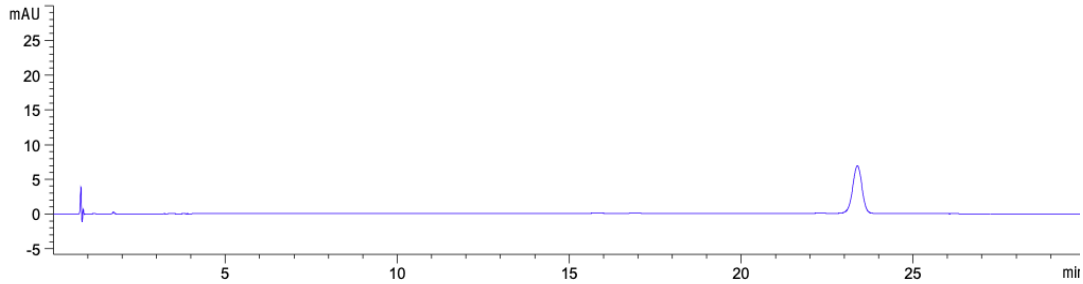

Figure 56 HPLC chromatograms of OXY-TAc with retention time at 23.4 min. The sample was taken after 1 h incubation in phosphate buffer pH 7.4 at 37 °C. The detection was measured at 320 nm.

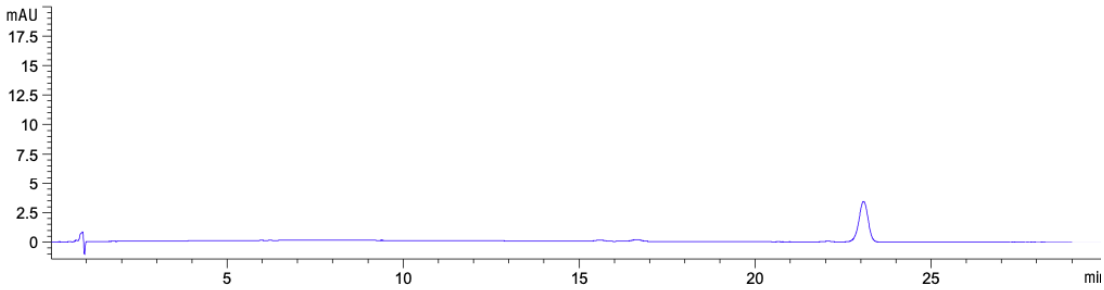

Figure 57 HPLC chromatograms of OXY-TAc with retention time at 23.1 min. The sample was taken after 30 min incubation in SGF at 37 °C. The detection was measured at 320 nm.

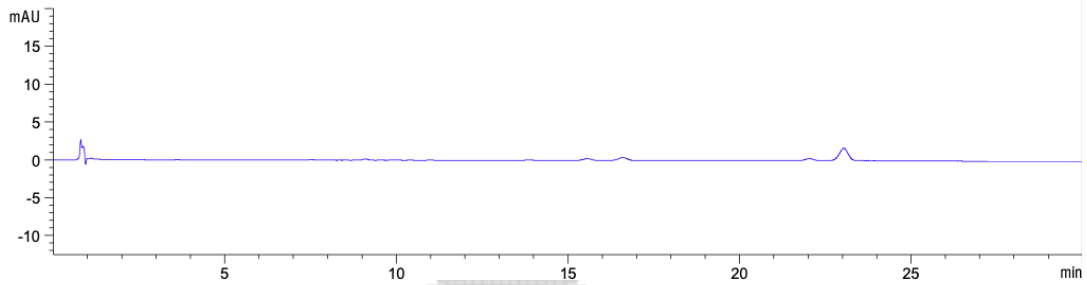

Figure 58 HPLC chromatograms of OXY-TAc with retention time at 23.0 min. The sample was taken after 15 min incubation in SIF at 37 °C. The detection was measured at 320 nm.

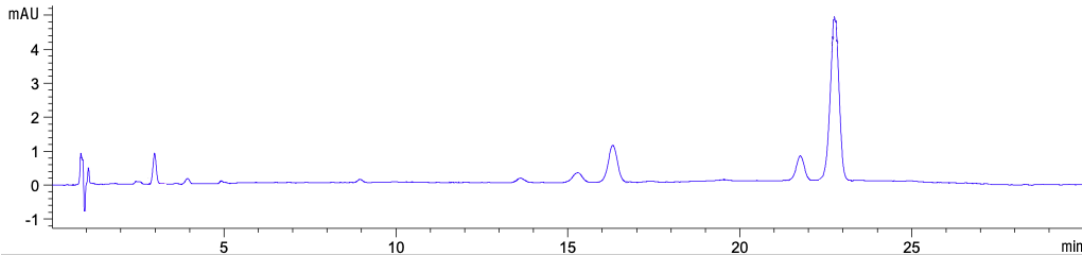

Figure 59 HPLC chromatogram of OXY-TAc with retention time at 22.8 min. The sample was taken after 10 s incubation in human plasma at 37 °C. The detection was measured at 320 nm.

APPENDIX C

REACTION OF ACID ANHYDRIDE AND ALCOHOL

General Reaction

Reactions of anhydrides use pyridine as a solvent

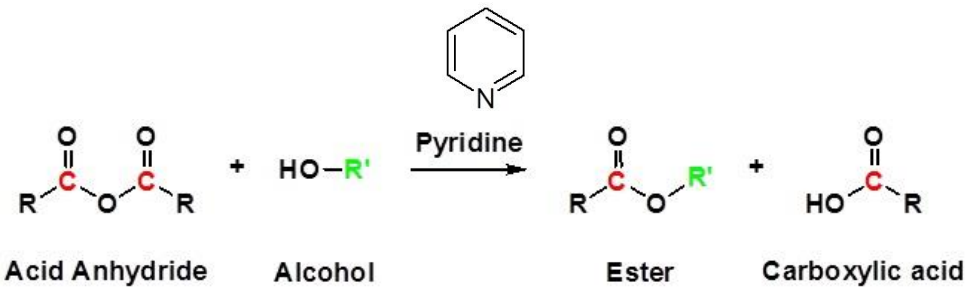

Mechanism

1. Nucleophilic attack by the alcohol

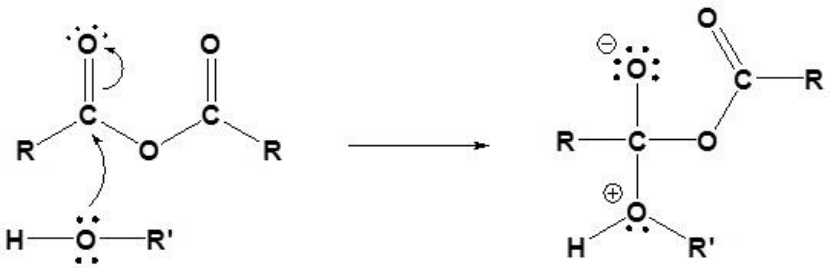

2. Deprotonation by pyridine

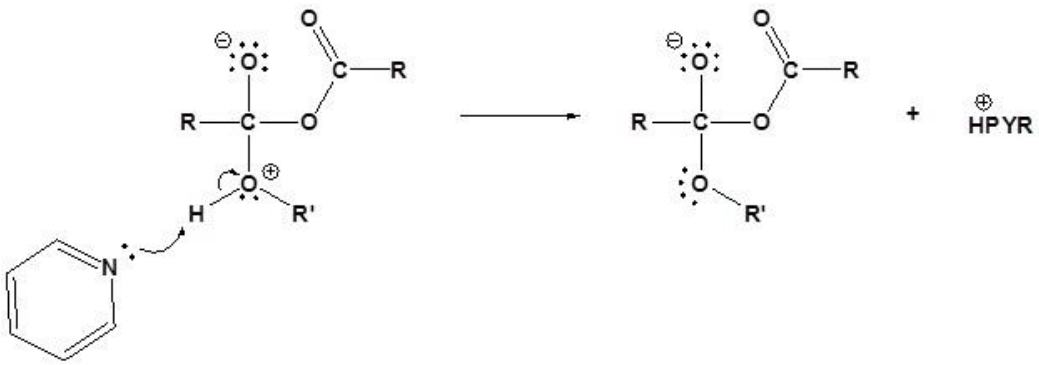

3. Leaving group removal

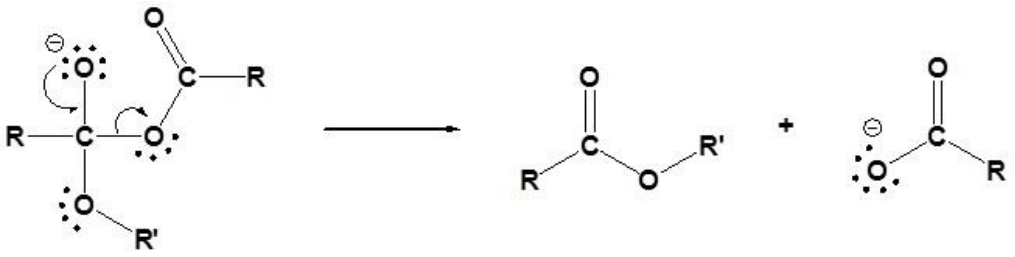

4. Protonation of the carboxylate

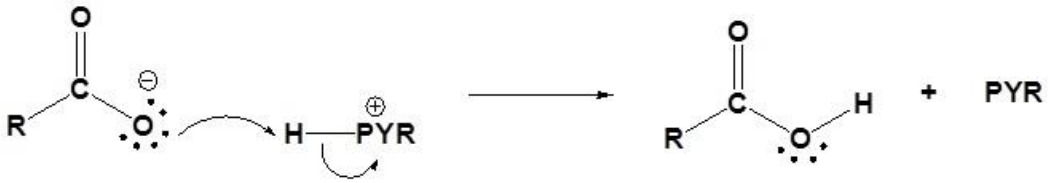

APPENDIX D

CULTURE MEDIA

1. Reagent

1.1 Dulbecco's modified Eagle's medium (DMEM)	(Gibco 12800, USA)
1.2 Fetal bovine serum (FBS)	(Gibco, 16000-044)
1.3 L-Glutamine 200 mM (100x)	(Gibco, 25030-081)
1.4 Nonessential amino acids	(Gibco, 11140-050)
1.5 Penicillin-Streptomycin	(Gibco, 15140-122)
1.6 Fungizone	(Gibco, 15290-081)
1.7 Sodium bicarbonate ($NaHCO_3$) (MW 84.01)	(Sigma Co. S5761)

2. Heat-inactivated fetal bovine serum (ΔFBS)

FBS was thawed in a water bath at 37 °C, and then FBS was incubated in a water bath at 56.7°C for 30 min and mix every 10 min.

3. Basal Dulbecco's Modified Minimum Essential Medium (D7777) (1 L)

(DEMEM or serum-free media)

3.1. 850 mL dH_2O slowly add contents from 1 pack of powdered DMEM (12800, Gibco) into the beaker with stir bar at moderate speed.

3.2. Stir at a moderate rate to dissolve for 30 min at room temperature

3.3. Add 3.7 g $NaHCO_3$ (44 mM) and stir until solubilized

3.4. Adjust pH to 7.2-7.3 with 1M HCl or 1 M

3.5. Transfer medium to a volumetric flask and adjust the volume to 1 L Filter sterilize, a label indicating contents, your initials and date, and store at 4^0C

4. Complete media (cDMEM) for Caco-2 cells

4.1 Preparation of cDMEM (complete DMEM) + 15% ΔFBS (100 ml) Sterile

4.1.1 Pipette 15 mL of FBS heat inactivate

4.1.2 Pipette 1 mL of penicillin-streptomycin

4.1.3 Pipette 1 mL of L-glutamine

4.1.4 Pipette 1 mL of nonessential amino acids

4.1.5 Pipette 0.2 mL of fungizone

4.1.6 Adjust total volume to 100 mL by basal DMEM

4.2 Preparation of cDMEM (complete DMEM) + 7.5% ΔFBS (100 mL) Sterile

4.2.1 Pipette 7.5 mL of FBS heat inactivate

4.2.2 Pipette 1 mL of penicillin-streptomycin

4.2.3 Pipette 1 mL of L-glutamine

4.2.4 Pipette 1 mL of nonessential amino acids

4.2.5 Pipette 0.2 mL of fungizone

4.2.6 Adjust total volume to 100 mL by basal DMEM

5. Complete media (cDMEM) for RAW264.7 macrophage cells

5.1 Preparation of cDMEM (complete DMEM) + 10% ΔFBS (100 mL) Sterile

5.1.1 Pipette 10 mL of FBS heat inactivate

5.1.2 Pipette 1 mL of penicillin-streptomycin

5.1.3 Adjust total volume to 100 mL by basal DMEM

APPENDIX E

CELL CULTURE

1. Resuscitation of frozen cells

1.1 cDMEM was warmed in a 37 ºC water bath for 30 min before removing the cryogenic tube from liquid nitrogen

1.2 cDMEM 12 mL was added of in 75 cm^2 flask and incubated in an incubator

1.3 cDMEM 4 mL was added of in 15 mL plastic tubes

1.4 The cryogenic tube was transferred to a 37 ºC water bath for 1-2 min until fully thawed. Quickly thawing the cryogenic tube will minimize any damage to the cell membranes. Be careful not to totally immerse the cryogenic tube - this may increase contamination risk

1.5 Wipe cryogenic tube with a tissue soaked in 70% alcohol prior to opening.

1.6 Total cell stock solution was transferred from a cryogenic tube into 15 mL plastic tubes containing 4 mL of cDMEM

1.7 Centrifuged at 800 rpm for 5 min

1.8 The supernatant was discarded and resuspend with 2-3 mL of cDMEM

1.9 The total cell solution was transferred into 75 cm^2 flask containing 13 mL of cDMEM Incubate in a CO_2 incubator

2. Growth and maintenance of live cell cultures

2.1 Media was placed in a water bath (37 ºC) for 15-20 min

2.2 A dish of cells was taken out of CO_2 incubator

2.3 Cells were examined under a microscope to determine health/condition.

2.4 In the hood, label the appropriate number of new dishes with the cell line name, the passage number, the date, and the initial name. Cells were subcultured when it showed 70-80%confluence

2.5 Old media was removed from the flask by aspiration. Cells were washed with 5 mL warmed DMEM

2.6 1X trypsin-EDTA 5 mL was added and then incubated at 37 °C for 5-10 min.

2.7 cDMEM 5 mL was added

2.8 Total solution was transferred to 15 mL tube

2.9 Centrifuged at 800 rpm for 5 min

2.10 The supernatant was discarded and resuspend with 2-3 mL of cDMEM + 15% FBS for count cell in a hemocytometer

2.11 Cells were seeded on a new 75 cm^2 flask at 0.4 $x10^6$/flask with 12 mL cDMEM + 15% FBS/flask, and the plate was returned to the CO_2 incubator

3. Cell Quantification

3.1 The hemocytometer was cleaned

3.2 Cells suspension 30 µL was pipetted of into 30 µL of trypan blue (dilution factor = 2) by gentle pipetting

3.3 Fill both sides of the chamber (approx. 10 µL) with cell suspension and view under a light microscope by using x20 magnification

3.4 The number of non-viable cells and viable cells was counted

3.5 The percentage of viable cells was calculated

4. Calculate total cell number as follows:

4.1 Means of 16 square x 2 (dilution into trypan blue) x 10^4 (volume of cell suspension per 16 squares is 0.1 µL) = number of cells per mL

4.2 For example, if 100 and 90 cells in two sets of 16 squares,

$$(110+90)/2 = 100$$

100 x 2 (dilution factor) x 10^4 = 2.00 x 10^6 cells/mL

Also count cells that accumulate trypan blue (dead cells)

in each set of 16 squares, viable cells/ (viable cells + dead cells) x 100 = % viability (routinely > 95% viability).

Calculate cell numbers needed for new T-75 flasks and new 6 or 12 well plates

Seeding number at 3.0 – 4.0 x 10^5 cells per T75-flask (12 mL/flask)

2.5-3.5 x 10^5 cells per well of a 6 well-dish (2 mL/well)

2.0-2.5 x 10^5 cells per well of insert (1.5 mL/insert)

4.3 When preparing cells for seeding new dishes or flasks, always make 1.2 flasks or for an extra well to account for pipetting errors.

APPENDIX F

PREPARATION OF BUFFER

1) 0.1 N HCl pH 1.2

The 0.1 N HCl solutions were prepared by combining a 0.2 M potassium chloride solution with a 0.2 M hydrochloric acid solution. The 0.2 M potassium chloride solution was prepared by charging 74.55 g of potassium chloride to a carboy and filling to 5 L with Milli-Q water. The 0.2 M hydrochloric acid solution was prepared by diluting 165.3 mL of HCl with milli-Q water to 10 L. To prepare the final solution (0.1N HCl), 5 L of potassium chloride solution was charged to a carboy followed by 8.5 L of 0.2 M hydrochloric acid solution. Milli-Q water was then added to 20 L. The final pH was recorded.

2) Phosphate Buffer pH 6.8 and 7.4

The phosphate buffers pH 6.8 and 7.4 were prepared with potassium phosphate monobasic and milli-Q water. The initial studies utilized potassium phosphate monobasic solutions and were prepared in accordance with procedures defined in the current USP. However, final studies utilized phosphate buffer prepared according to the following procedure. For 20 L of the buffer, 136 g of potassium phosphate monobasic was weighed and charged to a carboy. The carboy was filled to 20 L with Milli-Q water, and the initial pH was recorded. While stirring, potassium hydroxide was added to adjust the pH of the solution to 6.8 (or 7.4), and the final pH was recorded.

APPENDIX G

DETERMINATION OF PROTEIN CONCENTRATION BY BCA ASSAY

The BCA Assay combines the well-known reduction of Cu^{2+} to Cu^{+} by protein in the alkaline medium with the highly selective colorimetric and sensitive detection of Cu^{+} by bicinchoninic acid.

The first step is the chelation of Cu with protein to form a blue colored complex in an alkaline environment. In this reaction, biuret reaction, peptides containing three or more amino acid residues form a colored chelate complex with Cu^{2+} in an alkaline environment containing sodium potassium tartrate. This was known as the biuret reaction because of similar complex forms with the organic compound biuret (NH-CO-NH-CO-NH) and the cupric ion. Biuret, a product of excess urea and heat, reacts with copper to form a light blue tetradentate complex. Single amino acids and dipeptides do not produce a biuret reaction, but tripeptides and larger polypeptides or proteins react to produce the light blue to purple complex that absorbs light at 540 nm. One cupric ion forms a colored coordination complex with 4 - 6 peptides bonds. The intensity of the produced color is proportional to the number of peptide bonds involved in the reaction. The biuret reaction is, therefore, the basis for a simple and rapid colorimetric reagent of the same name for the quantitative determination of the total protein concentration. Since the working range for the biuret assay is between 5 and 160 mg/mL, the biuret assay is used in clinical laboratories to quantify the total protein in serum.

In the second step of the color reaction, BCA Reagent, a highly sensitive and selective colorimetric detection reagent reacts with Cu^{+} that was formed in step 1. The purple reaction product is formed by the chelation of two molecules of BCA Reagent with one cuprous ion (Figure 48). The complex is water-soluble and has a strong linear absorbance at 562 nm with increased protein concentrations.

Step 1

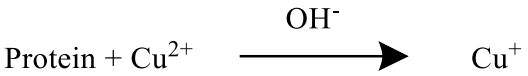

Step 2

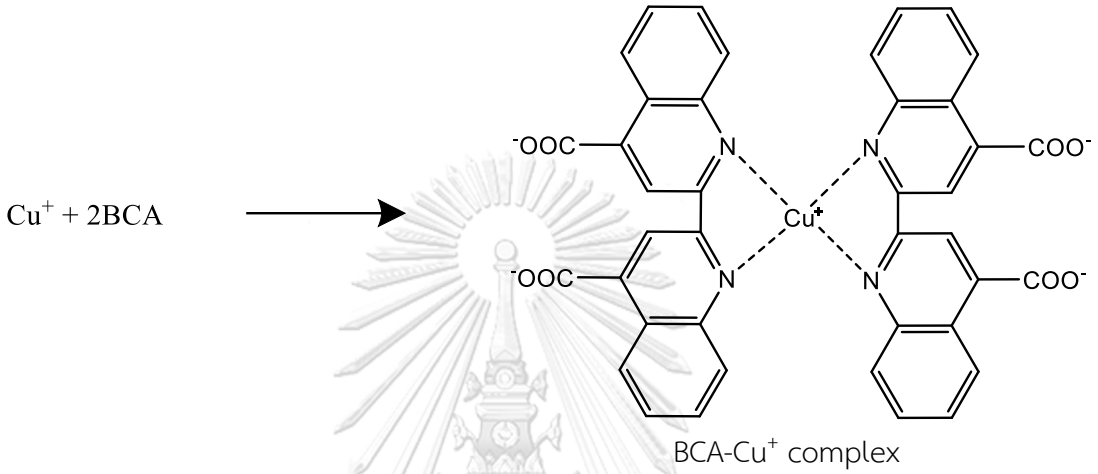

Figure 60 Reaction schematic for the bicinchoninic acid (BCA)-containing protein assay.

Reagents:

1. BCA™ Protein Assay Reagent A (Thermo Scientific cat.no. 23223)
2. Micro-reagent A

$NaHCO_3$ anhydrous	6.84 g
NaOH	1.6 g
KNa tartrate anhydrous	1.6 g

Add $NaHCO_3$ to adjust the pH 11.25, make up the volume to 100 ml with dH_2O

3. 4%$CuSO_4 \cdot 5H_2O$

$CuSO_4 \cdot 5H_2O$	4 g
Deionized water	100 mL

Working reagent (freshly prepared)	40 samples
BCA™ Protein Assay Reagent A	4 mL
Micro-reagent B	4 mL
4%$Cu_2SO_4 \cdot 5H_2O$	160 µL
Total	8.16 mL

Protocol:

1. Dilute protein lysate 1:10 (for RAW264.7) with deionized water.
2. Prepare serial dilution of standard BSA 0.125, 0.25, 0.5, 1 and 2 mg/mL, used deionized water as blank.
3. Pipette 10 µl of diluted lysate and standard protein to the microplate.
4. Add 200µl of working reagent, mix 30 s on shaker
5. Incubate 37 °c for 30 min
6. Read absorbance at 562 nm with a microplate reader
7. Generate the standard curve and quantitate the protein concentration of the unknown.

APPENDIX H

WESTERN BLOT

1. Lysis buffer for western blot

Stock	For 2 mL	Final concentration
1 M Tris-HCl (pH 7.4)	100 µL	50 mM
1.5 M NaCl	200 µL	150 mM
0.05 M EDTA (pH 8.0)	40 µL	1 mM
Triton-x 100	20 µL	1%
10%SDS	20 µL	0.1%
1 M Sodium fluoride	200 µL	50 mM
200 mM Sodium pyrophosphate	200 µL	10 mM
Protease inhibitor cocktail	10 µL	N/A
Water	1200 µL	N/A

2. Loading buffer (Laemmli buffer)

(10x, 62.5mM Tris pH 6.8, 0.625M β-mercaptoethanol, 10% glycerol, 2%SDS, 0.00125% bromophenol blue.)

Stock	For 8 mL	
dH_2O	3.0	mL
Glycerol	0.8	mL
10% SDS	1.6	mL
0.25M TrisHCl pH 6.8	2.0	mL
β -mercaptoethanol	0.4	mL

0.05% (w/v) bromophenol blue 0.2 mL or a few specs

To sample add ¼ volume of loading buffer before heating (used at 2x) (2x, 31.25mM Tris pH 6.8, 0.125M β-mercaptoethanol, 2% glycerol, 0.4% SDS, 0.00025% bromophenol blue)

3. **Separating gel buffer or Resolving gel buffer (**Tris-HCl 3M pH8.85) 100 mL

   Tris 36.33 g

   Add around 80 mL dH_2O and pH with HCl

   Make volume up to 100 mL

4. **Stacking gel buffer** (0.25M Tris-HCl pH6.8) 100 mL

   Tris 3.028 g

   Add around 80 mL dH_2O and pH with HCl

   Make volume up to 100 mL

5. **10% APS** (ammonium persulfate) 500uL

   0.05g in 500ul dH_2O

6. **10% SDS**

   50g in 50mL dH_2O

7. **5x running buffer** (1 L)

   (0.125M Tris, 1.25M Glycine, 0.5%SDS)

   Tris base 15.1 g

   Glycine 94 g

   10% SDS 50 mL

   Adjust volume to 1L

   Use at 1x. (0.25M glycine, 0.025M Tris, 0.1%SDS)

8. **Transfer buffer** (1L)

   5x running buffer 100 mL

   100% ethanol 233 mL

   make up to 1L with dH_2O

9. 10x TBS (0.2M Tris, pH7.6) 1 L

NaCl	80	g
Tris	24.2	g

Adjust pH to 7.6 with HCl and makeup to 1L with dH_2O

10. Wash buffer (0.2M Tris M NaCl pH7.6, 0.1% Tween-20) 1 L

10x TBS	100	mL
Tween-20	1	mL

Make volume up to 1000 mL with dH_2O

11. Blocking buffer (0.02M Tris Nacl pH7.6, 0.1% Tween-20 with 5%(w/v) non-fat dry milk) 100 mL

powdered milk	5	g
wash buffer	100	mL

APPENDIX I

ANTIOXIDANT ACTIVITY ASSAY

The available methods to quantify antioxidant activity can be classified based on the mechanism of action by which the applied compounds stop chain-breaking reactions. They can be categorized into two groups: hydrogen-atom transfer (HAT) reactions and single electron transfer (SET) (compound reduction reactions through electron transfer from an antioxidant) [132]. Several assays have frequently been used to estimate the antioxidant capacity of natural antioxidants, including DPPH, FRAP, and ORAC assays [138-141].

1. DPPH assay

DPPH assay is one of the most stable free radicals and is frequently used in the evaluation of radical scavengers in phenolic compounds [142, 143]. DPPH method is very simple and is also quick for manual analysis of antioxidant capacity. DPPH is not only specific to any specific antioxidant but also to the overall antioxidant content of the sample and can be employed for liquid or solid samples. The DPPH assay is based on the ability of the stable DPPH free radical to react with hydrogen donors. The DPPH radical displays an intense ultraviolet-visible (UV-vis) absorption spectrum. In this test, a solution of radicals is decolorized after reduction with an antioxidant (RH) in Figure 49 [144]. The DPPH analysis is a fast and uncomplicated test ensuring reliable results. Furthermore, it requires only a UV-vis spectrophotometer to perform, which explains its widespread use in screening antioxidant properties. The method is not a competitive reaction, since DPPH is both a radical probe and an oxidant. DPPH is a stable nitrogen radical that bears no similarity to the highly reactive and transient peroxyl radicals involved in lipid peroxidation.

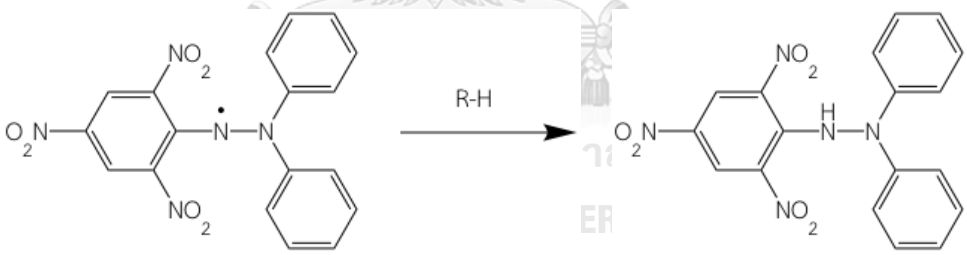

DPPH **DPPH-H**

(517 nm)

Figure 61 Mechanism of DPPH assay. DPPH free radical conversion to DPPH-H by antioxidant compound (RH).

2. ORAC assay

ORAC is a method for quantifying the antioxidant strength of substances. It involves combining the sample with being tested (i.e., the antioxidant) with a fluorescent compound as well as a compound that produces free radicals at a known rate. As free radicals are produced, the fluorescent compound is damaged, and then it loses its fluorescence. When antioxidants are present, free radicals are produced and therefore inhibit the loss of fluorescence as described above. The stronger the antioxidant properties of a substance, the higher is the degree of inhibition of fluorescence loss. The calculation is standardized Trolox, which has a defined ORAC value and is reported as Trolox equivalents (TE). This assay serves as an excellent way to quantify the ability of various compounds to quench free radicals. The free radicals in the ORAC method are produced by AAPH followed by the oxidation of the fluorescent indicator (Figure 50) [145]. The loss of fluorescence can be inhibited by antioxidants and was measured using a microplate fluorescence reader.

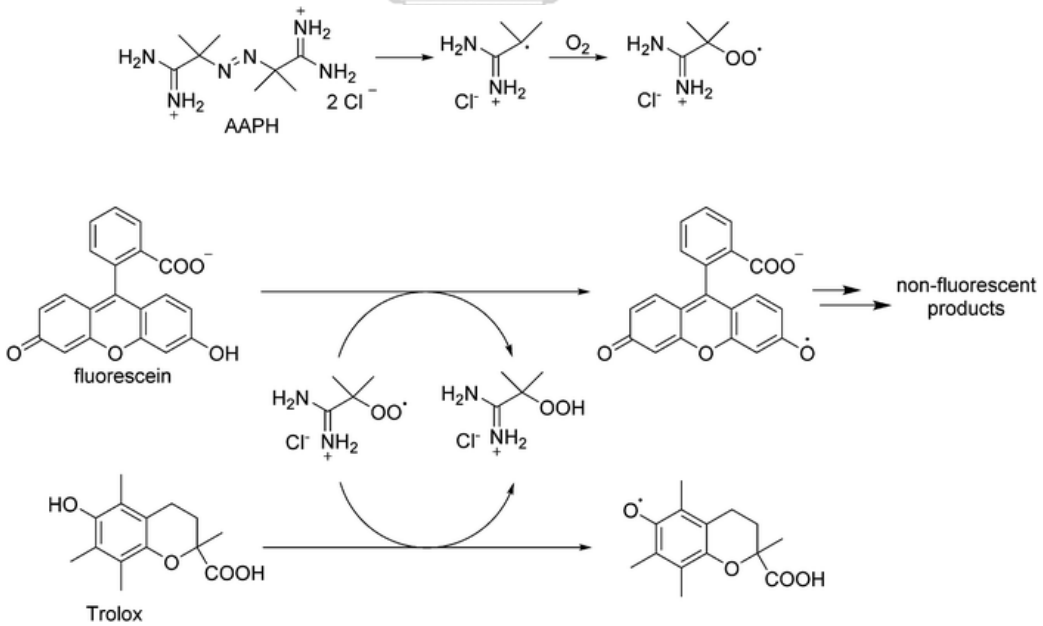

Figure 62 Mechanism of ORAC assay.

3. FRAP assay

The FRAP method is another method that can be used to assess the total antioxidant activity of phenolic compounds [142, 143]. The FRAP assay uses antioxidants as reductants in a redox-linked colorimetric method, using an easily reduced oxidant system present in stoichiometric excess. FRAP assay has so far been widely used to directly test the total antioxidant potential of several plant extracts and foods based on the reduction of complexes of 2,4,6-tri(2-pyridyl)-1,3,5-triazine (TPTZ) with ferric chloride hexahydrate ($FeCl_3 \cdot 6H_2O$), which are almost colorless. The FRAP assay relies on the reduction by the antioxidants of the complex ferric ion-TPTZ (Figure 51). The binding of Fe^{2+} to the ligand creates a very intense navy-blue color. The solution will gradually turn slightly brownish, forming blue ferrous complexes after complete reduction [146]. Increased absorbance of the reaction mixture suggested increased reducing power.

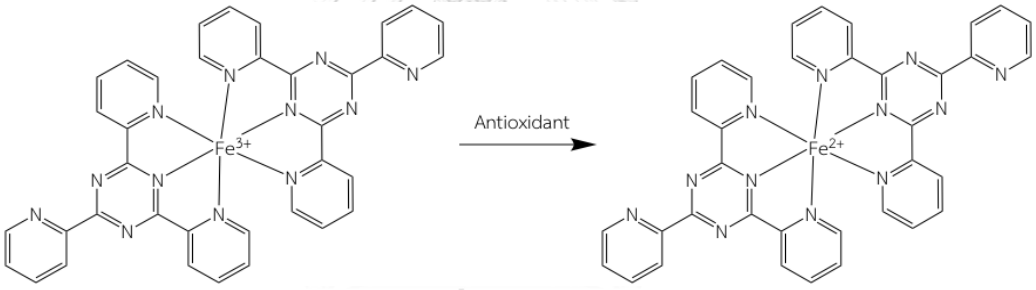

$[Fe(III)(TPTZ)_2]^{3+}$ $[Fe(III)(TPTZ)_2]^{2+}$

Figure 63 Mechanism of FRAP assay.

APPENDIX J

CERTIFICATE OF OXY

B&P INGREDIENTS LIMITED.
ADDRESS: NO. 28, MAJI RD, PUDONG, SHANGHAI, CHINA (200131)
PHONE: (8621) 3100-6931

CERTIFICATE OF ANALYSIS

PRODUCT NAME	OXYRESVERATROL
CAS NO.	29700-22-9
BATCH NUMBER	CY160409
BATCH QUANTITY	10KG
MANUFACTURE DATE	APR. 09, 2016
DATE OF CERTIFICATE	APR. 15, 2016

ANALYSIS	SPECIFICATION	RESULTS
APPEARANCE	SLIGHT YELLOW OR OFF WHITE POWDER	COMPLIES
ODOR	CHARACTERISTIC	COMPLIES
ASSAY (HPLC ON ANHYDROUS BASIS)	OXYRESVERATROL≥98.0%	99.25%
MELTING POINT	199-204°C	199-203°C
SIEVE ANALYSIS	NLT 95% PASS 80 MESH	COMPLIES
LOSS ON DRYING	≤0.5%	0.18%
HEAVY METAL	<10PPM	COMPLIES
AS	<2PPM	COMPLIES
RESIDUAL SOLVENTS	EUR.PHARM.	COMPLIES
MICROBIOLOGY		
TOTAL PLATE COUNT	<1000CFU/G	COMPLIES
YEAST & MOULDS	<100CFU/G	COMPLIES
E.COLI	NEGATIVE	COMPLIES
SALMONELLA	NEGATIVE	COMPLIES

CONCLUSION	CONFORM TO SPECIFICATION
STORAGE	STORE IN SEALED CONTAINERS AT COOL & DRY PLACE. PROTECT FROM LIGHT, MOISTURE AND PEST INFESTATION.
SHELF LIFE	2 YEARS WHEN PROPERLY STORED

APPENDIX K

CERTIFICATE OF HUMAN PLASMA

Certificate of Analysis

Product:	Pooled Normal Human Plasma		
Anticoagulant:	Na Heparin		
Lot:	17793		
Quantity:	2	Age:	Not Applicable
Volume:	100ml	Gender:	Not Applicable
Storage:	-20°	Race:	Not Applicable
Notes:			
Description:	Human Plasma is collected at an FDA Licensed commercial donor center / facility within the United States. Each unit is tested and found negative for: HBsAg, HCV, HIV-1, HIV-2, HIV-1Ag or HIV 1-NAT, ALT, and syphilis by FDA-Approved Methods.		
Expiration:	Based upon evaluation of the stability of "signal chemistries" (critical parameters of the sera from the biochemical profile) serum and plasma is stable for 3 years from date of manufacture when stored in unopened containers at temperatures of (– 20) deg C or below.		
Handling:	This material is sold for in-vitro use only in manufacturing and research. This material is not suitable for human use. It is the responsibility of the user to undertake sufficient verification and testing to determine the suitability of each product's application. The statements herein are offered for informational purposes only and are intended to be used solely for your consideration, investigation and verification.		

APPENDIX L

HYDROLYSIS OF OXY-TAc IN SIF

Zero-order

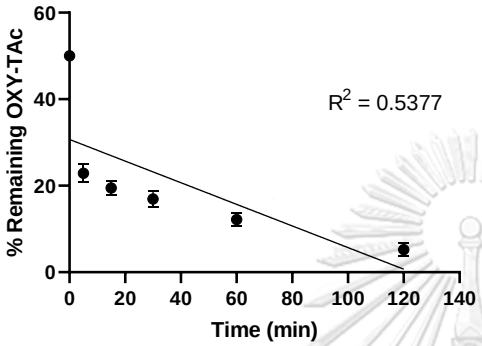

Pseudo-first order

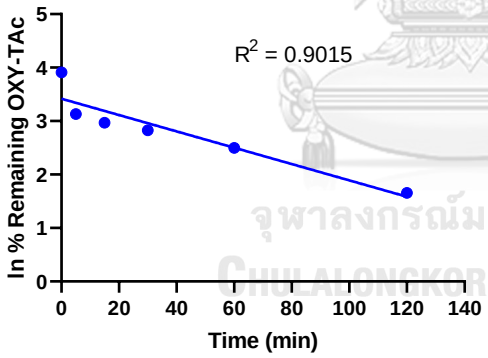

Second-order

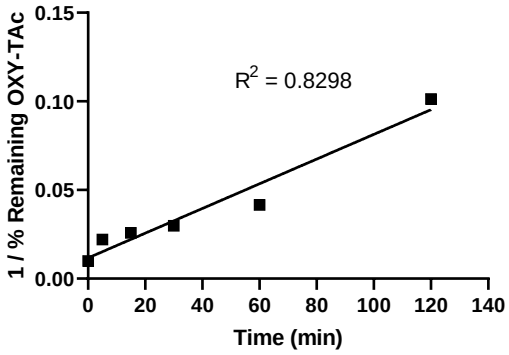

APPENDIX M

POSITIVE CONTROL

Vitamin C was selected as a positive control because Vitamin C has antioxidant activity. Vitamin C has been reported as a positive control in ROS production in LPS-induced macrophage cells [147-149].

Indomethacin was selected as a positive control because indomethacin is a standard anti-inflammatory. Indomethacin was reported as a positive control in PGE_2, TNF-α, IL-1β, IL-6, iNOS protein and COX-2 protein production in LPS-induced macrophage cells [150-152]

REFERENCES

[1] Caruso, G., et al. Carnosine Decreases PMA-Induced Oxidative Stress and Inflammation in Murine Macrophages. Antioxidants 8(8) (2019): 281.

[2] Sangsen, Y., Wiwattanawongsa, K., Likhitwitayawuid, K., Sritularak, B., and Wiwattanapatapee, R. Modification of oral absorption of oxyresveratrol using lipid based nanoparticles. Colloids and Surfaces B: Biointerfaces 131 (2015): 182-90.

[3] Chung, K.-O., et al. In-vitro and in-vivo anti-inflammatory effect of oxyresveratrol from Morus alba L. Journal of Pharmacy and Pharmacology 55(12) (2003): 1695-1700.

[4] Hwang, D., Jo, H., Kim, J.-K., and Lim, Y.-H. Oxyresveratrol-containing Ramulus mori ethanol extract attenuates acute colitis by suppressing inflammation and increasing mucin secretion. Journal of Functional Foods 35(Supplement C) (2017): 146-158.

[5] Fang, S.-C., Hsu, C.-L., and Yen, G.-C. Anti-inflammatory Effects of Phenolic Compounds Isolated from the Fruits of Artocarpus heterophyllus. Journal of Agricultural and Food Chemistry 56(12) (2008): 4463-4468.

[6] Aftab, N., Likhitwitayawuid, K., and Vieira, A. Comparative antioxidant activities and synergism of resveratrol and oxyresveratrol. Natural Product Research 24(18) (2010): 1726-1733.

[7] Povichit, N., Phrutivorapongkul, A., Suttajit, M., and Leelapornpisid, P. Antiglycation and antioxidant activities of oxyresveratrol extracted from the heartwood of Artocarpus lakoocha Roxb. Maejo International Journal of Science and Technology 4 (2010): 454-461.

[8] Hu, S., Chen, F., and Wang, M. Photoprotective Effects of Oxyresveratrol and Kuwanon O on DNA Damage Induced by UVA in Human Epidermal Keratinocytes. Chemical Research in Toxicology 28(3) (2015): 541-548.

[9] Oh, H., et al. Hepatoprotective and free radical scavenging activities of prenylflavonoids, coumarin, and stilbene from Morus alba. Planta Medica 68(10)

(2002): 932-4.

[10] Lorenz, P., Roychowdhury, S., Engelmann, M., Wolf, G., and Horn, T.F.W. Oxyresveratrol and resveratrol are potent antioxidants and free radical scavengers: effect on nitrosative and oxidative stress derived from microglial cells. Nitric Oxide 9(2) (2003): 64-76.

[11] Sasivimolphan, P., et al. Inhibitory activity of oxyresveratrol on wild-type and drug-resistant varicella-zoster virus replication in vitro. Antiviral Research 84(1) (2009): 95-97.

[12] Likhitwitayawuid, K., Sritularak, B., Benchanak, K., Lipipun, V., Mathew, J., and Schinazi, R.F. Phenolics with antiviral activity from Millettia Erythrocalyx and Artocarpus Lakoocha. Natural Product Research 19(2) (2005): 177-182.

[13] Jeon, Y.-H. and Choi, S.-W. Isolation, Identification, and Quantification of Tyrosinase and ฮฑ-Glucosidase Inhibitors from UVC-Irradiated Mulberry (Morus alba L.) Leaves. Preventive Nutrition and Food Science 24(1) (2019): 84-94.

[14] Jo, S.-P., Kim, J.-K., and Lim, Y.-H. Antihyperlipidemic effects of stilbenoids isolated from Morus alba in rats fed a high-cholesterol diet. Food and Chemical Toxicology 65(Supplement C) (2014): 213-218.

[15] Park, K.-T., Kim, J.-K., and Lim, Y.-H. Deglycosylation of stilbene glucoside compounds improves inhibition of 3-hydroxy-3-methylglutaryl coenzyme a reductase and squalene synthase activities. Food Science and Biotechnology 23(2) (2014): 647-651.

[16] He, H. and Lu, Y.-H. Comparison of Inhibitory Activities and Mechanisms of Five Mulberry Plant Bioactive Components against α-Glucosidase. Journal of Agricultural and Food Chemistry 61(34) (2013): 8110-8119.

[17] Andrabi, S.A., Spina, M.G., Lorenz, P., Ebmeyer, U., Wolf, G., and Horn, T.F.W. Oxyresveratrol (trans-2,3′,4,5′-tetrahydroxystilbene) is neuroprotective and inhibits the apoptotic cell death in transient cerebral ischemia. Brain Research 1017(1) (2004): 98-107.

[18] Chillemi, R., Sciuto, S., Spatafora, C., and Tringali, C. Anti-tumor properties of stilbene-based resveratrol analogues: Recent results. Natural Product

Communications 2 (2007): 499-513.

[19] Wu, L.-S., Wang, X.-J., Wang, H., Yang, H.-W., Jia, A.-Q., and Ding, Q. Cytotoxic polyphenols against breast tumor cell in Smilax china L. Journal of Ethnopharmacology 130 (2010): 460-464.

[20] Chen, W., Yeo, S.C.M., Elhennawy, M.G.A.A., and Lin, H.-S. Oxyresveratrol: A bioavailable dietary polyphenol. Journal of Functional Foods 22 (2016): 122-131.

[21] Falcón-Cano, G., Molina, C., and Cabrera-Pérez, M.Á. ADME Prediction with KNIME: Development and Validation of a Publicly Available Workflow for the Prediction of Human Oral Bioavailability. Journal of Chemical Information and Modeling 60(6) (2020): 2660-2667.

[22] Kim, M.T., Sedykh, A., Chakravarti, S.K., Saiakhov, R.D., and Zhu, H. Critical evaluation of human oral bioavailability for pharmaceutical drugs by using various cheminformatics approaches. Pharmaceutical Research 31(4) (2014): 1002-1014.

[23] Huang, H., Chen, G., Lu, Z., Zhang, J., and Guo, D.A. Identification of seven metabolites of oxyresveratrol in rat urine and bile using liquid chromatography/tandem mass spectrometry. Biomedical Chromatography 24(4) (2010): 426-32.

[24] Mei, M., et al. In vitro pharmacokinetic characterization of mulberroside A, the main polyhydroxylated stilbene in mulberry (Morus alba L.), and its bacterial metabolite oxyresveratrol in traditional oral use. Journal of Agricultural and Food Chemistry 60(9) (2012): 2299-308.

[25] Naylor, M.R., et al. Lipophilic Permeability Efficiency Reconciles the Opposing Roles of Lipophilicity in Membrane Permeability and Aqueous Solubility. Journal of Medicinal Chemistry 61(24) (2018): 11169-11182.

[26] Fang, Y., Cao, W., Xia, M., Pan, S., and Xu, X. Study of Structure and Permeability Relationship of Flavonoids in Caco-2 Cells. Nutrients 9(12) (2017): 1301.

[27] Rossi Sebastiano, M., et al. Impact of Dynamically Exposed Polarity on Permeability and Solubility of Chameleonic Drugs Beyond the Rule of 5. Journal of Medicinal Chemistry 61(9) (2018): 4189-4202.

[28] Rautio, J., et al. Prodrugs: design and clinical applications. Nature Reviews Drug

Discovery 7 (2008): 255.

[29] Hu, J.N., Zou, X.G., He, Y., Chen, F., and Deng, Z.Y. Esterification of Quercetin Increases Its Transport Across Human Caco-2 Cells. Journal of Food Science 81(7) (2016): H1825-32.

[30] Zhang, B., et al. Absorption mechanism of ginsenoside compound K and its butyl and octyl ester prodrugs in Caco-2 cells. Journal of Agricultural and Food Chemistry 60(41) (2012): 10278-84.

[31] Zhang, M., Xin, X., Lai, F., Zhang, X., Li, X., and Wu, H. Cellular Transport of Esculin and Its Acylated Derivatives in Caco-2 Cell Monolayers and Their Antioxidant Properties in Vitro. Journal of Agricultural and Food Chemistry 65(34) (2017): 7424-7432.

[32] Hu, C., Chen, Z., Yao, R., and Xu, G. Inhibition of protein kinase C by stilbene derivatives from Monus alba L. Natural Product Research and Development 8(2) (1996): 13-16.

[33] Zhao, W.J., Y.T. Guo Y. Tezuka and T. Kikuchi. Chemical research on the stilbenes from Veratrum nigrum L. var. ussuriense Nakai. Chinese. Journal of Medicinal Chemistry 8 (1998): 35-37.

[34] Deng, H., He, X., Xu, Y., and Hu, X. Oxyresveratrol from Mulberry as a dihydrate. Acta Crystallographica Section E Structure Reports Online 68(Pt 5) (2012): 1318-1319.

[35] Mongolsuk S, R.A., Towers R. 2,4,3',5'-Tetrahydroxystilbene from Artocarpus lakoocha. Journal of the Chemical Society (1957): 2231-2233.

[36] Ayinampudi, S., , Y.-H.W., , B.A., , T.S., and , I.K. Quantitative analysis of oxyresveratrol in different plant parts of Morus species and related genera by HPTLC and HPLC. Journal of Planar Chromatography - Modern TLC 24(2) (2011): 125-129.

[37] Shao, B., et al. Simultaneous determination of six major stilbenes and flavonoids in Smilax china by high performance liquid chromatography. Journal of Pharmaceutical and Biomedical Analysis 44(3) (2007): 737-742.

[38] Dapic, N., Darmati, Z., Filip, S., and Jankov, R. A stilben from heartwood from Maclura pomifera. Journal of the Serbian Chemical Society 68(3) (2003): 235-237.

[39] Hanawa, F., Tahara, S., and Mizutani, J. Antifungal stress compounds from Veratrum grandiflorum leaves treated with cupric chloride. Phytochemistry 31(9) (1992): 3005-3007.

[40] Tran, H.N.K., et al. Anti-inflammatory activities of compounds from twigs of Morus alba. Fitoterapia 120 (2017): 17-24.

[41] Matencio, A., Garcia-Carmona, F., and Lopez-Nicolas, J.M. The inclusion complex of oxyresveratrol in modified cyclodextrins: A thermodynamic, structural, physicochemical, fluorescent and computational study. Food Chemistry 232(Supplement C) (2017): 177-184.

[42] Chen, Y.C., et al. Morus alba and active compound oxyresveratrol exert anti-inflammatory activity via inhibition of leukocyte migration involving MEK/ERK signaling. BMC Complementary and Alternative Medicine 13(1472-6882) (2013).

[43] Zhou, J., et al. Variations in the Levels of Mulberroside A, Oxyresveratrol, and Resveratrol in Mulberries in Different Seasons and during Growth. The Scientific World Journal 2013 (2013): 7.

[44] Kim, J.K., Kim, M., Cho, S.-G., Kim, M.-K., Kim, S.W., and Lim, Y.-H. Biotransformation of mulberroside A from Morus alba results in enhancement of tyrosinase inhibition. Journal of Industrial Microbiology and Biotechnology 37(6) (2010): 631-637.

[45] Oh, H., et al. Hepatoprotective and Free Radical Scavenging Activities of Prenylflavonoids, Coumarin, and Stilbene from Morus alba. Planta Medica 68 (2002): 932-934.

[46] Kumar, S. and Pandey, A.K. Free Radicals: Health Implications and their Mitigation by Herbals. British Journal of Medicine and Medical Research 7 (2015): 438-457.

[47] Bartsch, H. and Nair, J. Chronic inflammation and oxidative stress in the genesis and perpetuation of cancer: role of lipid peroxidation, DNA damage, and repair. Langenbeck's Archives of Surgery 391(5) (2006): 499-510.

[48] Goossens, V., et al. Redox regulation of TNF signaling. BioFactors 10(2-3) (1999): 145-156.

[49] Chang, C.-H., Yu, F.-Y., Wu, T.-S., Wang, L.-T., and Liu, B.-H. Mycotoxin Citrinin Induced Cell Cycle G2/M Arrest and Numerical Chromosomal Aberration Associated with Disruption of Microtubule Formation in Human Cells. Toxicological Sciences 119(1) (2010): 84-92.

[50] Wang, C., et al. Platycodin D and D3 isolated from the root of Platycodon grandiflorum modulate the production of nitric oxide and secretion of TNF-α in activated RAW 264.7 cells. International Immunopharmacology 4(8) (2004): 1039-1049.

[51] Lei, Y., Wang, K., Deng, L., Chen, Y., Nice, E.C., and Huang, C. Redox Regulation of Inflammation: Old Elements, a New Story. Medicinal Research Reviews 35(2) (2015): 306-340.

[52] Chatterjee, S. Chapter Two - Oxidative Stress, Inflammation, and Disease. in Dziubla, T. and Butterfield, D.A. (eds.),Oxidative Stress and Biomaterials, pp. 35-58: Academic Press, 2016.

[53] Newton, K. and Dixit, V.M. Signaling in innate immunity and inflammation. Cold Spring Harbor Perspectives in Biology 4(3) (2012).

[54] Dvorakova, M. and Landa, P. Anti-inflammatory activity of natural stilbenoids: A review. Pharmacological Research 124 (2017): 126-145.

[55] Lewis, A.J. and Manning, A.M. New targets for anti-inflammatory drugs. Current Opinion in Chemical Biology 3(4) (1999): 489-94.

[56] Tambuwala, M.M. Natural Nuclear Factor Kappa Beta Inhibitors: Safe Therapeutic Options for Inflammatory Bowel Disease. Inflammatory Bowel Diseases 22(3) (2015): 719-723.

[57] Ko, Y.J., et al. Piceatannol inhibits mast cell-mediated allergic inflammation. International Journal of Molecular Medicine 31(4) (2013): 951-8.

[58] Santini, A., Tenore, G.C., and Novellino, E. Nutraceuticals: A paradigm of proactive medicine. European Journal of Pharmaceutical Sciences 96 (2017): 53-61.

[59] Woo, E.-R., Pokharel, Y., Won Yang, J., Yi Lee, S., and Wook Kang, K. Inhibition of nuclear factor-kappaB activation by 2',8''-biapigenin. Biological and

Pharmaceutical Bulletin 29 (2006): 976-980.

[60] Mitchell, J.A., Larkin, S., and Williams, T.J. Cyclooxygenase-2: Regulation and relevance in inflammation. Biochemical Pharmacology 50(10) (1995): 1535-1542.

[61] Aggarwal, B.B., Shishodia, S., Sandur, S.K., Pandey, M.K., and Sethi, G. Inflammation and cancer: How hot is the link? Biochemical Pharmacology 72(11) (2006): 1605-1621.

[62] Gallego, J.G., and Tunon, M. J. . Anti-inflammatory properties of dietary flavonoids. Nutrition Hospitalaria 22(3) (2007): 287-293.

[63] Kim, S.F. Chapter Nine - The Nitric Oxide-Mediated Regulation of Prostaglandin Signaling in Medicine. in Litwack, G. (ed.)Vitamins and Hormones, pp. 211-245: Academic Press, 2014.

[64] Schönfeld, P., Kruska, N., and Reiser, G. Antioxidative activity of the olive oil constituent hydroxy-1-aryl-isochromans in cells and cell-free systems. Biochimica et Biophysica Acta (BBA) - General Subjects 1790(12) (2009): 1698-1704.

[65] Zhao, Z., Jin, J., Fang, W., and Ruan, J. Antioxidant activity of polyphenolic constituents from Smilax china. Herald of Medicine 27 (2008): 765-767.

[66] Wang, Y.C., Wu, C., Chen, H., Zheng, Y., Xu, L., and Huang, X.Z. Antioxidant activities of resveratrol, oxyresveratrol, esveratrol, mulberroside a from cortex mori. Food Science 32 (2011): 135-138.

[67] Sureda, A., Tejada Gavela, S., Bibiloni, M.d.M., Antoni Tur, J., and Pons, A. Polyphenol Supplementation and Exercise-Induced Oxidative Stress and Inflammation. Critical Reviews in Food Science and Nutrition 15 (2014): 7.

[68] Alam, M., Subhan, N., Rahman, M.M., Uddin, S., Reza, H., and Sarker, S. Effect of Citrus Flavonoids, Naringin and Naringenin, on Metabolic Syndrome and Their Mechanisms of Action. Advances in Nutrition 5(4) (2014): 404-417.

[69] Choi, H.Y., Lee, J.-H., Jegal, K.H., Cho, I.J., Kim, Y.W., and Kim, S.C. Oxyresveratrol abrogates oxidative stress by activating ERK–Nrf2 pathway in the liver. Chemico-Biological Interactions 245(Supplement C) (2016): 110-121.

[70] Chen, C.-Y., Jang, J.-H., Li, M.-H., and Surh, Y.-J. Resveratrol upregulates heme oxygenase-1 expression via activation of NF-E2-related factor 2 in PC12 cells.

Biochemical and Biophysical Research Communications 331(4) (2005): 993-1000.

[71] Choi, E.-M. and Hwang, J.-K. Effects of Morus alba leaf extract on the production of nitric oxide, prostaglandin E2 and cytokines in RAW264.7 macrophages. Fitoterapia 76(7) (2005): 608-613.

[72] Wongwat, T., Srihaphon, K., Pitaksutheepong, C., Boonyo, W., and Pitaksuteepong, T. Suppression of inflammatory mediators and matrix metalloproteinase (MMP)-13 by Morus alba stem extract and oxyresveratrol in RAW 264.7 cells and C28/I2 human chondrocytes. Journal of Traditional and Complementary Medicine (2019).

[73] Lee, H.S., Kim, D.H., Hong, J.E., Lee, J.Y., and Kim, E.J. Oxyresveratrol suppresses lipopolysaccharide-induced inflammatory responses in murine macrophages. Human and Experimental Toxicology 34(8) (2015): 808-18.

[74] Chung, K.-O., et al. In-vitro and in-vivo anti-inflammatory effect of oxyresveratrol from Morus alba L. Journal of Pharmacy and Pharmacology 55(12) (2003): 1695-1700.

[75] Eswara Rao Bharani, S., Asad, M., Samson Dhamanigi, S., and Kallenahalli Chandrakala, G. Immunomodulatory activity of methanolic extract of Morus alba Linn. (mulberry) leaves. Pakistan Journal of Pharmaceutical Sciences 23(1) (2010): 63-68.

[76] Lee, H.S., Kim, D.H., Hong, J.E., Lee, J.Y., and Kim, E.J. Oxyresveratrol suppresses lipopolysaccharide-induced inflammatory responses in murine macrophages. Human and Experimental Toxicology 34(1477-0903) (2015): 808-18.

[77] Park, G.-S., Kim, J.-K., and Kim, J.-H. Anti-inflammatory action of ethanolic extract of Ramulus mori on the BLT2-linked cascade. BMB Reports 49(4) (2016): 232-237.

[78] Linde, A., Mosier, D., Blecha, F., and Melgarejo, T. Innate immunity and inflammation – New frontiers in comparative cardiovascular pathology. Cardiovascular Research 73(1) (2007): 26-36.

[79] Cheung, D.W.-S., et al. A herbal formula containing roots of Salvia miltiorrhiza (Danshen) and Pueraria lobata (Gegen) inhibits inflammatory mediators in LPS-

stimulated RAW 264.7 macrophages through inhibition of nuclear factor **K**B (NF**K**B) pathway. Journal of Ethnopharmacology 145(3) (2013): 776-783.

[80] Mittal, M., Siddiqui, M.R., Tran, K., Reddy, S.P., and Malik, A.B. Reactive oxygen species in inflammation and tissue injury. Antioxidants and Redox Signaling 20(7) (2014): 1126-67.

[81] Zhang, L. and Wang, C.-C. Inflammatory response of macrophages in infection. Hepatobiliary and Pancreatic Diseases International 13(2) (2014): 138-152.

[82] Funaro, A., et al. Enhanced Anti-Inflammatory Activities by the Combination of Luteolin and Tangeretin. Journal of Food Science 81(5) (2016): H1320-H1327.

[83] Taciak, B., et al. Evaluation of phenotypic and functional stability of RAW 264.7 cell line through serial passages. PLOS ONE 13(6) (2018): e0198943.

[84] Jiang, F.A.-O., Guan, H., Liu, D., Wu, X., Fan, M., and Han, J. Flavonoids from sea buckthorn inhibit the lipopolysaccharide-induced inflammatory response in RAW264.7 macrophages through the MAPK and NF-kB pathways. Food and Function 8(3) (2017): 1313-1322.

[85] Huang, H.-l., Zhang, J.-q., Chena, G.-t., Lu, Z.-q., Sha, N., and Guo, D.-a. Simultaneous Determination of Oxyresveratrol and Resveratrol in Rat Bile and Urine by HPLC after Oral Administration of Smilax china Extract. Natural Product Communications 4(6) (2009): 825-830.

[86] Huang, H., Chen, G., Lu, Z., Zhang, J., and Guo, D.-A. Identification of seven metabolites of oxyresveratrol in rat urine and bile using liquid chromatography/tandem mass spectrometry. Biomedical Chromatography 24(4) (2010): 426-432.

[87] Mei, M., et al. In Vitro Pharmacokinetic Characterization of Mulberroside A, the Main Polyhydroxylated Stilbene in Mulberry (Morus alba L.), and Its Bacterial Metabolite Oxyresveratrol in Traditional Oral Use. Journal of Agricultural and Food Chemistry 60(9) (2012): 2299-2308.

[88] Hidalgo, I., Raub, T., and T. Borchardt, R. Characterization of the Human Colon Carcinoma Cell Line (Caco-2) as a Model System for Intestinal Epithelial Permeability. Gastroenterology 96 (1989): 736-749.

[89] Zeng, Z., et al. Transport of curcumin derivatives in Caco-2 cell monolayers. European Journal of Pharmaceutics and Biopharmaceutics 117 (2017): 123-131.

[90] Gan, L.-S., Hsyu, P.-H., Pritchard, J.F., and Thakker, D. Mechanism of Intestinal Absorption of Ranitidine and Ondansetron: Transport Across Caco-2 Cell Monolayers. Pharmaceutical Research 10(12) (1993): 1722-1725.

[91] Hubatsch, I., Ragnarsson, E.G.E., and Artursson, P. Determination of drug permeability and prediction of drug absorption in Caco-2 monolayers. Nature Protocols 2(9) (2007): 2111-2119.

[92] Lind, M.L., Jacobsen, J., Holm, R., and Müllertz, A. Development of simulated intestinal fluids containing nutrients as transport media in the Caco-2 cell culture model: Assessment of cell viability, monolayer integrity and transport of a poorly aqueous soluble drug and a substrate of efflux mechanisms. European Journal of Pharmaceutical Sciences 32(4) (2007): 261-270.

[93] Imai, T. Human carboxylesterase isozymes: catalytic properties and rational drug design. Drug Metabolism and Pharmacokinetics (1347-4367 (Print)).

[94] Gallardo, E., Sarria, B., Espartero, J.L., Gonzalez Correa, J.A., Bravo-Clemente, L., and Mateos, R. Evaluation of the Bioavailability and Metabolism of Nitroderivatives of Hydroxytyrosol Using Caco-2 and HepG2 Human Cell Models. Journal of Agricultural and Food Chemistry 64(11) (2016): 2289-2297.

[95] Deferme, S., Annaert, P., and Augustijns, P. In Vitro Screening Models to Assess Intestinal Drug Absorption and Metabolism. in Ehrhardt, C. and Kim, K.-J. (eds.),Drug Absorption Studies: In Situ, In Vitro and In Silico Models, pp. 182-215. Boston, MA: Springer US, 2008.

[96] Albert, A. Chemical Aspects of Selective Toxicity. Nature 182(4633) (1958): 421-423.

[97] Kevin Beaumont, R.W., Iain Gardner, Kevin Dack. Design of Ester Prodrugs to Enhance Oral Absorption of Poorly Permeable Compounds: Challenges to the Discovery Scientist. Current Drug Metabolism 4(6) (2003): 461-485.

[98] Stella, V.J. and Nti-Addae, K.W. Prodrug strategies to overcome poor water solubility. Advanced Drug Delivery Reviews 59(7) (2007): 677-694.

[99] Chung, C.M., et al. Prodrugs for the Treatment of Neglected Diseases. Molecules

13(3) (2007): 616-177.

[100] Rautio, J., et al. Prodrugs: design and clinical applications. Nature Reviews Drug Discovery 7(3) (2008): 255-270.

[101] Taylor, M.D. Improved passive oral drug delivery via prodrugs. Advanced Drug Delivery Reviews 19(2) (1996): 131-148.

[102] Liederer, B.M. and Borchardt, R.T. Enzymes involved in the bioconversion of ester-based prodrugs. Journal of Pharmaceutical Sciences 95(6) (2006): 1177-1195.

[103] DJ, E. Relative amounts of hepatic and renal carboxylesterase in mammalian species. Research Communications in Chemical Pathology and Pharmacology 3(3) (1972): 629-636.

[104] Balant, L.P., Doelker, E., and Buri, P. Prodrugs for the improvement of drug absorption via different routes of administration. European Journal of Drug Metabolism and Pharmacokinetics 15(2) (1990): 143-53.

[105] Di, L. and Kerns, E.H. Chapter 39 - Prodrugs. in Di, L. and Kerns, E.H. (eds.),Drug-Like Properties (Second Edition), pp. 471-485. Boston: Academic Press, 2016.

[106] Chatsumpun, N., et al. Oxyresveratrol: Structural Modification and Evaluation of Biological Activities. Molecules 21(4) (2016): 489-489.

[107] Park, J., Park, J.H., Suh, H.-J., Lee, I.C., Koh, J., and Boo, Y.C. Effects of resveratrol, oxyresveratrol, and their acetylated derivatives on cellular melanogenesis. Archives of Dermatological Research 306(5) (2014): 475-487.

[108] Li, C., Wainhaus, S., Uss, A.S., and Cheng, K.-C. High-Throughput Screening Using Caco-2 Cell and PAMPA Systems. in Ehrhardt, C. and Kim, K.-J. (eds.),Drug Absorption Studies: In Situ, In Vitro and In Silico Models, pp. 418-429. Boston, MA: Springer US, 2008.

[109] DiMarco, R.L., Hunt, D.R., Dewi, R.E., and Heilshorn, S.C. Improvement of paracellular transport in the Caco-2 drug screening model using protein-engineered substrates. Biomaterials 129 (2017): 152-162.

[110] Ozdemir, K.G., Yilmaz, H., and Yilmaz, S. In vitro evaluation of cytotoxicity of soft lining materials on L929 cells by MTT assay. Journal of Biomedical Materials Research Part B: Applied Biomaterials 90(1) (2009): 82-6.

[111] 33, U.S.P.N.F. Test Solutions. USA: United Book Press, Inc., 2015.

[112] Asafu-Adjaye, E.B., et al. Validation and application of a stability-indicating HPLC method for the in vitro determination of gastric and intestinal stability of venlafaxine. Journal of Pharmaceutical and Biomedical Analysis 43(5) (2007): 1854-1859.

[113] Lu, Y., N. Shipton, F., J. Khoo, T., and Wiart, C. Antioxidant Activity Determination of Citronellal and Crude Extracts of Cymbopogon citratus by 3 Different Methods. Journal of Pharmacy and Pharmacology 05 (2014): 395-400.

[114] Thaipong, K., Boonprakob, U., Crosby, K., Cisneros-Zevallos, L., and Hawkins Byrne, D. Comparison of ABTS, DPPH, FRAP, and ORAC assays for estimating antioxidant activity from guava fruit extracts. Journal of Food Composition and Analysis 19(6) (2006): 669-675.

[115] Pellegrini, N., et al. Total Antioxidant capacity of plant foods, beverages and oils consumed in Italy assessed by three different in vitro assays. Journal of Nutrition 133 (2003): 2812-2819.

[116] Benzie, I.F.F. and Strain, J.J. The Ferric Reducing Ability of Plasma (FRAP) as a Measure of "Antioxidant Power": The FRAP Assay. Analytical Biochemistry 239(1) (1996): 70-76.

[117] Huang, D., Ou, B., Hampsch-Woodill, M., A Flanagan, J., and Prior, R. High-Throughput Assay of Oxygen Radical Absorbance Capacity (ORAC) Using a Multichannel Liquid Handling System Coupled with a Microplate Fluorescence Reader in 96-Well Format. Journal of Agricultural and Food Chemistry 50 (2002): 4437-4444.

[118] Ou, B., Huang, D., Hampsch-Woodill, M., A Flanagan, J., and K Deemer, E. Analysis of Antioxidant Activities of Common Vegetables Employing Oxygen Radical Absorbance Capacity (ORAC) and Ferric Reducing Antioxidant Power (FRAP) Assays: A Comparative Study. Journal of Agricultural and Food Chemistry 50 (2002): 3122-3128.

[119] Soh, N.J.A. and Chemistry, B. Recent advances in fluorescent probes for the detection of reactive oxygen species. Analytical and Bioanalytical Chemistry 386(3) (2006): 532-543.

[120] Banskota, A.H., Tezuka, Y., Nguyen, N.T., Awale, S., Nobukawa, T., and Kadota, S. DPPH radical scavenging and nitric oxide inhibitory activities of the constituents from the wood of Taxus yunnanensis. Planta Medica 69(6) (2003): 500-5.

[121] Verley, A. and Bölsing, F. Ueber quantitative Esterbildung und Bestimmung von Alkoholen resp. Phenolen. Berichte der Deutschen Chemischen Gesellschaft 34(3) (1901): 3354-3358.

[122] Amidon, S., Brown, J.E., and Dave, V.S. Colon-targeted oral drug delivery systems: design trends and approaches. AAPS PharmSciTech 16(4) (2015): 731-41.

[123] Benzie, I.F. and Strain, J.J. The ferric reducing ability of plasma (FRAP) as a measure of "antioxidant power": the FRAP assay. Analytical Biochemistry 239(1) (1996): 70-6.

[124] Kaldas, M.I., Walle, U.K., and Walle, T. Resveratrol transport and metabolism by human intestinal Caco-2 cells. Journal of Pharmacy and Pharmacology 55(3) (2003): 307-312.

[125] Suzuki, Y., et al. Exploring Novel Cocrystalline Forms of Oxyresveratrol to Enhance Aqueous Solubility and Permeability across a Cell Monolayer. Biological and Pharmaceutical Bulletin 42(6) (2019): 1004-1012.

[126] Ohura, K., Nishiyama, H., Saco, S., Kurokawa, K., and Imai, T. Establishment and Characterization of a Novel Caco-2 Subclone with a Similar Low Expression Level of Human Carboxylesterase 1 to Human Small Intestine. Drug Metabolism and Disposition 44(12) (2016): 1890-1898.

[127] Stockdale, T.P., Challinor, V.L., Lehmann, R.P., De Voss, J.J., and Blanchfield, J.T. Caco-2 Monolayer Permeability and Stability of Chamaelirium luteum (False Unicorn) Open-Chain Steroidal Saponins. ACS Omega 4(4) (2019): 7658-7666.

[128] Chagas, C.M., Moss, S., and Alisaraie, L. Drug metabolites and their effects on the development of adverse reactions: Revisiting Lipinski's Rule of Five. International Journal of Pharmaceutics 549(1-2) (2018): 133-149.

[129] Yu, J., et al. Intestinal transportations of main chemical compositions of polygoni multiflori radix in caco-2 cell model. Evidence-Based Complementary and Alternative Medicine 2014 (2014): 483641.

[130] He, X., Sugawara, M., Takekuma, Y., and Miyazaki, K. Absorption of ester prodrugs in Caco-2 and rat intestine models. Antimicrob Agents Chemother 48(7) (2004): 2604-9.

[131] Cacciatore, I., et al. Carvacrol codrugs: a new approach in the antimicrobial plan. PLOS ONE 10(4) (2015): 20.

[132] Prior, R.L., Wu, X., and Schaich, K. Standardized Methods for the Determination of Antioxidant Capacity and Phenolics in Foods and Dietary Supplements. Journal of Agricultural and Food Chemistry 53(10) (2005): 4290-4302.

[133] Maia, I.R.D., Trevisan, M.T.S., Silva, M.G.D., Breuer, A., and Owen, R.W. Characterization and Quantitation of Polyphenolic Compounds in Senna gardneri and S. georgica from the Northeast of Brazil. Natural Product Communications 13(11) (2018): 1511-1514.

[134] Passos, C.L., Ferreira, C., Soares, D.C., and Saraiva, E.M. Leishmanicidal Effect of Synthetic trans-Resveratrol Analogs. PLOS ONE 10(10) (2015): 16.

[135] Köhler, B.M., Günther, J., Kaudewitz, D., and Lorenz, H.-M. Current Therapeutic Options in the Treatment of Rheumatoid Arthritis. Journal of Clinical Medicine 8(7) (2019): 938.

[136] Du, H., Ma, L., Chen, G., and Li, S. The effects of oxyresveratrol abrogates inflammation and oxidative stress in rat model of spinal cord injury. Molecular Medicine Reports 17(3) (2018): 4067-4073.

[137] Junsaeng, D., Anukunwithaya, T., Songvut, P., Sritularak, B., Likhitwitayawuid, K., and Khemawoot, P. Comparative pharmacokinetics of oxyresveratrol alone and in combination with piperine as a bioenhancer in rats. BMC Complementary and Alternative Medicine 19(1) (2019): 235-235.

[138] González, C.M., Martínez, L., Ros, G., and Nieto, G. Evaluation of nutritional profile and total antioxidant capacity of the Mediterranean diet of southern Spain. Food Science and Nutrition 7(12) (2019): 3853-3862.

[139] Lakshmi, B., Tilak, J.C., Adhikari, S., Devasagayam, T.P.A., and Janardhanan, K.K. Evaluation of antioxidant activity of selected Indian mushrooms. Pharmaceutical Biology 42(3) (2004): 179-185.

[140] Jayawardena, N., Watawana, M.I., and Waisundara, V.Y. The total antioxidant

capacity, total phenolics content and starch hydrolase inhibitory activity of fruit juices following pepsin (gastric) and pancreatin (duodenal) digestion. Journal für Verbraucherschutz und Lebensmittelsicherheit 10(4) (2015): 349-357.

[141] Leyton, M., Mellado, M., Jara, C., Montenegro, I., González, S., and Madrid, A. Free radical-scavenging activity of sequential leaf extracts of Embothrium coccineum. Open Life Sciences 10 (2015): 260–268.

[142] Aryal, S., Baniya, M.K., Danekhu, K., Kunwar, P., Gurung, R., and Koirala, N. Total Phenolic Content, Flavonoid Content and Antioxidant Potential of Wild Vegetables from Western Nepal. Plants 8(4) (2019): 96.

[143] Chaves, N., Santiago, A., and Alías, J.C. Quantification of the Antioxidant Activity of Plant Extracts: Analysis of Sensitivity and Hierarchization Based on the Method Used. Antioxidants 9(1) (2020): 76.

[144] Parejo, I., Codina, C., Petrakis, C., and Kefalas, P. Evaluation of scavenging activity assessed by Co(II)/EDTA-induced luminol chemiluminescence and DPPH· (2,2-diphenyl-1-picrylhydrazyl) free radical assay. Journal of Pharmacological and Toxicological Methods 44(3) (2000): 507-512.

[145] Gheldof, N., Wang, X.H., and Engeseth, N.J. Identification and quantification of antioxidant components of honeys from various floral sources. Journal of Agricultural and Food Chemistry 50(21) (2002): 5870-7.

[146] Benzie, I.F.F. and Strain, J.J. Ferric reducing/antioxidant power assay: Direct measure of total antioxidant activity of biological fluids and modified version for simultaneous measurement of total antioxidant power and ascorbic acid concentration. in Methods in Enzymology, pp. 15-27: Academic Press, 1999.

[147] Chen, Y., et al. Vitamin C Mitigates Oxidative Stress and Tumor Necrosis Factor-Alpha in Severe Community-Acquired Pneumonia and LPS-Induced Macrophages. Mediators of Inflammation 2014 (2014): 426740.

[148] Shang, H.-M., Zhou, H.-Z., Yang, J.-Y., Li, R., Song, H., and Wu, H.-X. In vitro and in vivo antioxidant activities of inulin. PLOS ONE 13(2) (2018): 12.

[149] More, G.K. and Makola, R.T. In-vitro analysis of free radical scavenging activities and suppression of LPS-induced ROS production in macrophage cells by Solanum sisymbriifolium extracts. Scientific Reports 10(1) (2020): 6493.

[150] Huang, C., et al. Anti-inflammatory activities of Guang-Pheretima extract in lipopolysaccharide-stimulated RAW 264.7 murine macrophages. BMC Complementary and Alternative Medicine 18(1) (2018): 46.

[151] Silva, P., et al. (E)-2-Cyano-3-(1H-Indol-3-yl)-N-Phenylacrylamide, a Hybrid Compound Derived from Indomethacin and Paracetamol: Design, Synthesis and Evaluation of the Anti-Inflammatory Potential. International Journal of Molecular Sciences 21(7) (2020): 2591.

[152] Wang, X., et al. Anti-inflammatory effects and mechanism of the total flavonoids from Artemisia scoparia Waldst. et kit. in vitro and in vivo. Biomedicine and Pharmacotherapy 104 (2018): 390-403.

VITA

NAME	Wuttinont Thweesest
DATE OF BIRTH	2 December 1988
PLACE OF BIRTH	Udonthani
INSTITUTIONS ATTENDED	2011-2013 M.Sc. (Biotechnology), Chulalongkorn University, Bangkok, Thailand. 2008-2011 B.Sc. (Chemistry), Kasetsart University Kamphaeng Saen Campus, Nakhon Pathom, Thailand
HOME ADDRESS	17 Moo 1 Wari U-Thit Road, Ban Dung, Udon Thani, 41190, Thailand
PUBLICATION	Thaweesest W., Muangnoi C., Sritularak B., Rashatasakhon P. and Rojsitthisak P. Enhancement of antioxidant and anti-inflammatory effects of oxyresveratrol on lipopolysaccharide-stimulated RAW264.7 macrophage cells by oxyresveratrol ester prodrug Antioxidants (In processing)